UNIVERSITA' DEGLI STUDI DI PARMA

Dottorato di ricerca in Fisica

Ciclo XXVI

Photochromism of flavin-based photoreceptors: new perspectives for super-resolution microscopy and optogenetics

Coordinatore:
Chiar.mo Prof. Pier Paolo Lottici

Tutor:
Dott. ssa Aba Losi

Dottoranda: Mandalari Carmen

M’illumino d’immenso.

(G. Ungaretti)

Summary

Flavin-binding blue-light (BL) sensor proteins (Fl-Blues) of bacterial origin have been investigated in this work with diverse biophysical methods, with the aim to characterize their photophysical and photochemical properties. Investigations have been carried out both *in vitro* and *in vivo*, to explore their potential in advance cellular applications and establish novel methods of analysis. Besides the lab work, extensive *in silico* analysis have been performed, in the attempt to optimize searching in public databanks, identify novel Fl-Blues and gain hints on their evolution patterns.

Main object of lab work has been the protein YtvA from *Bacillus subtilis*, a BL-photoreceptor involved in environmental stress responses. Its photosensing unit is a LOV (Light, Oxygen and Voltage) domain, that binds oxidized flavin mononucleotide (FMN) as a photoactive chromophore, brightly fluorescent in the dark-adapted state. BL illumination triggers a photocycle with formation of a FMN-cysteine covalent adduct (light adapted or lit state), with complete loss of fluorescence and concomitant activation of a biological response (signaling). The adduct thermally recovers to the dark-state with breakage of the covalent bond, on a time scale of hours at room temperature. This protein is thus naturally bi-stable, both for its optical and biological properties.

Using steady-state and time resolved optical spectroscopies, we could show here that application of violet or UVA light to the adduct is able to induce a photoequilibrium, with partial recovery of the dark-adapted state and of FMN fluorescence. In other words, YtvA was demostrated to be a photochromic system. It was possible to calculate the quantum yield of the photoinduced light-to-dark reaction as ca. 0.05, that is about 1/10 the efficiency of the forward dark-to-light photochemical step. This newly discovered photochromism of YtvA, allowed us to show its potential in super-resolution microscopy, in particular using Fluorescence Photo-activation Localization Microscopy (FPALM) to visualize YtvA fluorescence inside transformed *Escherichia coli* cells with nanometer precision [1]. In order to try to optimize and tune the photochromic, photochemical and spectral properties of YtvA, a set of mutagenized variants has been designed and investigated. In particular we were able to identify amino acids that act as major spectral tuners in the UVA region, and other residues able to strongly affects the dynamics of the photocycle [2].

Another notable property of YtvA has emerged by performing epifluorescence microscopy experiments on living cells expressing the proteins. During these studies, still at a preliminary stage, it became clear that the level of hydration is able to affect the thermal recovery rate of

the photocycle, a property that is relevant to understand the effects of water on this kind of systems and for applications *in vivo*.

Genome digging has revealed, during the last decade, that LOV domains are widespread among the three life domains and are emerging as BL sensing systems not only in plants, but also in prokaryotes. On full-length proteins LOV modules they are usually linked to diverse effector domains that determine the biological functionality of the protein itself. A second and different type of BL-sensor, also widespread among prokaryotes, is the so-called BLUF (Blue Light sensing Using Flavins), that upon light-activation undergoes a rapidly reversible hydrogen-bond (HB) switch. In this work we performed an extensive database search in order to have a comprehensive scenario of LOV and BLUF proteins in the prokaryotic world, inspect phylogenetic pathways and discover possible novel functionalities for effector domains, a feature connected with optogenetics [3, 4]. From distance-trees obtained by using neighbouring-methods, it was observed that most LOV and BLUF domains from organisms belonging to the same phylum are neighbour, but that in many cases clustering occurs according to effector functions associated to the photosensing domains [3]. Metagenomics and bio-informatic analysis have only recently been initated, but signatures are beginning to emerge that allow definition of a *bona fide* LOV or BLUF domain, aiming at better selection criteria for novel BL sensors based on sequence logos [4]. Taking advantage of these new criteria it was built, for the first time, the phylogenetic tree for archaeal LOV domains that have reached a statistically significant number, but have not at all been investigated so far [4].

1. A. Losi, W. Gärtner, S.Raffelberg, F. Cella Zanacchi, P.Bianchini, A.Diaspro, **C.Mandalari**, S.Abbruzzetti and C.Viappiani, “A photochromic bacterial photoreceptor with potential for super-resolution microscopy”, *Photochem. Photobiol. Sci*., 2013,

2. S. Raffelberg, A.Gutt, W. Gärtner, **C. Mandalari**, S. Abbruzzetti, C. Viappiani and A. Losi, “The amino acids surrounding the flavin 7a-methyl group determine the UVA spectral features of a LOV protein”, *Biol. Chem.*, 2013, 394: 1517-1528

3. C. Mandalari, A. Losi and W. Gärtner, “Distance-tree analysis, distribution and co-presence of bilin- and flavin-binding prokaryotic photoreceptors for visible light”, *Photochem. Photobiol. Sci*., 2013, 12:1144-1157

4. A. Losi, **C. Mandalari**, W. Gärtner, “From plant infectivity to growth patterns: the role of blue-light sensing in the prokaryotic world”, *Plants*, 2014, accepted for pubblication.

Abbreviations

The following list contains all abbreviations repeatedly used in this thesis excluding common SI units. For DNA bases and amino acids the standard one or three letter codes were used, respectively.

aa: amino acid
AMP: adenosine monophosphate (5'-adenylic acid)
*As*phot: *Avena sativa* phototropin
ATP: adenosine-triphosphate
*At*phot: *Arabidopsis thaliana* phototropin
BL: blue-light
BLUF: sensor of blue-light using FAD domain
$BLUF_{RED}$: BLUF domain red-shifted signalling state
*Bs*YtvA: *Bacillus subtilis* YtvA
cAMP: cyclic adenosine monophosphate
c-di-GMP: cyclic diguanylate
cGMP: cyclic guanosine monophosphate
CRY: cryptochrome
EAL: diguanylate phosphodiesterase domain
*Ec*YcgF: *Escherichia coli* YcgF
EM: electron microscopy
EPS: extracellular polymeric substances
FAD: flavin adenine dinucleoctide
FbFPs: FMN-binding fluorescent proteins
FCS: fluorescence correlation spectroscopy
Fl-Blues: flavin-binding blue/UVA light sensors
FLIM: fluorescence lifetime imaging microscopy
FMN: flavin mononucleotide
FP: fluorescent protein
FPALM: fluorescence photoactivation localization microscopy
GAF: cGMP phosphodiesterase, adenylyl cyclase and FhlA protein
GFP: green fluorescent protein
GGDEF: diguanylate cyclise

GMP: diguanylate

GSR: general stress response

GTP: guanosine-triphosphate

HB: hydrogen bond/-ing

HK: histidine kinase (domain)

HTH: helix- turn- helix DNA-binding domain

LFP: laser flash photolysis

LIOAS: laser induced optoacustic spectroscopy

LOV: light, oxygen, voltage (domain)

LOV_{390} LOV signaling state, also called light-adapted or lit state

LOV_{447}: LOV dark-adapted state

LOV_{660}: LOV excited triplet-state

LOV-HK: LOV histidine kinase

MCP: Methyl-accepting chemotaxis proteins

ORF: open reading frame

ox, sq, hq: oxidized, semiquinone, hydroquinone

PAC: photoactivated adenylyl cyclase

PALM: photoactivation localization microscopy

PAS: Per Arnt Sim domain

Phot: phototropin

PHY: phytochrome

PL: photolyase

PpsR: dimeric repressor

PSF: point spread function

PYP: photoactive yellow protein

RESOLFTS: reversible saturable optical fluorescence transition

RF: riboflavin

RR: response regulator

Rs AppA: *Rhodobacter sphaeroides* AppA

SCHIC: sensor containing heme instead of cobalamin

SPOIIE: Sporulation stage II, protein E C-terminal/Protein phosphatase 2C-related

SSIM: saturated structured illumination microscopy

STAS: sulfate transporter anti-sigma factor antagonist (domain)

STED: stimulated emission depletion

STORM: stochastic optical reconstruction microscopy

TPE: two-electron excitation

UV: ultraviolet

VIS: visible light

YtvA-WT: wild type YtvA

YFP: yellow fluorescent protein

YtvaD: dark-adapted state of YtvA

YtvaL: light-adapted state of YtvA

Table of contents

1. Introduction

During this research work I have studied flavin-binding blue-light(BL)/UVA sensor proteins (Fl-Blues) with the aim to: **i.** develop new investigation methods for their photophysical and functional characterization, both for *in vitro* and *in vivo* studies; **ii.** identify and/or optimize via an extended mutagenesis approach, their potential for advanced biophysical and biotechnological applications, such as superresolution microscopy and optogenetics; **iii.** develop methods to facilitate the *in silico* search for novel Fl-Blues, important for the identification of novel proteins and novel associated functions, with relevance for the above mentioned applications and to get insights into the evolutionary pathways of these increasingly important photoreceptors. The proteins I have worked with, comprise photosensors of the Light-Oxygen-Voltage (LOV) and Blue-Light-sensing Using Flavin (BLUF) superfamilies, introduced below.

1.1. Fl-Blues, ubiquitous and versatile blue-light/UVA sensing proteins

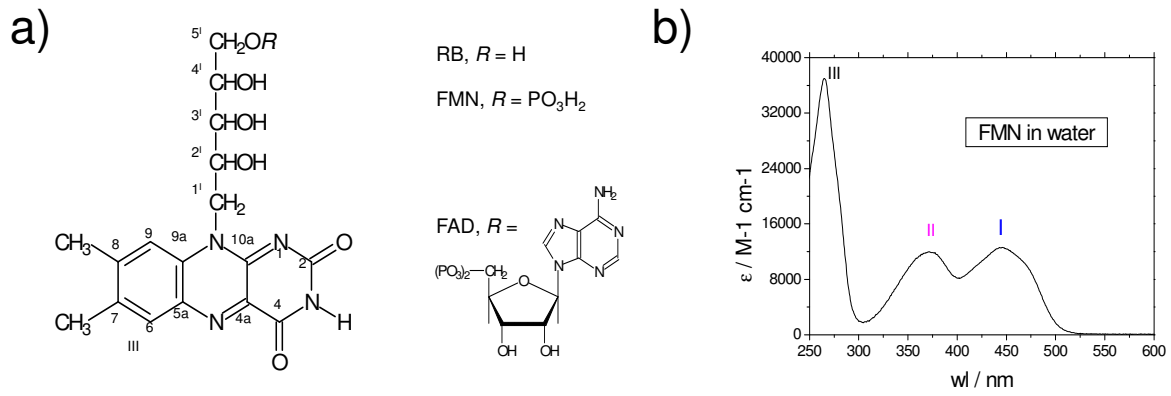

Figure 1.1. a) The three flavin chromophores of BL sensors. Riboflavin (RB) consists of a 7,8-dimethyl-isoalloxazine ring linked to D-ribitol. FMN and FAD are the phosphorylated and adenosylated forms of riboflavin, respectively. **b)** Absorption spectrum of FMN in water, scaled to show the absorption coefficients at the different wavelengths. This spectrum exemplifies a fully oxidized form of the chromophore and is basically the same for the three derivatives. I, II, III indicate the three major electronic transitions in the visible, UVA and UVB region respectively.

During the last decade the study of Fl-Blues belonging to the cryptochrome (Cry), LOV and BLUF proteins, has registered a continuously growing interest. For almost 200 years scientists

had reported on light color effects on plant growth and morphogenesis, but BL-photoreceptors could be identified and characterized only at the beginning of this century, followed by an outburst of structural and functional data [1]. It became soon clear that plant BL-photoreceptors bind riboflavin (RF) derivatives, such as flavin mononucleotide (FMN) and flavin adenine dinucleotide (FAD) (Figure 1.1), immediately initiating a new discussion, as the dogma of chromophore isomerization in photoreceptors (e.g. in rhodopsins and phytochromes) was broken [2]. Flavins can switch between different oxidation states, referred to as *"ox"*= fully oxidized, *"sq"* = one electron reduced or semiquinonic form,*"hq"* = hydroquinone, two electron reduced form. s*q* and *hq* can be protonated/deprotonated with pK_a-values of ca. 8 and 6, respectively [3]. All these species show different absorbance and photoreactivity features in the UVB-, UVA-, and visible range. The absorption spectrum of *ox* is composed of three major $\pi\pi^*$ bands, centered at ca. 446, 370 and 265 nm and characterizes (Figure 1.1) the dark-adapted state of LOV and BLUF proteins (see paragraph 1.2). The *sq* species is strongly red shifted, with a maximum at ca. 650 nm, while *hq* species shows an unstructured spectrum with a maximum in the UVB range. Upon light excitation, the redox potential dramatically shifts from ca. -0.3 V to + 1.9 V, i.e. photoexcited flavins state are strongly oxidant. Other important photophysical properties are the high triplet quantum yield (ca. 0.5-0.7) of the *ox* state and its noticeable fluorescence quantum yield (Φ_F) of 0.25-0.3 (for FMN and riboflavin).

Fl-Blues exhibit multiple photo-regulated functions in the living world. In plants, phot and Cry are originally related to phototropism and to the inhibition of hypocotyl elongation during photomorphogenesis respectively [2]. Other BL-regulated processes include circadian rhythms entrainment and flowering, stomatal opening, leaf expansion, chloroplast accumulation/avoidance movements, inhibition of hypocothyl growth during photomorphogenesis. The multiple roles of plant FL-Blues are mirrored now by a growing understanding of their involvement in light-to-signal conversion in microorganisms. In other words, Fl-Blues are rapidly conquering the field of BL photobiology in all three domains of life. Physiology, chronobiology, microbiology, evolutionary biology, biophysics, and biotechonology are the major research areas involved (Figure 1.2). Although still few case stories have been described, Fl-Blues seem to constitute light-perceptive systems also in prokaryotes, a sort of primitive visual tools integrated with other signal-transduction systems for screening and responding to environmental conditions. The

widespread occurrence of Fl-Blues offers a unique possibility of exploring the evolution and ecological significance of BL through soluble photoreceptors.

Last but not least, Fl-Blues have a large potential as tools for light-control of cellular functions (optogenetics) [4] and as fluorescent reporters in conditions not suitable for green-fluorescent proteins and derivatives, e.g., anaerobic/microaerobic systems or small viral genomes [5].

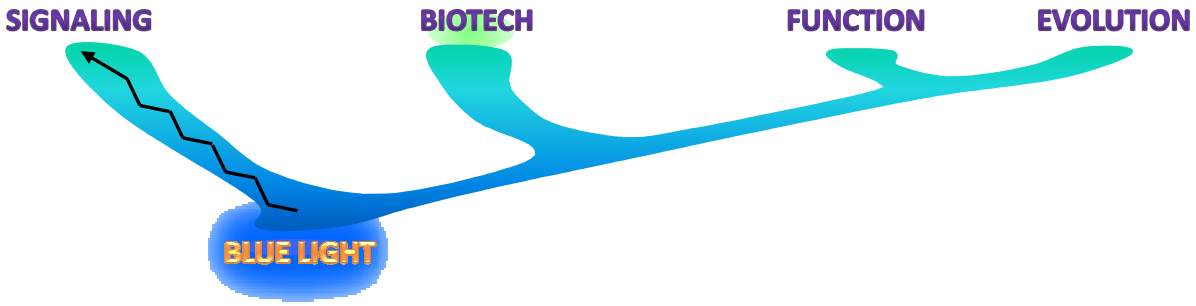

Figure 1.2. Research topics for flavin-binding, BL receptors (Fl-Blues). Besides their mechanism of activation, signal propagation and signal transduction, their function *in vivo* is being actively investigated. The wide-spread occurrence of Fl-Blues in the prokaryotic world prompts investigation of their evolution pathways and phylogenetic history [6]. Flavins are ubiquitous chromophores, thus favoring intracellular biotechnological applications, where Fl-blues are being exploited as fluorescent reporters, photochromic proteins for nanoscopy or photoactivable tools for optogenetics.

As mentioned above, Fl-Blues can be classified as three distinct types: LOV, BLUF and Cry proteins. LOV and BLUF domains are relatively small and compact folds (ca. 100-110 aa), binding a single flavin chromophore (FMN or FAD). Their photosensing and photoresponding properties, characterized by defined photochemical reactions and spectral features (par. 1.2) are linked to diverse effector/regulator functions in a large array of different proteins [6]. Cry instead are two-chromophore proteins, structurally and functionally related to the DNA-repairing enzymes photolyases (PL), with which they form the large Cry/PL family [7]. Contrary to PL, that catalyze the light-dependent repair of UV-induced DNA lesions, Cry proteins mainly function as sensors and have lost or show a strongly reduced capability of DNA repair activity. The divergent Cry/PL superfamily [8] spread with diverse functional significance in Archaea, Bacteria and Eukarya (including animals), is still a matter of debate as for the distinction between sensorial and photo-activated PL-like activity and will not be dealt further here. Here we will

focus on LOV and BLUF proteins, given their peculiar relevance and versatility in the prokaryotic world and their applicability in advanced biophysical techniques.

1.2 Structural and spectral properties of LOV and BLUF domains

LOV and BLUF domains are minimal and compact photosensing modules (ca 100–110 aa) with characteristic and well defined α/β folds (Figure 1.3) [2],[9]. The secondary structure elements of the core domains are conventionally named AβBβCαDαEαFαGβHβIβ (LOV) and $\beta_1\alpha_1\beta_2\beta_3\alpha_2\beta_3$ (BLUF) [27]. In LOV domains, a subgroup of the PAS (Per Arnt Sim) superfamily, the five antiparallel β-strands form a robust β-sheet surface that anchors the flexible helical connector CαDαEαFα [9]. The reactive cysteine responsible for photochemistry (*vide infra*) (Figure 1.3, 1.4a) is located within the Dα-Eα loop, at the N-terminal side of helix E. In BLUF domains the β-scaffold is also formed by five strands, partially organized in a parallel arrangement and basically running perpendicular to the isoalloxazine ring. The two Tyr and Gln residues that determine BLUF photocycle are placed on β_1 and β_3 respectively (Figures 1.3, 1.4b). Variable, mostly helical regions flank the α/β core and are often part of interfaces in oligomeric structures [2].

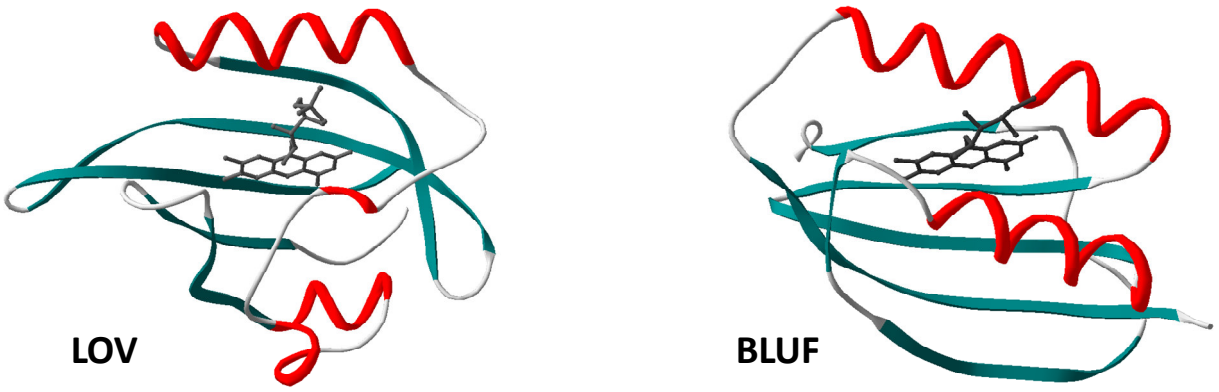

Figure 1.3. Three-dimensional structures of (left) LOV and (right) BLUF domains (core regions) showing the bound flavin chromophore (in black) and the secondary structure elements (red: helices, blue: strands). Figures created from the PDB entries 2PR5 (YtvA from *Bacillus subtilis*) and 1X0P (Tll0078 protein from *Thermosynechococcus elongatus*) respectively.

The photocycle of LOV domains starts from the dark-adapted state LOV_{447} (the subscript indicates the absorption maximum) in which *ox* FMN is non-covalently bound within an amphipatic cavity (Figure 1.4a), showing a vibrationally resolved absorption spectrum and Φ_F ca. 0.25 [9]. The photoprocess involves transient formation of a covalent bond between FMN-C(4a) and a conserved cysteine (light-adapted or lit-state, LOV_{390}), via the short µs decay of the FMN triplet state, with loss of fluorescence and a dramatic change in the absorption spectrum (Figure 1.5). Formation of LOV_{390} involves the establishment of new C(4a)-S and N-H(5) bonds, suggested to proceed via the fast decay of a $FMNH^{\bullet}$-$H_2CS^{\bullet}$ radical pair after spin inversion [10]. The driving force for the thermal recovery reaction to LOV_{447} is given by the high energy content of LOV_{390} (ca. 110-140 kJ/mol) that suggests a strained protein conformation [11].

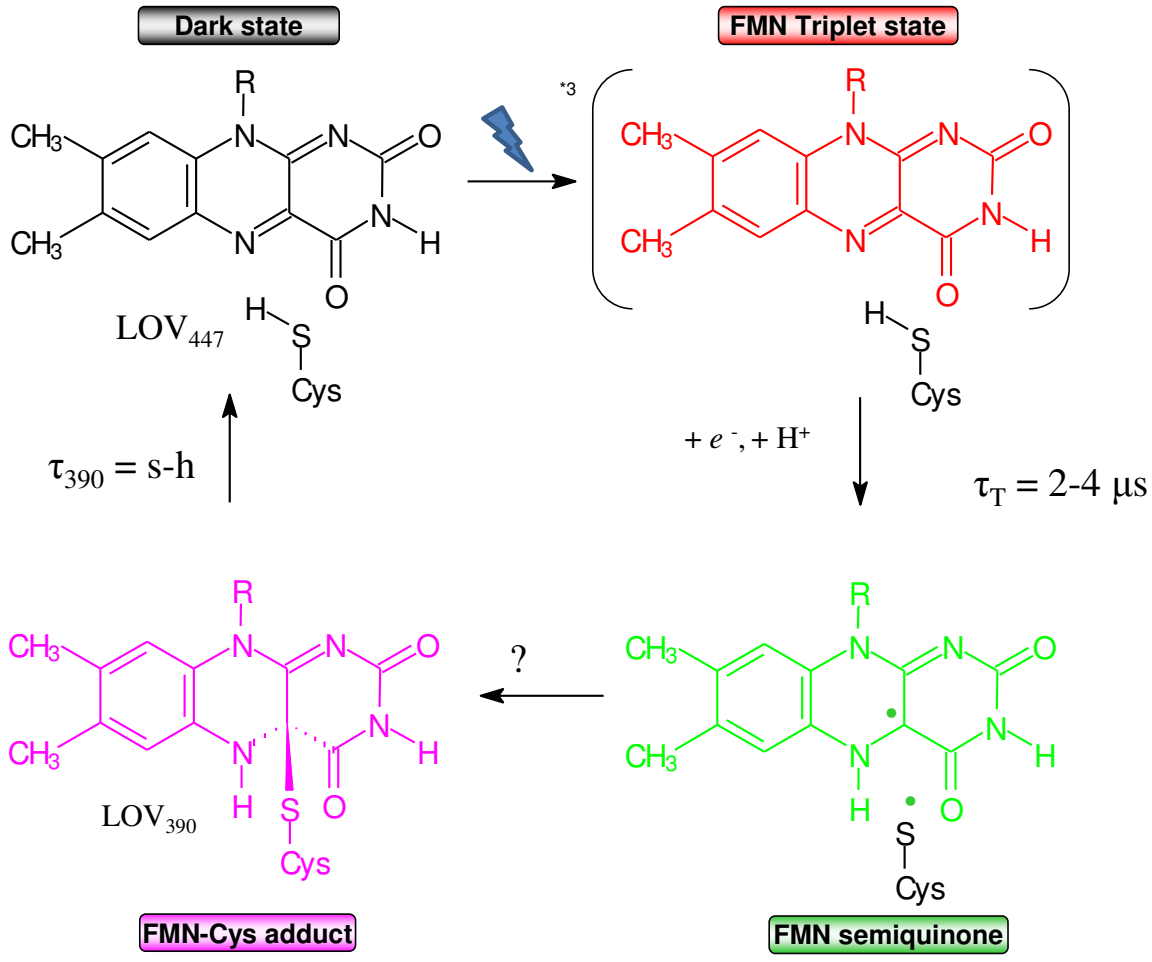

Figure 1.4a. Blue-light triggered photocycle of a LOV domain, with thermal recovery. The adduct is formed via the triplet state decay on the µs time-scale, possibly with a FMN radical, still uncharacterized, as an intermediate species. Modified from [12].

Nevertheless, breakage of the covalent FMN-C(4a) bond implies a high activation barrier of ca. 100 kJ/mol, thus rendering the overall duration of the photocycle strongly temperature dependent and sensitive to amino acids substitutions, especially in close vicinity of the chromophore [13], [14].

The thermal recovery rate is also highly variable among LOV domains, despite their high structural homology, ranging from few seconds to several hours around 20-25 °C (Figure 1.4a) [9], [15]. The first bacterial protein for which a LOV-type photocycle has been identified, is YtvA from the soil bacterium *Bacillus subtilis* (*Bs*YtvA) [11].

Intriguingly, LOV domains appear to be photochromic systems, in that LOV_{390} can be photoswitched back to LOV_{447}, yet with low efficiency, by using UVA/violet light [16], a feature that, for YtvA, has been explored and thoroughly investigated during this research work (see Results section), given its importance in superresolution microscopy [17].

In BLUF domains light excitation of the FAD chromophore induces a reversible red-shifted absorption spectrum, corresponding to the putative signaling state $BLUF_{RED}$ (Figure 1.4b and Figure 1.5) [9]. This spectral change is dictated by a hydrogen bonds- (HB-) switch reaction involving N(5), O(4), and a conserved tyrosine-glutamine couple (Figure 1.4b) [9], [18], [19]. The lifetime for recovery of the dark-adapted state ranges from a few seconds to several minutes. $BLUF_{RED}$ formation involves light-driven, ultrafast electron and proton transfer from the conserved tyrosine residue to FAD, followed by HB rearrangement and radical-pair recombination [20].

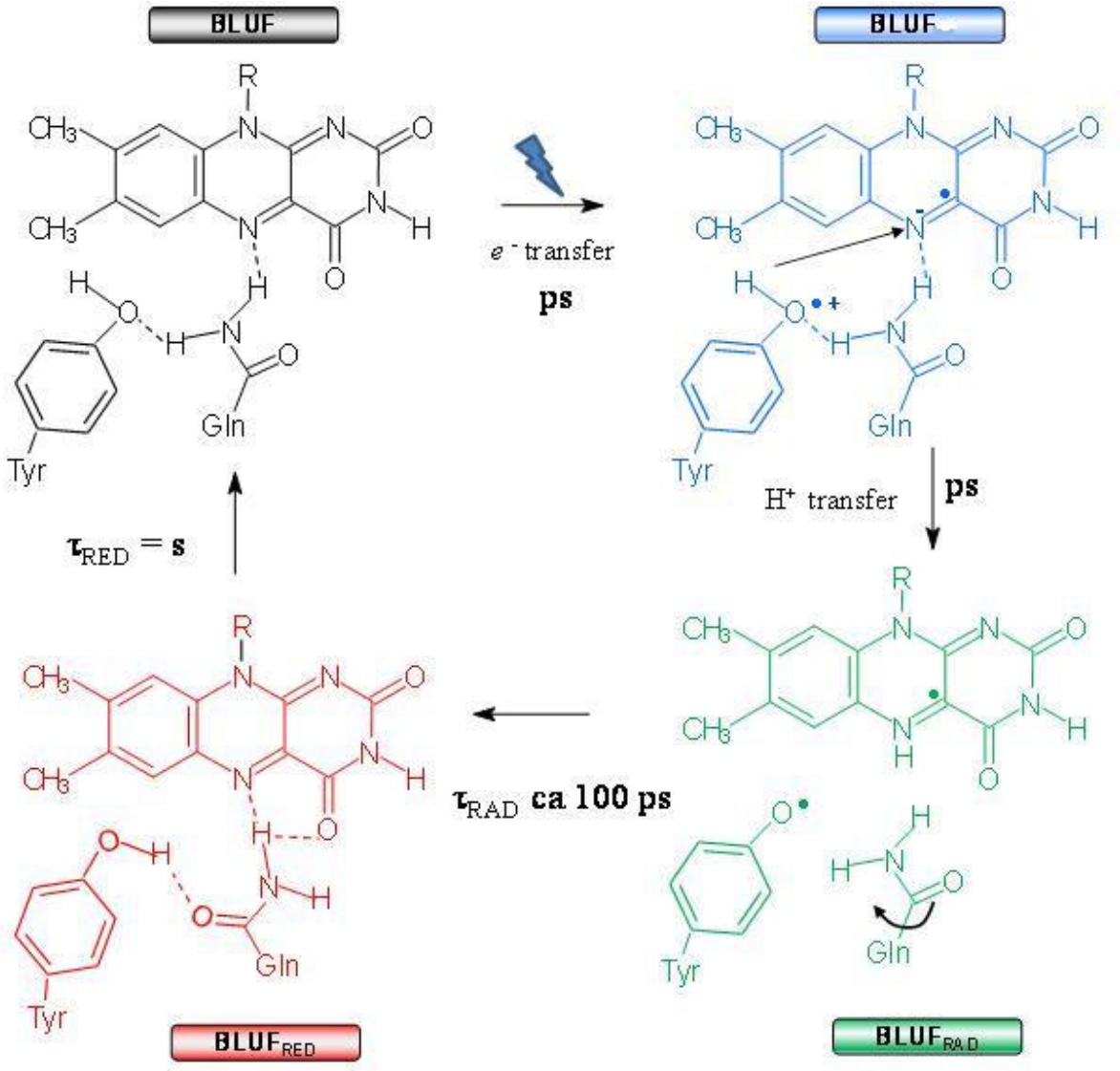

Figure 1.4b. A proposed reaction mechanism for photoinduced hydrogen-bond switching in BLUF domains. Ultrafast sequential electron and proton transfer for a radical pair that recombines promoting a flipping of a glutamine side chain, ultimately resulting in hydrogen bonds rearrangement, without a change in flavin oxidation state. Modified from [20].

Electron transfer could also facilitate glutamine tautomerization, a mechanism that has been put forward based on theoretical calculations to account for discrepancies, in structural studies, regarding the orientation of Gln lateral chain [21]. The first bacterial protein for which a BLUF-type photocycle has been characterized, is AppA from the facultative phototroph *Rhodobacter sphaeroides* (*Rs*AppA) [22].

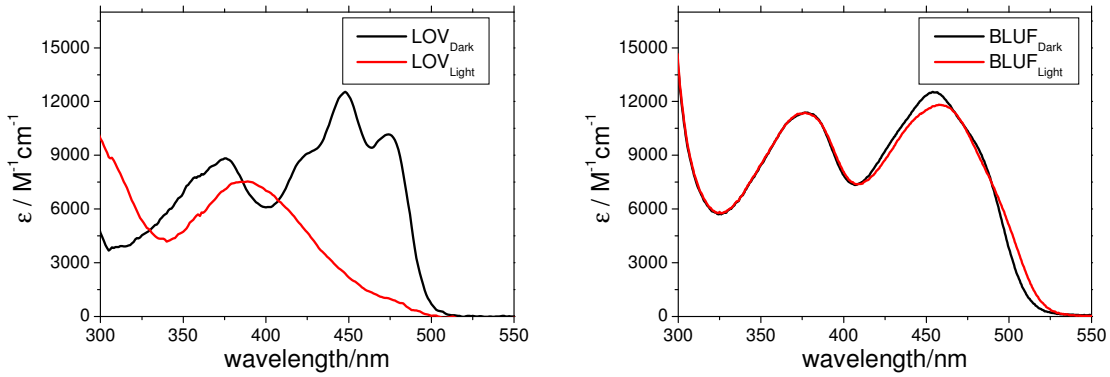

Figure 1. 5. Left, absorption spectra of a LOV domain (here the protein YtvA from *Bacillus subtilis*) in its dark-adapted (black line) and light-activated state (red) [11]; right, the same for a BLUF domain (here the protein YcgF from *Escherichia coli*, Aba Losi unpublished).

LOV and BLUF photocycles require that the flavin chromophore is fully oxidized in the dark-adapted state, raising the possibility that these photoreceptors could be transiently light-insensitive under reducing conditions, that may occur within the cell [23].

Besides the substrate cysteine, the sole residue responsible for photochemistry, a set of super conserved amino acids seem to be necessary to define a functionally active, photochemically competent LOV domain. The same holds for BLUF proteins, for which also super conserved and essential amino acids can be identified [6] These super conserved residues form the basis for sequence search and optimization described in this work.

1.3 Propagating signals: coupling photons to signal transduction

In full length LOV and BLUF proteins, the small and structurally well defined, globular photosensing units (LOV and BLUF domains) are linked to diverse effector domains that determine the functionality of the protein itself; in prokaryotic Fl-Blues typical associated functions are represented by HK (histidine kinases) of the two-component systems, phosphatases of the SPOIIE (Sporulation stage II, protein E C-terminal/Protein phosphatase 2C-related) type, cyclases, and phosphodiesterases for the bacterial second messenger c-di-GMP (cyclic diguanylate) [6], [24],. The photochemical events depicted in subsection 1.2 trigger intradomain and intraprotein signal propagation, via conformational changes that travel from the chromophore cavity to molecular surfaces, ultimately affecting interdomain and/or protein-protein interactions, and regulating the activity of the associated effectors or/and the interplay with regulator domains [25].

The high variability and modularity of LOV and BLUF proteins still allows identification of some common mechanisms for signal propagation and delivery. In LOV domains the extended β-sheet is a true chromophore/ environment interface: on the cavity side it hosts residues directly interacting with the isoalloxazine ring of FMN, affecting chromophore stability, spectroscopic properties and the dynamics of the photocycle [14]; at its external surface side, the β-sheet contacts helical regions flanking the LOV-core or effector domains, or is part of LOV-LOV dimerization interfaces [13]. As an example, it is now generally accepted that a conserved "flipping" glutamine (Q123 in *Bs*YtvA), located on strand Iβ and directly interacting with the chromophore, is important both in signal propagation and for the dynamics of the photocycle [13], [26].

The importance of the LOV-core β-sheet during signal transmission has been first highlighted for plant phototropins (phot). Phot are light-regulated Sr/Thr-kinases bearing two LOV domains in tandem, where BL illumination triggers the unfolding and detachment of the so-called Jα-linker that connects LOV2 to the kinase domain, thus stimulating autophosphorylation of phot [27]. In the dark-adapted state Jα instead is mostly docked on the β-scaffold of LOV2. The light-induced unfolding of Jα presently constitutes the basis for most LOV-based optogenetic applications [4].

An alternative mechanism of signaling has been proposed for *Bs*YtvA that forms dimers stabilized via the LOV domain β-sheet, whereby the Jα-linker is arranged as a coiled-coil in the dimeric structure: signal transmission to a linked effector domain should proceed via a torque mechanism of the coiled Jα-linker [28]. This proposal has received strong support from the published structure of a chimeric protein, SHK YF1, bearing the LOV domain of *Bs*YtvA fused to a heterologous kinase [29].

A third variant of signal transmission in LOV proteins has been described for EL222 from *Erythrobacter litoralis*. EL222 bears a HTH motif, and is able to bind to its target only after being illuminated with BL and having undergone dimerization. In the dark-adapted state, a helix involved in HTH dimerization is sequestered into interactions with the β-sheet surface of the LOV domain, and the latter also competes for the same surface of HTH devoted to DNA-binding [30].

For other LOV proteins, dimerization involving the central β-sheet surface and/or helical caps located N- or C-terminally to the LOV core, are seen as dynamic processes important for signaling, but the relevance of this phenomenon in full-length proteins is unclear [2]. Nevertheless, we can state that, as a whole, the scenario for early signal propagation and transmission steps in LOV proteins, points to a general involvement and variations of a β-sheet/helical cap mechanism on the LOV domain itself.

Signal propagation and transduction mechanisms in BLUF proteins have been recently reviewed [31]. Recent structural information on full length *Rs*AppA [32], combined with previous studies on other BLUF proteins, suggest that the β-sheet (in particular β_5) and helices α_3 and α_4 (C-terminal to β_5 and flanking the BLUF core) are important for signal propagation. This is reminiscent of the β-sheet/helical cap mechanism depicted above for LOV domains. In *Kp*BlrP1, BLUF is associated to an EAL domain with phosphodiesterase activity (hydrolysis of c-di-GMP) [33]. The *Kp*BlrP1-BLUF is monomeric, whereas the full-length protein is dimeric and enzymatically active, regulated via allosteric communication between the two monomers [34]. Full length *Ec*YcgF, structurally similar to *Kp*BlrP1, also exists in a fast and temperature–dependent monomer-dimer equilibrium: light excitation results in transient dimerization of the monomeric species, thought to be important for signaling [35].

An important concept has been aquired in recent times such that light is able to switch-on the LOV and BLUF domains, but a photoactivated photosensing domain does not necessarily correspond to an activated associated functional activity. Today we understand such processes as dynamic shifts in equilibria, e.g., the Jα-linker in the dark-adapted state of phot-LOV2 is "mostly docked" on the β-sheet surface and light activation of LOV2 shifts the equilibrium to "mostly undocked": in other words, these kind of photoreceptors seem to possess also in the dark a constitutive activity of the associated function, i.e., they are intrinsically noisy [20], [36]. This issue is extremely important when LOV and BLUF proteins are exploited as photoswitches in optogenetics.

Molecular downstream partners for bacterial LOV and BLUF proteins are known only for few cases (the reader is referred to recent literature on this subject [2], [20]). In the following paragraph we focus instead on biological roles of prokaryotic LOV and BLUF proteins.

1.4 Photobiological responses mediated by LOV and BLUF proteins

It is not yet possible to delineate a general concept about the physiological roles of LOV and BLUF proteins in bacteria: genome mining and structural/ functional studies in vitro proceed obviously much faster that photophysiological investigations, but some basic ideas are starting to emerge. BL seems to affect, through LOV and BLUF proteins, certain growth and metabolic patterns that imply differential gene expression, with relevance to complex phenomena such as cell adhesion and biofilm formation. A special attention is presently devoted to the role of these photoreceptors in animal and plant pathogens, but also in environmental and symbiotic bacteria. It is also emerging that in many cases Fl-Blues have both light-dependent and light-independent roles (see Figure 1.6 for selected examples and Table 1.1-1.2).

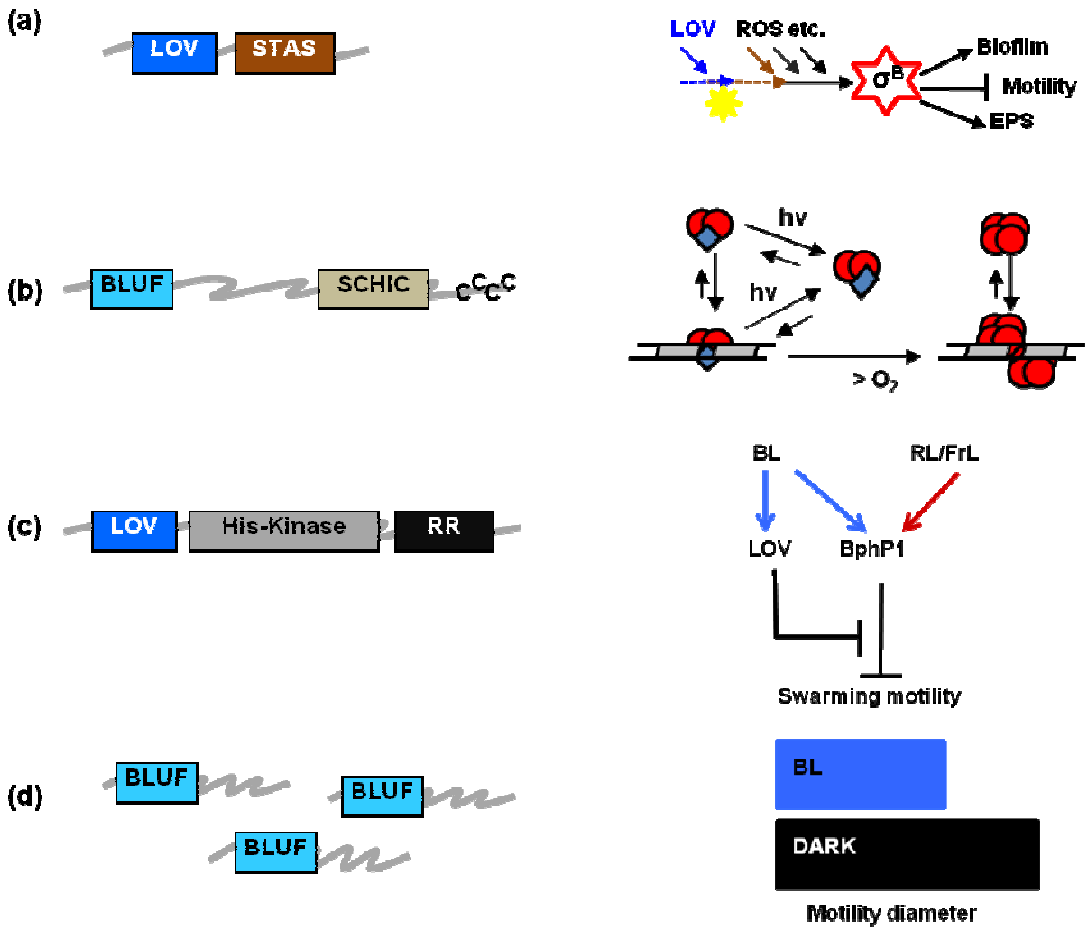

Figure 1.6. Examples of light-regulated in vivo effects for bacterial Fl-Blues, whose architecture is shown on the left: (a) A LOV protein from *Listeria monocytogenes* affects motility and growth patterns by activating the alternative transcription factor σ^B, acting together with other proteins and other signals [59]; (b) AppA from *Rhodobacter sphaeroides* senses BL through its BLUF domain and oxygen through its SCHIC domain; a simplified model for its action is presented on the right hand side (modified from [32]): AppA (blue squares) acts as an antirepressor for photosynthesis gene expression by binding the dimeric repressor PpsR (red circles), a complex that can also associate to DNA; illumination reduces the affinity of AppA-PpsR2 for DNA and an octamer of PpsR can bind to its target sequence, thus switching off gene expression. Increased O_2 concentration favors PpsR8 binding. (c) A LOV-kinase from *Pseudomonas syringae pv syringae* promotes swarming motility by releasing the inhibition mediated by bacteriophytochrome 1 (BphP1) [52]. (d) Three similar BLUF proteins additively regulate the twitching motility of *Acinetobacter baylyi* in a light-dependent pathway [48].

In *Bacillus subtilis* the LOV protein YtvA is a constitutive part of the stressosome, a large molecular hub that integrates environmental stimuli and initiates a signaling cascade, ultimately up-regulating the alternative transcription factor σB (σ^B) [37]. σ^B is one of the key components in the general stress response (GSR) and controls the transcription of 150-200 genes in *B. subtilis* [38]. In transformant cells overexpressing YtvA, GSR is readily induced by BL, but in WT *B. subtilis* the effect is more moderate and BL plays a role as stressor only if associated to an

additional salt stress [39]. Mutagenesis studies *in vivo* have identified residues responsible for light-to-signal transduction [40] and a quantitative model has recently been built, correlating the photocycle dynamics *in vitro* with the efficiency of BL effects *in vivo* [41]. Nevertheless it is clear that YtvA also can exert light-independent effects [42].

The important animal pathogen *Listeria monocytogenes* also bears a YtvA-like photoreceptor, Lmo0799 [43], that up-regulates σ^B in response to BL [44]. Lmo0799 is involved in colony differentiation under alternating dark-light periods [43] and enhanced invasiveness towards enterocytes [44].

Besides *L. monocytogenes* prokaryotic LOV proteins are present in a large number of animal pathogens and they are considered to be involved in infectivity by influencing bacterial lifestyle. The first break-through publication about the physiological role of a bacterial LOV protein in a human pathogen was published in 2007, when Swartz et al. demonstrated that in *Brucella abortus* blue light stimulates infection of host cells through a LOV-HK [45] Other bacteria important for human health for which Fl-Blues have been demonstrated to play a physiological role. are the opportunistic pathogens of the genus *Acinetobacter* [46], [47], [48] and *Escherichia coli* [35] (Table 1.2). BLUF-dependent responses in bacteria appear to be related, in several cases, to the turnover of cyclic nucleotides, important second messengers in prokaryotes [49]. Besides few example of BLUF and LOV domains linked to AMP/GMP cyclase [50], a considerable number of these proteins are predicted to be involved in the turnover of di-c-GMP, a second messenger regulating, among others, the formation of biofilms, motility and virulence [51].

During the last two years investigations have been initiated also on plant pathogens aiming to identify a possible influence of bacterial photoreceptors (often resembling plant counterparts, such as phototropins and phytochromes), on responses related to plant-pathogen interactions, such as motility, adhesion to leaves, infectivity and virulence. As a whole, the results up to now available for LOV proteins in plant pathogens of the genus *Xanthomonas* and *Pseudomonas* indicate that, upon BL activation, they regulate motility and bacterial growth patterns, promote bacterial adhesion to plant leaves and inhibit certain aspects of virulence. The cross-talk with other photosensors is still largely unexplored, but is likely to play an important role both for bacterial lifestyle and virulence [52], [53], [54].

Plant-bacteria interaction are also important for symbiotic relationships: in these cases, Fl-Blues seem to be involved in EPS (extracellular polymeric substances) and biofilm formation, and number of competent (N_2 fixing) root nodules in host plants [55], [56].

Other responses regulated by Fl-Blues in bacteria include positive phototaxis in *Synechocystis* sp. PCC6803, [31] and cell-cell attachment in *Caulobacter crescentus* [57] (see Tables 1 2).

Table 1.1. Known photobiological effects mediated by LOV-proteins in bacteria.

	LOV protein	**Blue light-regulated phenomena**
B. subtilis	*Bs*YtvA	Activation of σ^B stress factor[a] [39], [40], [41], [37].
B. amyloliquefaciens	YtvA-like?	Antifungal lipopeptide synthesis[a] [58].
L. monocytogenes	Lmo0799 (YtvA-like)	σ^B –mediated invasiveness, swimming motility, salt stress[a] [44]; colony differentiation [59].
R. leguminosarum	LOV-HK	Biofilm; EPS[b]; flagella; proliferation within roots; competence for N_2 fixing [56].
C. crescentus	LovK	Cell-cell adhesion [57].[c]
E. litoralis	EL222	Binding to DNA consensus sequences [60].
B. abortus	LOV-HK	Infectivity [45].
X. axonopodis pv. citri	*Xac*LOV	Adhesion; virulence [53].
X. campestris pv. campestris		Growth [61].
P. syringae pv. tomato	*Pst*LOV	Growth; motility (swarming); adhesion; virulence; invasiveness; σ factor gene expression [62], [54].
P. syringae pv. syringae	*Pss*LOV	Motility (swarming)[d] [52].
R. sphaeroides	*Rs*LOV	Genes for photosynthesis and photo-oxidative stress under σ^F control [63][e]

[a]: additionally, red-light effects have been described; [b]: EPS = exopolysaccharides; [c]: co-regulation by cell-redox state; [d]: signaling network with bacteriophytochrome 1 (BphP1) protein; [e]: possible signaling network with AppA

Table 1.2. Known photobiological effects by BLUF-proteins in bacteria.

	BLUF protein	**Blue light-regulated phenomena**
R. sphaeroides	*Rs*AppA	Photosynthesis gene transcription; [22]; integration of light and redox sensing[a] [32], [65], [69].
Synechocystis sp. PCC6803	PixD/Slr1694	Phototaxis [31].
Acinetobacter	BLUF	Surface motility; biofilm [47].
A. baumannii	BLUF	Virulence; surface motility; biofilm[b] [46]
A. baylyi ADP1	BLUF	Surface motility; biofilm[b] [47], [48],.
R. palustris	PapB	Biofilm [55]
E. coli	YcgF	Biofilm[b] [35], [70]

[a]: possible signaling network with CryB [68] and a LOV protein [56]; [b]: co-regulation by temperature.

Finally we refer to *Rhodobacter sphaeroides*, a paradigmatic example of how BL sensing relies on diverse Fl-Blues, interplaying with each other and being connected to other environmental stimuli. *R. sphaeroides* can switch between photosynthesis and aerobic respiration via a complex regulation mechanism that includes the BLUF protein *Rs*AppA. AppA binds the dimeric repressor PpsR constitutively at low oxygen tension, whereas under fully aerobic conditions $PpsR_2$ is released from AppA and binds to the promoter of certain photosynthesis genes, repressing their transcription [64]. These responses are light-independent, but at intermediate oxygen concentration, BL reduces the affinity of AppA for $PpsR_2$ that can now bind to its target DNA sequence [32]. Thus, *Rs*AppA integrates both BL and redox signaling [65]. Redox sensing relies chiefly on the heme binding SCHIC (Sensor Containing Heme Instead of Cobalamin) domain, possibly involving a C-terminal cysteine-rich sequence [66], [67] and the photoactive flavin bound within the BLUF domain [23]. Recently the *Rs*LOV protein has been shown to act synergetically with *Rs*AppA and to down-regulate the expression of genes involved in

photosynthesis and in photo-oxidative stress response under control of the σ^F factor [63]. As a further complication, an interaction between *Rs*AppA and a Cry protein has been demonstrated [68]. Apparently, the activity of these systems in *R. sphaeroides* is aimed to maximize photosynthesis under favorable conditions and to reduce it if the risk of photooxidative damage is high (see Table 1.2).

1.5 Spreading and evolution of Fl-Blues

Despite their physiological role as photosensors in prokaryots is still poorly understood and has been established only for few cases (par. 1.4), the widespread occurrence of FL-Blues offers a unique possibility of exploring the evolution of the light-sensing capability. In fact, the interplay between detrimental and beneficial effects of light and their impact in evolution is most evident in the UVA/Blue range. Potential damage to nucleic acids and photosensitizing effects, mediated by endogenous absorbers, are counteracted by stimulation of growth and photosynthesis [71]. In addition, BL penetrates deepest of all spectral qualities into a water column and constitutes a ubiquitous information source. BL is thus an ambivalent environmental factor: it represents an attracting light quality allowing activation of the photosynthetic apparatus and it is essential for the function of light-activated DNA-repairing enzymes [72]; on the other hand, ubiquitous porphyrins and flavins, the same cofactors that optimize respiration and photosynthesis, are powerful photosensitizers, mainly by forming toxic oxygen species [50].

An extensive phylogenetic analysis on prokaryotic and eukaryotic LOV domains suggested that these protein modules are of bacterial origin and their genes must have undergone frequent horizontal gene transfer, massive gene duplication, and gene loss in prokaryots [73]. Environmental genomics or metagenomics is likely to rapidly change the scenario, with novel proteins discovered, as recently demonstrated with BLUF and LOV proteins [74], [75].

A recent survey showed that ca. 10-12 % of fully sequenced bacteria bear genes for LOV, BLUF proteins or both, and that a similar percentage of LOV proteins occur in Archaea [76]. BLUF proteins are up to now solely found in bacteria and protists, and in most cases these proteins consist of a stand-alone BLUF domain with flanking regions [50]. The same observation holds for metagenomes, for which in this case gene neighborhood analysis is probably the best tool to characterize novel functionalities. Mining in metagenome databases yielded also for the LOV

domains a relatively small number (ca. 230) of open-reading frames with signatures strictly conserved in this BL-photoreceptor domain [74], [77].

Definition of a positive hit for a LOV domain turned out to be relatively difficult, as LOV domains share a great sequential and structural similarity with the ubiquitous PAS domains. In addition, an individual inspection of each marked sequence had to identify those amino acids that are essential for the photochemistry and stabilization of the chromophore in the binding pocket. One of the aim of this work was the optimization of the search algorithms for uncovering new LOV and BLUF proteins as an increasing number of prokaryotic genomes becomes available (see 1.8).

1.6 Advanced biophysical applications: microscopy, nanoscopy and optogenetics

For LOV proteins, the fluorescence of the dark-adapted state, LOV_{447}, allows applications in fluorescence imaging [78]. As fluorescence is lost upon formation of the LOV_{390} adduct, this last process can be annihilated by mutating the reactive cysteine. Such applications are becoming so feasible that a novel name as been introduced for LOV domains employed as fluorescent tools: FMN-binding fluorescent proteins (FbFPs). FbFPs have been originally designed such that the reactive cysteine is mutated into alanine and the system retains permanent fluorescence. This mutation can also increase Φ_F from 0.2-0.3 to ca. 0.4 [79], [80]. Different to Green Fluorescent protein (GFP), the FMN fluorophore is formed also in anaerobic and microaerobic environments, FbFPs are thus ideally suited as fluorescent reporters of bacterial location or gene expression in obligate anaerobes, for example some opportunistic pathogens and facultative anaerobes. FbFPs have also been proposed as fluorescent tools to study fungine colonization of hypoxic niches during infections [78].

A small molecular weight (ca. 10 kDa) FbFP denominated iLOV has been designed for studying the dynamics of viral infections in plants and animal cells. Tagging viruses with GFP-derivatives often results in decreased infectivity and loss of FP through recombination events, due to the limited size of viral genomes and high recombination. The smaller size of iLOV seems to overcome this problem, allowing optimal packing within the genetic material of a virus. iLOV

bears several mutations beyond the Cys-to-Ala outlined above, aimed to enhance fluorescence to a Φ_F = 0.44 and minimize irreversible photobleaching [81]. Other recent applications include real-time monitoring of O_2 levels in *Escherichia coli* cells during batch cultivation [82] and of in vivo gene expression [83].

As seen above, fluorescence is lost upon formation of the adduct LOV_{390}. Since the latter is considered to be the biologically active (signaling) state, it may be stated that fluorescence is ON when the biological photoresponses are OFF, and vice versa, i.e., LOV_{447} and LOV_{390} can be labeled $Fluo_{ON}Bio_{Off}$ and $Fluo_{OFF}Bio_{ON}$, respectively (Figure 1.7).
Interestingly, an early report on the LOV2 domain from the phy3 receptor of *Adiantum* indicated that for this protein the light adapted species can be photoconverted in good yield to the dark adapted, fluorescent state, by shining near UV-violet light on the photoreceptor [16]: in other words LOV domains can be considered photochromic systems. The finding of photoswitching phenomena in LOV domain proteins went largely unnoticed and the potential of this property was almost completely unexplored. The availability of genetically encodable fluorescent reporters with photochromic properties is of fundamental relevance to super-resolution microscopy (nanoscopy) studies, based on the stochastic photoactivation of single molecules, like in FPALM [84] (see par. 1.7.1)
It is also noted that LOV proteins have the potential to function at the same time as optogenetic tools (initiating a biological function, e.g., enzyme activities) and as photoswitchable proteins in superresolution microscopy, given the possibility to establish a photoequilibrium between the LOV_{447} and LOV_{390}. Although this opportunity needs to be demonstrated in living cells, it represents a novel potential application of LOV proteins [12].

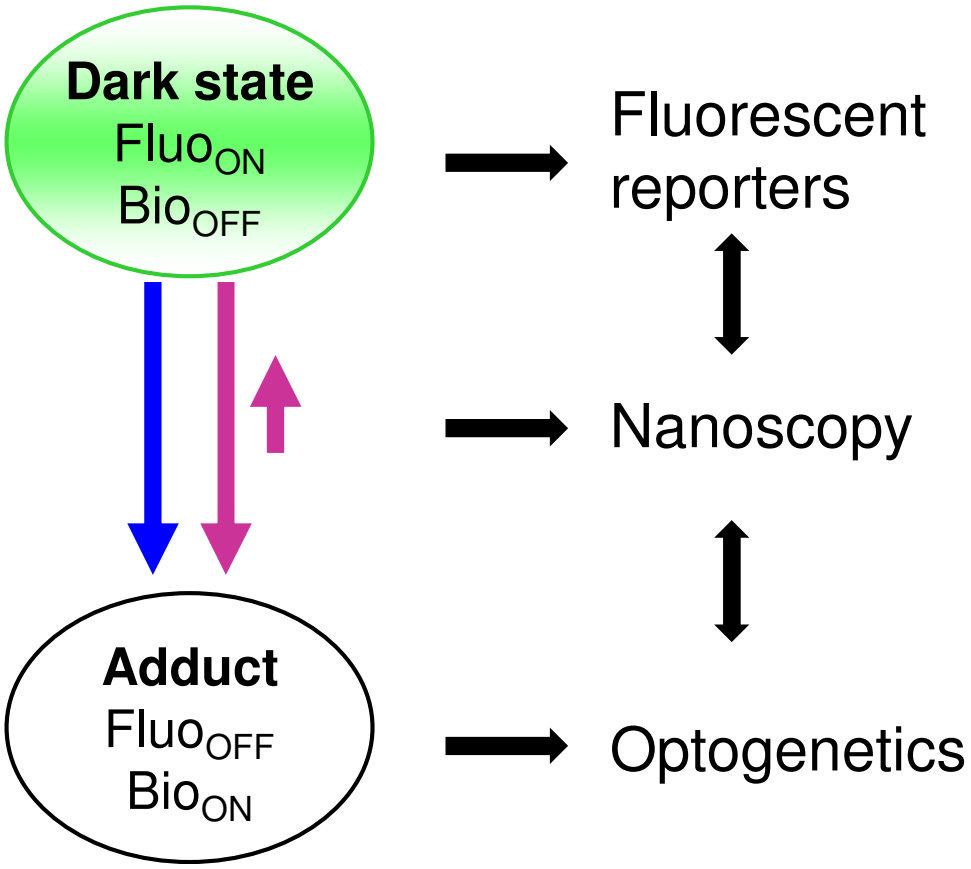

Figure 1.7. LOV domains biotechnology applications. The fluorescence of the dark adapted state can be exploited to engineer reporter genes. Blue-light excitation results in adduct formation, i.e., the signaling state, that may in turn regulate a variety of metabolic processes. This feature is exploited in optogenetics. The adduct is biologically active and non fluorescent (Fluo$_{OFF}$/ Bio$_{ON}$), but the system can be driven into a photoequilibrium by means of violet/UVA light, with a very low yield for recovery of fluorescence. This photoswitching feature has potential application in superresolution fluorescence microscopy (nanoscopy) [12].

1.7 Super resolution fluorescence microscopy

Our knowledge regarding biological processes at the cellular and subcellular level had come from the ability to directly visualize them. Among the various microscopy techniques, fluorescence microscopy is one of the most widely used because of its two principal advantages:

- specific cellular components may be observed through molecule-specific labelling;
- light microscopy allows the observation of structures inside a live sample in real time.

A comparison between different imaging techniques such as electron microscopy (EM) and conventional light microscopy, shows that the latter is limited by relatively low spatial resolution because of the diffraction of light. This diffraction limit, about 200–300 nm in the lateral direction and 500–700 nm in the axial direction, is comparable to or larger than many subcellular structures, i.e. they are too small to be observed in detail and in real time. In recent years, a number of "super-resolution" fluorescence microscopy techniques have been invented to overcome the diffraction barrier, including techniques that employ nonlinear effects to sharpen the point-spread function of the microscope, such as stimulated emission depletion (STED) microscopy [85], [86], related methods using other reversible saturable optically linear fluorescence transitions (RESOLFTs) [87], and saturated structured-illumination microscopy (SSIM) [88], as well as techniques that are based on the localization of individual fluorescent molecules, such as stochastic optical reconstruction microscopy (STORM) [89], photoactivated localization microscopy (PALM) [90], and fluorescence photoactivation localization microscopy (FPALM) [91] (Figure 1.8.). Thank to these methods we could yield an order of magnitude improvement in spatial resolution in all three dimensions over conventional light microscopy. For this, with these techniques it is possible to observe unresolved details of cellular structures and elucidate biological processes at the cellular and molecular scale.

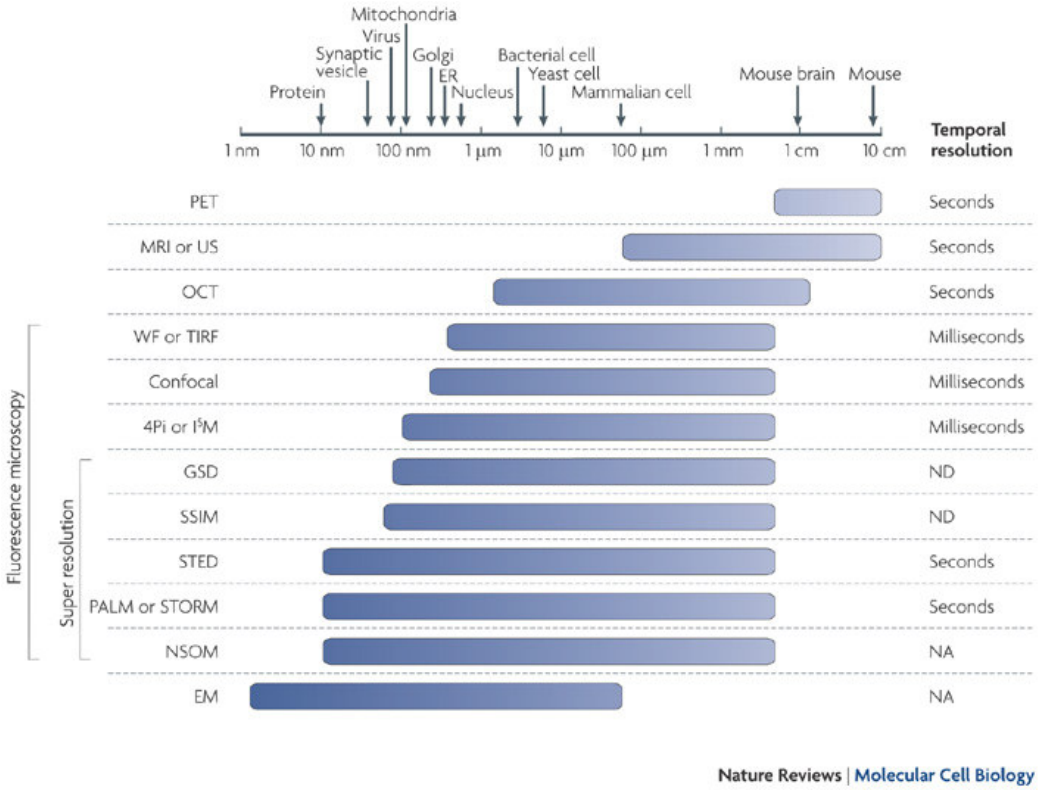

Figure 1. 8: Riassumptive scheme of different optical microscopy with relative spatial and temporal resolution.

In the following paragraph we analyze FPALM technique because we demonstrated that YtvA from *B. subtilis*, object of our studies, was a good probe for this imaging technique [17].

1.7.1 Fluorescence Photoactivation localization microscopy (FPALM)

This technique is based on stochastic activation of photoswitchable-fluorescent molecules localized with nm accuracy and builds a super-resolution image from many image cycles, using low level activation to create sets of well-separated spots from probes [84]. In particular probes used are photo-switchable fluorescent molecules – molecules that can be reversibly switched from non-fluorescent (off-state) to fluorescent (on-state) by stimulation of light with specific wavelengths for different imaging cycles.

To achieve super resolution with stochastic activation it is necessary to have a microscope optics and a detector that must be able to detect very few photons, a fluorescent dyes and/or proteins that enable photoswitching, permitting stochastic activation.

At the end it is important to obtain an analysis of thousands of images and their reconstruction into a super-resolved image [84].

The density of activated molecules in each single image must be kept very low, such that the images (in this case point spread function <PSF>) of individual fluorophores do not overlap, permetting single-particle detection. In each step of this imaging process a small number of molecules are activated, imaged and deactivated. Repeating this cycle creates a sequence of images in which most of the photo-switchable population will appear sequentially distributed over a large number of temporal slices, allowing for individual spot detection and localization.

For PALM, the choice of the right photoswitchable fluorophores is critical because the speed of acquisition and localization accuracy of the techniques depend from them. Desirable fluorescent molecules should be extremely bright, have both a large absorption coefficient (ε) and quantum yield (*QY*) to allow for the detection of the maximum possible amount of photons per molecule (*N*).

Non-overlapping of PSF's molecules and single-molecule super-resolution can be achieved by maintaining a good ratio between the amounts of photons emitted in the fluorescent activated state and the residual photons emitted in the non-activated state. Acquisition speed is dependent on the activation and deactivation rates of the fluorophores.

Analysis and reconstruction are one of the major parts of PALM. Post-acquisition processing infer the characteristics of each molecule present in the large amount of images that constitute the dataset. In a typical experiment 1000–10 000 images are generated in which tens to hundreds of

particles are present in each frame. Although the acquisition by itself takes few minutes, the data analysis can take up to several hours.

1.8 Our approach: novel BL-switched applications and novel investigation tools for Fl-Blues

Fl-Blues are relatively newcomers in photobiology and photobiophysics, but exhibit several points of great interest. These range from their structure and function, to advanced applications, as detailed above. At the very beginning of our research work, it became evident that the LOV protein YtvA from *B. subtilis* is a photochromic system that could find application in FPALM (see par. 3.4 in Results chapter). The study and characterization of this property was performed with several approaches, that required the development of LED-assisted spectroscopy (steady state and time-resolved) to manipulate photochemical events, and data analysis to determine conversion *QY* for the violet-induced light-to-dark (LD) process (see pars. 3.2-3.3). YtvA photochromism also allowed to measure fluorescence lifetimes under photoequilibrium conditions and fluorescence correlation spectroscopy (FCS), thus avoiding artefacts coming from long-lasting measurements under BL (see paragraph 3.1). Photochromism could be studied both *in vitro* and *in vivo*, i.e. in cells overexpressing YtvA, thanks to the usage of an epifluorescence microscope (see paragraph 3.6).
Given that Fl-Blues-based applications require optimization of photophysical and photochemical parameters and of the photocycle dynamics, we characterized with the same techniques a large set of mutated proteins, thanks to a collaboration with the Max Planck Institute for Chemical Energy Conversion that provided the samples (see paragraph 3.5). A further collaboration with the Italian Institute of Technology (IIT), led to the first applications of FPALM to cells expressing YtvA (see paragraph 3.4).

Biophysical applications and photobiology studies, require a continuos update of *in silico* search for novel Fl-Blues, providing both novel light-regulated functions and hints for the biological roles of these increasingly important photoreceptors We thus developed a search pattern that was proven to greatly facilitate and speed up the recovery of LOV and BLUF domains from genome mining (see paragraph 3.7.3). Further analysis led to the building of distance-trees evidencing clustering into phylogenetic and/or functionally related protein groups (see paragraph 3.7.2).

Chapter bibliography

[1] Briggs WR., "Blue/UV-A: historical overview.," in in *Photomorphogenesis in plants and bacteria*, E, Schäfer, F, Nagy, Ed. Dordrecht: Springer, pp. 171–197, 2006.

[2] Losi A.and Gärtner W., "The evolution of flavin-binding photoreceptors: an ancient chromophore serving trendy blue-light sensors.," *Annu. Rev. Plant Biol.*, vol. 63, pp. 49–72, Jan. 2012.

[3] Kritsky M. S., a Telegina T., Vechtomova Y. L., Kolesnikov M. P., a Lyudnikova T., and a Golub O., "Excited flavin and pterin coenzyme molecules in evolution.," *Biochem. Biokhimiicha*, vol. 75, no. 10, pp. 1200–16, Oct. 2010.

[4] Pathak G.P, Vrana J.D.; Tucker C.L, "Optogenetic control of cell function using engineered photoreceptors.," *Biol. Cell*, vol. 105, pp. 59–72, 2013.

[5] Drepper, T.; Gensch, T.; Pohl M., "Advanced in vivo applications of blue light photoreceptors as alternative fluorescent proteins.," *Photochem. Photobiol. Sci.*, vol. 12, pp. 1125–1134, 2013.

[6] Mandalari C., Losi A., Gärtner W., "Distance-tree analysis, distribution and co-presence of bilin- and flavin-binding prokaryotic photoreceptors for visible light," *Photochem. Photobiol. Sci.*, vol. 12, pp. 1144–1157, 2013.

[7] Chaves I., Pokorny R., Byrdin M., Hoang N., Ritz T., Brettel K., Essen L.-O., van der Horst G. T. J., Batschauer A., and Ahmad M., "The cryptochromes: blue light photoreceptors in plants and animals.," *Annu. Rev. Plant Biol.*, vol. 62, pp. 335–64, Jan. 2011.

[8] Geisselbrecht Y., Frühwirth S., Schroeder C., Pierik A. J., Klug G., and Essen L.-O., "CryB from Rhodobacter sphaeroides: a unique class of cryptochromes with new cofactors.," *EMBO Rep.*, vol. 13, no. 3, pp. 223–9, Mar. 2012.

[9] Losi A., "Flavin-based Blue-light Photosensors : A Photobiophysics Update.", *Photochem. Photobiol.*, 83, pp. 1283–1300, 2007.

[10] Bauer C., Rabl C., Heberle J., and Kottke T., "Indication for a Radical Intermediate Preceding the Signaling State in the LOV Domain Photocycle ", *Photochem. Photobiol.*, 87, pp. 548-553 2011.

[11] Losi A., Polverini E., Quest B., and Gartner W., "First Evidence for Phototropin-Related Blue-Light Receptors in Prokaryotes," vol. 82, no. May, pp. 2627–2634, 2002.

[12] Losi A., "LOV proteins photobiophysics.," in in *Encyclopedia of Biophysics*, G.C.K. Rob., Springer-Verlag Berlin Heidelberg, pp. 1312–1316, 2013.

[13] Raffelberg S., Mansurova M., Gärtner W., Losi A., "Modulation of the photocycle of a LOV domain photoreceptor by the hydrogen-bonding network.," *J. Am. Chem. Soc.*, vol. 133, no. 14, pp. 5346–56, Apr. 2011.

[14] Raffelberg S., Gutt A., Gärtner W., Mandalari C., Abbruzzetti S., Viappiani C., Losi A., "The amino acids surrounding the flavin 7a-methyl group determine the UVA spectral features of a LOV protein," *Biol. Chem.*, vol. 394, pp. 1517–1528, 2013.

[15] Rani R., Jentzsch K., Lecher J., Hartmann R., Willbold D., Jaeger K., and Krauss U., "Conservation of Dark Recovery Kinetic Parameters and Structural Features in the Pseudomonadaceae ' Short ' Light, Oxygen, Voltage (LOV) Protein Family: Implications for the Design of LOV-Based Optogenetic Tools,", Biochemistry, 52, pp. 4460-4473, 2013.

[16] Kennis J. T. M., van Stokkum I. H. M., Crosson S., Gauden M., Moffat K.and van Grondelle R., "The LOV2 domain of phototropin: a reversible photochromic switch," *J. Am. Chem. Soc.*, vol. 126, pp. 4512–4513, 2004.

[17] Losi A., Gärtner W., Raffelberg S., Cella Zanacchi F., Bianchini P., Diaspro A., Mandalari C., Abbruzzetti S., and Viappiani C., "A photochromic bacterial photoreceptor with potential for super-resolution microscopy.," *Photochem. Photobiol. Sci.*, vol. 12, no. 2, pp. 231–5, Feb. 2013.

[18] Iwata T., Watanabe A., Iseki M., Watanabe M., and Kandori H., "Strong Donation of the Hydrogen Bond of Tyrosine during.", *J. Phys. Chem. Lett.*, 2, pp. 1015–1019, 2011.

[19] Mathes T., Van Stokkum I. H. M., Bonetti C., Hegemann P., and Kennis J. T. M., "The Hydrogen-Bond Switch Reaction of the Blrb Bluf Domain of Rhodobacter sphaeroides.", *J. Phys. Chem. B*, 115, pp. 7963–7971, 2011.

[20] Kennis J. T. M., Mathes T., "Molecular eyes : proteins that transform light into biological information Molecular eyes : proteins that transform light into biological information," *Interface Focus*, no. August, 2013.

[21] Khrenova M. G., a Nemukhin V, and Domratcheva T., "Photoinduced electron transfer facilitates tautomerization of the conserved signaling glutamine side chain in BLUF protein light sensors.," *J. Phys. Chem. B*, vol. 117, no. 8, pp. 2369–77, Feb. 2013.

[22] Masuda S.and Bauer C. E., "AppA Is a Blue Light Photoreceptor that Antirepresses Photosynthesis Gene Expression in Rhodobacter sphaeroides.", *Cell*, vol. 110, pp. 613–623, 2002.

[23] Arents J. C., Perez M. A., Hendriks J., and Hellingwerf K. J., "On the midpoint potential of the FAD chromophore in a BLUF-domain containing photoreceptor protein," *FEBS Lett.*, vol. 585, no. 1, pp. 167–172, 2011.

[24] Herrou J.and Crosson S., "Function, structure and mechanism of bacterial photosensory LOV proteins," *Nat. Publ. Gr.*, vol. 9, no. 10, pp. 713–723, 2011.

[25] Zoltowski B. D.and Gardner K. H., "Tripping the light fantastic: blue-light photoreceptors as examples of environmentally modulated protein-protein interactions.," *Biochemistry*, vol. 50, no. 1, pp. 4–16, Jan. 2011.

[26] Jones M. A., Feeney K. A., Kelly S. M., and Christie J. M., "Mutational Analysis of Phototropin 1 Provides Insights into the Mechanism Underlying LOV2 Signal Transmission.," *J. Biol. Chem.*, vol. 282, no. 9, pp. 6405–6414, 2007.

[27] Harper S. M., Neil L. C., and Gardner K. H., "Structural basis of a phototropin light switch.," *Science (80-.).*, vol. 301, no. 5639, pp. 1541–4, Sep. 2003.

[28] Möglich A., and Moffat K., "Engineered photoreceptors as novel optogenetic tools.," *Photochem. Photobiol. Sci.*, vol. 9, pp. 1286–1300, 2010.

[29] Diensthuber R. P., Bommer M., Gleichmann T., and Mo A., "Full-Length Structure of a Sensor Histidine Kinase Pinpoints Coaxial Coiled Coils as Signal Transducers and Modulators.", *Structure*, 21, pp. 1127–1136, 2013.

[30] Zoltowski B. D., Motta-mena L. B., and Gardner K. H., "Blue Light-Induced Dimerization of a Bacterial LOV − HTH DNA- Binding Protein.", *Biochemistry*, 52, pp. 6653-6661, 2013.

[31] Masuda S., "Light Detection and Signal Transduction in the BLUF Photoreceptors.", *Plant Cell Physiol.*, vol. 54, no. 2, pp. 171–179, 2013.

[32] Winkler A., Heintz U., Lindner R., Reinstein J., Shoeman R. L., and Schlichting I., "A ternary AppA – PpsR – DNA complex mediates light regulation of photosynthesis-related gene expression," *Nat. Publ. Gr.*, vol. 20, no. 7, pp. 859–867, 2013.

[33] Sondermann H., Shikuma N. J., and Yildiz F. H., "You've come a long way: c-di-GMP signaling," *Curr. Opin. Microbiol.*, vol. 15, no. 2, pp. 140–146, 2012.

[34] Barends T. R. M., Hartmann E., Griese J. J., Beitlich T., Kirienko N. V, Ryjenkov D. A., Reinstein J., Shoeman R. L., Gomelsky M., and Schlichting I., "Structure and mechanism of a bacterial light-regulated cyclic nucleotide phosphodiesterase," *Nature*, vol. 459, no. 7249, pp. 1015–1018, 2009.

[35] Tschowri N., Busse S., and Hengge R., "The BLUF-EAL protein YcgF acts as a direct anti-repressor in a blue-light response of *Escherichia coli*.", *Gene Dev.*, 23, pp. 522–534, 2009.

[36] Strickland D., Yao X.L., Gawlak G.; Rosen M.K.; Gardner K.H., Sosnick, T.R., "Rationally improving LOV domain-based photoswitches.," *Nat. Meth.*, vol. 7, pp. 623–U18, 2010.

[37] Jurk M., Schramm P., and Schmieder P., "The blue-light receptor YtvA from Bacillus subtilis is permanently incorporated into the stressosome independent of the illumination state," *Biochem. Biophys. Res. Commun.*, vol. 432, no. 3, pp. 499–503, 2013.

[38] Akbar S., Gaidenko T. A., Kang C. M., Reilly M. O., Devine K. M., Price C. W., and Kang C. M. I. N., "New Family of Regulators in the Environmental Signaling Pathway Which Activates the General Stress Transcription Factor ς B of Bacillus subtilis New Family of Regulators in the Environmental Signaling Pathway Which Activates the General Stress Transcripti." *J. Bacteriol.*, 183, pp. 1329-1338, 2001.

[39] Avila-Pérez M., Hellingwerf K. J., and Kort R., "Blue light activates the sigmaB-dependent stress response of Bacillus subtilis via YtvA.," *J. Bacteriol.*, vol. 188, no. 17, pp. 6411–4, Sep. 2006.

[40] Avila-Pérez M., Vreede J., Tang Y., Bende O., Losi A., Gärtner W., and Hellingwerf K., "In vivo mutational analysis of YtvA from Bacillus subtilis: mechanism of light activation of the general stress response.," *J. Biol. Chem.*, vol. 284, no. 37, pp. 24958–64, Sep. 2009.

[41] Van Der Steen J. B.and Nakasone Y., "Modeling the functioning of YtvA in the general stress response in Bacillus subtilis." *Mol. Biosyst.*, pp. 2331–2343, 2013.

[42] Gaidenko T. A., Kim T., Weigel A. L., Brody M. S., and Price C. W., "The Blue-Light Receptor YtvA Acts in the Environmental Stress Signaling Pathway of Bacillus subtilis.", *J. Bacteriol.*, vol. 188, no. 17, pp. 6387–6395, 2006.

[43] Chan R. H., Lewis J. W., and Bogomolni R. A., "Photocycle of the LOV-STAS Protein from the Pathogen Listeria monocytogenes." *Photochem. Photobiol.*, 89, pp. 361–369, 2013.

[44] Ondrusch N., "Blue and Red Light Modulates SigB-Dependent Gene Transcription , Swimming Motility and Invasiveness in Listeria monocytogenes," vol. 6, no. 1, 2011.

[45] Swartz T. E., Tseng T.S.; Frederickson M.A., Paris G.; Comerci D.J., Rajashekara G., Kim J.G.; Mudgett M.B.; Splitter G.A, Ugalde R.A., et al., "Blue-Light-Activated Histidine Kinases: Two-Component Sensors in Bacteria.," *Science (80-.).*, vol. 317, pp. 1090–1093, 2007.

[46] Mussi M. A., Gaddy J. A., Cabruja M., Arivett B. A., Viale A. M., Rasia R., and Actis L. A., "The Opportunistic Human Pathogen Acinetobacter baumannii Senses and Responds to Light." *J. Bacteriol*, vol. 192, no. 24, pp. 6336–6345, 2010.

[47] Golic A., Vaneechoutte M., Nemec A., Viale A. M., Actis L. A, and Mussi M. A., "Staring at the cold sun: blue light regulation is distributed within the genus Acinetobacter.," *PLoS One*, vol. 8, no. 1, p. e55059, Jan. 2013.

[48] Bitrian M.; González R.M., Paris G., Hellingwerf K.J., Nudel C.B., "Blue-light-dependent inhibition of twitching motility in Acinetobacter baylyi ADP1: additive involvement of three BLUF-domain-containing proteins.," *Microbiology*, vol. 159, pp. 1828–1841, 2013.

[49] Gomelsky M., "cAMP, c-di-GMP, c-di-AMP and now cGMP: bacteria use them all!," *Mol. Microbiol.*, vol. 79, no. 3, pp. 562–5, Feb. 2011.

[50] Losi A., Gärtner W., "Old Chromophores, New Photoactivation Paradigms, Trendy Applications: Flavins in Blue Light-Sensing Photoreceptors," *Photochem. Photobiol.*, vol. 87, pp. 491–510, 2011.

[51] Römling U.and Amikam D., "Cyclic di-GMP as a second messenger.," *Curr. Opin. Microbiol.*, vol. 9, no. 2, pp. 218–28, Apr. 2006.

[52] Wu L., Mcgrane R. S., Beattie G. A., Wu L., Mcgrane R. S., and Beattie G. A., "Protein Light Regulation of Swarming Motility in Pseudomonas syringae Integrates Signaling Pathways Mediated by a Bacteriophytochrome and a LOV Protein," *MBio*, vol. 4, pp. e00334–13, 2013.

[53] Kraiselburd I., Alet A. I., Tondo M. L., Petrocelli S., Daurelio L. D., Monzón J., a Ruiz O., Losi A., and Orellano E. G., "A LOV protein modulates the physiological attributes of Xanthomonas axonopodis pv. citri relevant for host plant colonization.," *PLoS One*, vol. 7, no. 6, p. e38226, Jan. 2012.

[54] Río-Álvarez, I.; Rodríguez-Herva, J.J.; Martínez, P.M.; González-Melendi, P.; García-Casado, G.; Rodríguez-Palenzuela, P.; López-Solanilla, E., "Light regulates motility, attachment and virulence in the plant pathogen Pseudomonas syringae pv tomato DC3000.," *Environ. Microbiol.*, pp. 10.1111/1462–2920.12240, 2013.

[55] Kanazawa T., Ren S., Maekawa M., Hasegawa K., Arisaka F., Hyodo M., Hayakawa Y., Ohta H., and Masuda S., "Biochemical and Physiological Characterization of a BLUF Protein - EAL Protein Complex Involved in Blue Light-Dependent Degradation of Cyclic Diguanylate in the Purple Bacterium Rhodopseudomonas palustris" *Biochemistry*, pp. 10647–10655, 2010.

[56] Bonomi H. R., Posadas D. M., Paris G., Carrica C., and Frederickson M., "Light regulates attachment , exopolysaccharide production , and nodulation in Rhizobium leguminosarum through a LOV-histidine kinase photoreceptor," *PNAS*, vol. 109, no. 30, pp. 12135–12140, 2012.

[57] Purcell E. B., Siegal-gaskins D., Rawling D. C., Fiebig A., and Crosson S., "A photosensory two-component system regulates bacterial cell attachment." *PNAS*, vol. 104, no. 46, pp. 18241–18246, 2007.

[58] Ramkumar G., Yu S., and Lee Y. H., "Influence of light qualities on antifungal lipopeptide synthesis in Bacillus amyloliquefaciens JBC36.", pp. 243–248, 2013.

[59] Tiensuu T., Andersson C., Rydén P., and Johansson J., "Cycles of light and dark co-ordinate reversible colony differentiation in Listeria monocytogenes," *Mol. Microbiol.*, vol. 87, no. January, pp. 909–924, 2013.

[60] Rivera-cancel G., Motta-mena L. B., and Gardner K. H., "Identi fi cation of Natural and Arti fi cial DNA Substrates for Light- Activated LOV − HTH Transcription Factor EL222.", Biochemistry, 51, pp. 10024-10034, 2012.

[61] Mao D., Tao J., Li C., Luo C., Zheng L., and He C., "Light signalling mediated by Per-ARNT-Sim domain-containing proteins in Xanthomonas campestris pv. campestris.", *FEMS Microbiol. Lett.*, vol. 326, pp. 31–39, 2012.

[62] Moriconi V., Sellaro R., Ayub N., Soto G., Rugnone M.a., Shah R., Pathak P., Gärtner W., Casal J.J., , "LOV-domain photoreceptor, encoded in a genomic island, attenuates the virulence of Pseudomonas syringae in light-exposed Arabidopsis leaves.," *Plant J*, vol. 76, pp. 322–331, 2013.

[63] Metz S., Jager A., and Klug G., "Role of a short light , oxygen , voltage (LOV) domain protein in blue light- and singlet oxygen-dependent gene regulation in Rhodobacter sphaeroides.", *Microbiology*, 158, pp. 368–379, 2012.

[64] Metz S., Jäger A., and Klug G., "In vivo sensitivity of blue-light-dependent signaling mediated by AppA/PpsR or PrrB/PrrA in Rhodobacter sphaeroides.," *J. Bacteriol.*, vol. 191, no. 13, pp. 4473–7, Jul. 2009.

[65] Niederman R. A, "Membrane development in purple photosynthetic bacteria in response to alterations in light intensity and oxygen tension.," *Photosynth. Res.*, vol. 116, no. 2–3, pp. 333–48, Oct. 2013.

[66] Yin L., Dragnea V., Feldman G., Hammad L. A., Karty J. A., Iii E. D., and Bauer E., "Redox and Light Control the Heme-Sensing Activity of AppA.", *mBio*, vol. 4, no. 5, pp. 1–9, 2013.

[67] Domains H. S., Moskvin O. V, and Gomelsky M., "The PpaA / AerR Regulators of Photosynthesis Gene Expression from Anoxygenic Phototrophic Proteobacteria Contain Heme-binding SCHICH domains," *J. Bacteriol*, vol. 192, no. 19, pp. 5253–5256, 2010.

[68] Metz S., Haberzettl K., Fru S., Teich K., Hasewinkel C., and Klug G., "Interaction of two photoreceptors in the regulation of bacterial photosynthesis genes.", *Nucleic. Acids. Res.*, vol. 40, no. 13, pp. 5901–5909, 2012.

[69] Pandey R., Flockerzi D., Hauser M.J.B., Straube R., "An extended model for the repression of photosynthesis genes by the AppA/PpsR system in Rhodobacter sphaeroides.," *FEBS J.*, vol. 279, pp. 3449–3461, 2012.

[70] Tschowri N., Lindenberg S., and Hengge R., "Molecular function and potential evolution of the biofilm-modulating blue light-signalling pathway of *Escherichia coli*.", *Mol. Microbiol.*, vol. 85, no. July, pp. 893–906, 2012.

[71] Hockberger P., "A history of ultraviolet photobiology for humans, animals and microorganisms.," *Photochem. Photobiol.*, vol. 76, pp. 561–79, 2002.

[72] Sancar A., "Photolyase and cryptochrome blue-light photoreceptors.," *Adv. Prot. Chem.*, vol. 69, pp. 73–100, 2004.

[73] Krauss U., Minh B. Q., Losi A., Gärtner W., Eggert T., von Haeseler A., and Jaeger K.-E., "Distribution and phylogeny of light-oxygen-voltage-blue-light-signaling proteins in the three kingdoms of life.," *J. Bacteriol.*, vol. 191, no. 23, pp. 7234–42, Dec. 2009.

[74] Pathak G., Ehrenreich A., Losi A., Streit WR., Gärtner W., "Novel blue light-sensitive proteins from a metagenomic approach.," *Environ. Microbiol.*, vol. 11, pp. 2388–99, 2009.

[75] Singh B. P.A.H, Doerks T, Letunic I, Raes J, "Discovering Functional Novelty in Metagenomes: Examples from Light-Mediated Processes," *J. Bacteriol.*, vol. 191, pp. 32–41, 2009.

[76] Losi A. and Gärtner W., "Bacterial bilin- and flavin-binding photoreceptors.," *Photochem. Photobiol. Sci.*, vol. 7, pp. 1168–1178, 2008.

[77] Pathak G., Losi A.and Gärtner W., "Metagenome-based screening reveals worldwide distribution of LOV-domain proteins.," *Photochem. Photobiol.*, vol. 88, pp. 107–118, 2012.

[78] Losi A., Viappiani C., "Flavin Mononucleotide-binding fluorescent proteins.," in in *Encyclopedia of Biophysics*, G.C.K. Roberts, Ed. Springer-Verlag Berlin Heidelberg, pp. 768–771,2013.

[79] Drepper T., Eggert T., Circolone F., Heck A., Krauss U., Guterl J.-K., Wendorff M., Losi A., Gärtner W., and Jaeger K.-E., "Reporter proteins for in vivo fluorescence without oxygen.," *Nat. Biotechnol.*, vol. 25, no. 4, pp. 443–5, Apr. 2007.

[80] Drepper T., Huber R., Heck A., Circolone F., and Hillmer A., "Flavin Mononucleotide-Based Fluorescent Reporter Proteins Outperform Green Fluorescent Protein-Like Proteins as Quantitative In Vivo Real-Time Reporters." vol. 76, no. 17, pp. 5990–5994, 2010.

[81] Chapman S., Faulkner C., Kaiserli E., Garcia-mata C., Savenkov E. I., Roberts A. G., Oparka K. J., and Christie J. M., "The photoreversible fluorescent protein iLOV outperforms GFP as a reporter of plant virus infection.", *PNAS*, 105, pp. 20038-43, 2008.

[82] Potzkei J., Kunze M., Drepper T., and Gensch T., "Real-time determination of intracellular oxygen in bacteria using a genetically encoded FRET-based biosensor.",

[83] Król J. E., Rogers L. M., Krone S. M., and Top E. M., "Dual Reporter System for In Situ Detection of Plasmid Transfer under Aerobic and Anaerobic Conditions Dual Reporter System for In Situ Detection of Plasmid Transfer under Aerobic and Anaerobic Conditions." 2010.

[84] Patterson G., Davidson M., Manley S., and Lippincott-Schwartz J., "Superresolution Imaging using Single- Molecule Localization.," *Annu. Rev. Phys. Chem.*, vol. 61, pp. 345–367, 2010.

[85] Hell S. W. J., "Breaking the diffraction resolution limit by stimulated-emission: stimulated emission- depletion fluorescence microscopy.," *Opt. Lett.*, vol. 19, pp. 780–782, 1994.

[86] Klar T. A and Hell S. W., "Subdiffraction resolution in far-field fluorescence microscopy.," *Opt. Lett.*, vol. 24, no. 14, pp. 954–6, Jul. 1999.

[87] Hell SW., "Far-field optical nanoscopy.," *Science (80-.).*, vol. 316, pp. 1153–1158, 2007.

[88] Gustafsson M. G. L., "Nonlinear structured-illumination microscopy: wide-field fluorescence imaging with theoretically unlimited resolution.," *Proc. Natl. Acad. Sci. U. S. A.*, vol. 102, no. 37, pp. 13081–6, Sep. 2005.

[89] Rust MJ., Bates M., Zhuang X., "Sub-diffraction-limit imaging by stochastic optical reconstruction microscopy (STORM).," *Nat. Methods*, vol. 3, pp. 793–795, 2006.

[90] Betzig E., Patterson G. H., Sougrat R., Lindwasser O. W., Olenych S., Bonifacino J. S., Davidson M. W., Lippincott-Schwartz J., and Hess H. F., "Imaging intracellular fluorescent proteins at nanometer resolution.," *Science*, vol. 313, no. 5793, pp. 1642–5, Sep. 2006.

[91] Hess S. T., Girirajan T. P. K., and Mason M. D., "Ultra-high resolution imaging by fluorescence photoactivation localization microscopy.," *Biophys. J.*, vol. 91, no. 11, pp. 4258–72, Dec. 2006.

2. Materials and methods

2.1 Mutagenesis, protein expression and purification

The His_6-tagged proteins were provided by the lab of Wolfgang Gärtner, Max-Planck-Institute for Chemical Energy Conversion (MH, GER). Briefly, mutations were induced by site-directed PCR using the QuikChange method (QuikChange II XL, Stratagene), as recently described [1]. Primers for PCR were designed by the "DNA-based" option of PrimerX (Copyright © 2003 by Carlo Lapid). PCR products were treated with the restriction enzyme DpnI (New England BioLabs) that especially digests methylated and hemimethylated parental DNA. Sequencing revealed that all mutations were successfully introduced.

After transformation and expression in *E. coli* BL21 cells (induction by 0.4 mM isopropyl-β-D-thiogalactopyranoside), the His-tagged proteins were purified via affinity chromatography (Ni-IMAC column, 4°C) with gradient elution (10 to 200 mM imidazole); after removal of imidazole, the samples were stored in sodium-phosphate buffer (10 mM NaCl, 10 mM NaPi, pH 8.0) at -20°C. Details of protein expression and purification are given in reffs. [1], [2].

2.2 Steady state and transient spectroscopy

Absorbance spectra were recorded with a Jasco 7850 UV/Vis spectrophotometer. Steady-state fluorescence measurements were carried out with a Perkin-Elmer LS50 luminescence spectrometer.

The fluorescence quantum yield, Φ_F, of the bound flavin for the wild-type protein and the mutated ones was measured at 20°C, using FMN as standard ($\Phi_F = 0.26$) [3].

In laser flash photolysis experiments, photoexcitation was achieved with the third harmonic (355 nm) of a Q-switched Nd:YAG laser (Surelite II-10, Continuum, Santa Clara, CA). The 633 nm line of a He-Ne laser (NEC Corp., 10 mW) was used as probe source for transient absorption signals. The transmitted intensity of the cw beam was monitored by a preamplified (Avtech AV149) avalanche silicon photodiode (Hamamatsu, S2382). A 0.25-m monochromator (H25, Jobin Yvon) was placed before the photodiode in order to remove scattering light from the pump laser. The voltage signal was digitized by a digital sampling oscilloscope (LeCroy 9370, 1GHz, 1GS/s) (Figure 2.1). The sample was changed after each

flash. The data were handled and analyzed using Origin Professional version 8.5 (Microcal Software, Inc., Northampton, MA, USA).

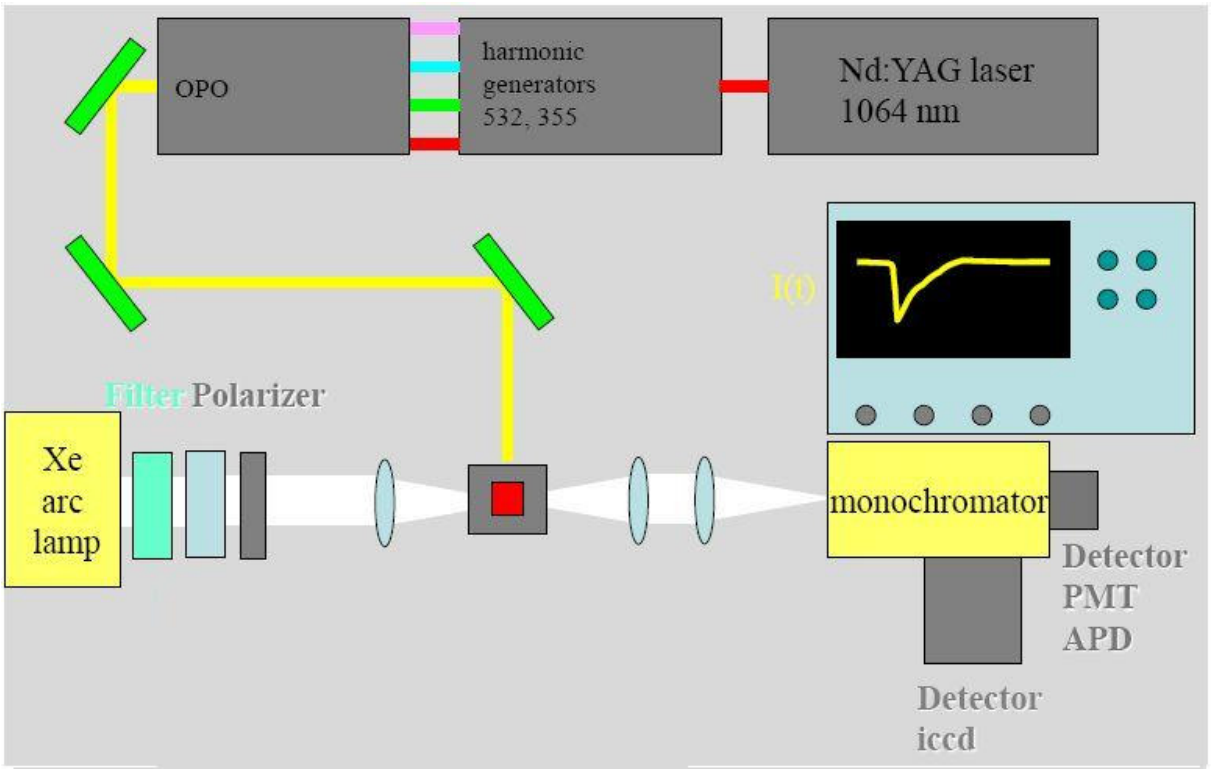

Figure 2. 1. Diagram of a Laser-Flash-Photolysis experiment.

Arrhenius and Eyring plots for the dark recovery reaction of the photoadduct were built by recording the recovery of FMN fluorescence (λ_{ex} = 330 nm, λ_{em} = 500 nm). The kinetics traces were fitted with a mono- or biexponential function, furnishing the recovery lifetime (τ_{rec}) as a function of temperature, in the range of the protein stability (11-25°C). Excitation was at 330 nm, in order to minimize secondary photochemistry leading to the formation of the photoproduct during recording of the traces [1].

Some experiments were performed with the aid of LEDs with emission peaks at 356 nm (LED356), 405 nm (LED405), and 465 (LED465) and FWHM of ~ 25 nm (Roithner Lasertechnik GmbH, Vienna, Austria). LED465 and LED405 were used for complete dark to light conversion and to establish photoequilibrium, respectively. LED356 and LED465 were also employed to determine the quantum yield of adduct formation upon UVA and BL excitation.

The emission curves are reported in Figure 2.2 and calibration curves in Figure 2.3. In photoconversion experiments, the LED emission covered the whole volume of the solution inside the cuvette.

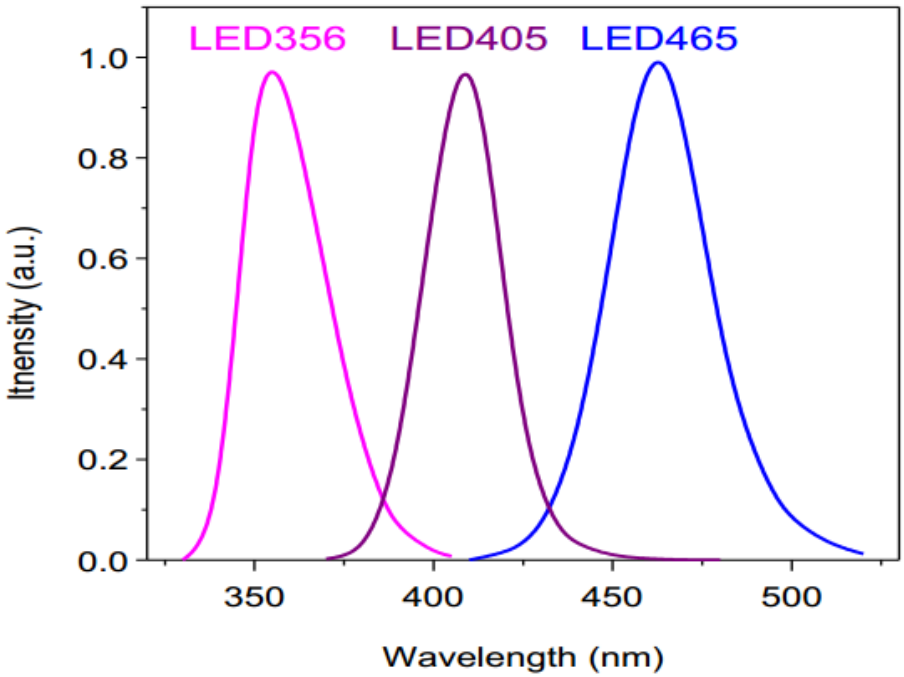

Figure 2.2. Emission spectra of LEDs used in the bulk photoconversion experiments. Magenta, LED356; purple, LED405; blue, LED465.

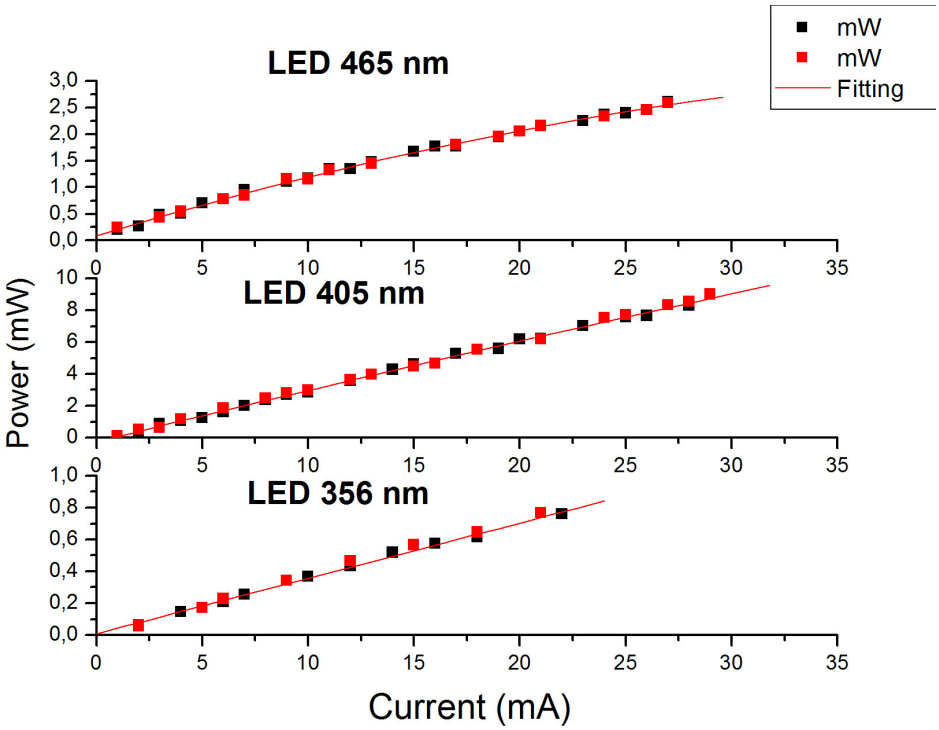

Figure 2.3. Calibration curves of used LED, 472 nm to induce fluorescence off, 405 and 356 nm to monitor photoconversion.

To calculate yield of photoinduced light-to-dark conversion (Φ_{LD}) two methods have been applied:

i. We define *SO(YtvAD)* and *SO(YtvAL)* as the spectral overlaps between the LED emission and the absorption spectra of the specified YtvAL and YtvAD variants. The value of Φ_{LD} can thus be calculated under photostationary conditions (eq. 2.1) , under the assumption that the thermal (dark) relaxation of YtvAL to YtvAD is much slower than the light-induced reactions at high photon density:

$$\Phi_{LD} = \frac{SO(YtvAD)[YtvAD]_{eq}}{SO(YtvAL)[YtvAL]_{eq}} \Phi_{DL} \qquad \text{(eq. 2.1)}$$

where $[YtvAL]_{eq}$ and $[YtvAD]_{eq}$ are the concentrations of the two molecular species under photostationary conditions. These concentrations are determined from the absorption spectrum of the mixture, which can be described as linear combination of the pure YtvAL and YtvAD spectra under LED405 illumination.

ii. Reverse reaction yields were estimated also by following the kinetics of establishment of the photoequilibrium under steady state illumination. In these experiments, we monitored fluorescence emission at 500 nm under 330 nm excitation. Starting from an YtvaL solution,

LED405 was switched on and the recovery of the fluorescence emission was followed. Saturation curves measured at different LED powers were analyzed using numerical solution of the rate equation (eq. 2.2). For details see par. 3.2 in the Results section.

$$\frac{d[YtvAD]}{dt} = \frac{P}{V}\ln 10\left(-A_D\Phi_{DL} + A_L\Phi_{LD}\right) + k_{LD}\left([YtvA_{tot}] - [YtvAD]\right) \quad \text{(eq. 2.2)}$$

where P is the light power, V is the illuminated volume, A_D and A_L are the absorbances at the excitation wavelength (405 nm) of YtvAD and YtvAL, respectively, k_{LD} is the rate constant for the reverse dark reaction and the concentration of YtvAD can be calculated with the knowledge that this is the only fluorescent state of the protein.

2.3 Fluorescence microscopy

Fluorescence lifetimes were measured using a Microtime 200 from Picoquant, based on an inverted confocal microscope (Olympus IX70) and equipped with two SPADs (single photon avalanche diodes). Switch-off of proteins' dark state was achieved by a 475 nm picosecond diode laser, also used as excitation for fluorescence emission. From lit state, proteins were switched on by a 405 nm picosecond diode laser, which also served as excitation for fluorescence emission. Fluorescence emission was split with a 50/50 splitter between the two detection channels and collected through matched bandpass filters (AHF, SMDEmitter HQ 520/40) (Figure 2.4). The concentration of all proteins was 100 nM. SymPhoTime software (PicoQuant) was used for data handling and analysis. Data accumulation time was 2 minutes for all samples. We fitted experimental curves with a two exponential function in case of violet illumination and with one exponential in BL- illumination.

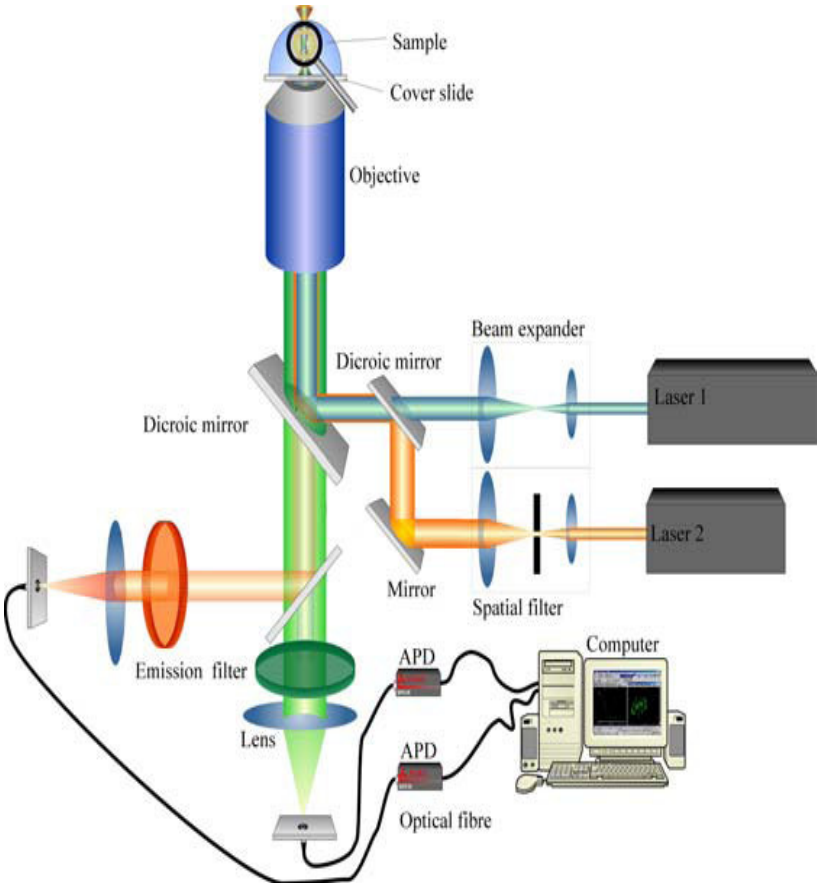

Figure 2.4. Setup of a fluorescence correlation experiment (PicoQuant).

The experimental setup described above allows us to reach a single-molecule condition, in fact the presence of a pinhole in the confocal microscope focuses light in a detection volume of femtolitersr; concentration of samples is in the nM range, so it is possible to follow what happens to a molecule diffusing within the excitation volume. The parameters of primary interest are spontaneous intensity fluctuations caused by the minute deviations of the small system from thermal equilibrium [4]. Any molecular processes that causes alteration in the emission of the chromophore, from diffusion to triplet formation, can be monitored with high precision with FCS and characteristic parameters relative to these processes can be measured (Figure 2.5). It is possible to obtain diffusion constants in aqueous enviroments, pH, viscosity, concentrations and parameters relative to chemical or photophysical reactions.

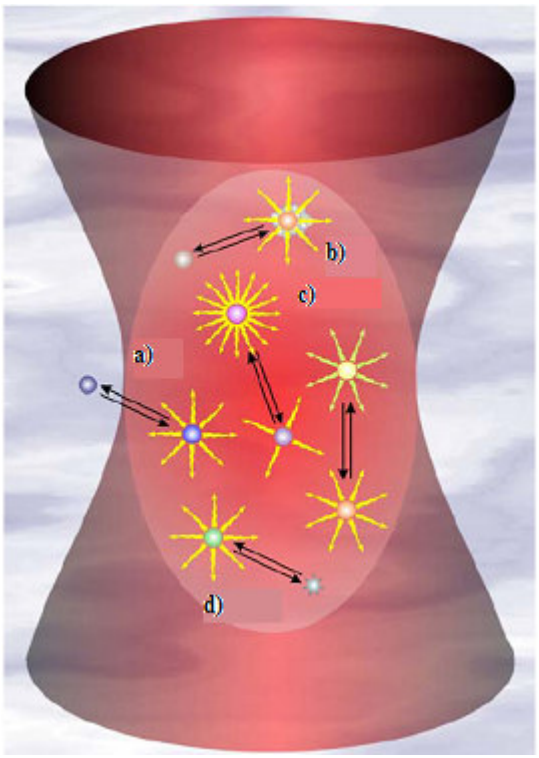

Figure 2.5. Molecular reactions that could cause alteration to fluorescence fluctuations: a) particle movements; b) conformational changes; c) chemical or d) photophysical reactions. Imaged modificated from [4].

Instead the fluorescence emission by *E. coli* colonies over-expressing YtvA was collected through an upright epifluorescence microscope (Nikon Eclipse E600) equipped with a 10X long working distance objective (Plan Fluor10X/0.30 DIC L WD 16.0). A 150 W Xe arc lamp (LOT-Oriel) was used as the excitation source. The white light intensity was modulated with a mechanical chopper (EG&G PARC 192) and entered into the epifluorescence excitation port through a fiber bundle. The filter cube allowed to excite the fluorescence emission by

390 nm light (Thorlabs MF390-18 excitation filter, Thorlabs MD416 Dichroic Filter) and collect fluorescence emission by YtvA through a proper emission filter (Thorlabs MF525-39) (Figure 2.6). The intensity modulated wide field fluorescence emission (collected over a ~ 2 mm diameter area) was detected by a single channel photometer (model 814, PTI). The voltage output was fed into a dual channel lock-in amplifier (EG&G PARC, 5208) which allowed to efficiently reject the noise. The retrieved DC amplitude was recorded on a computer using an acquisition board (National Instruments 6013). Finally, actinic beams at 465 nm (LED465) and 405 nm (LED405) were entered through the bottom port of the microscope. Maximum available power on the focal plane of LED465 and LED405 were 84 µW and 8 µW, respectively.

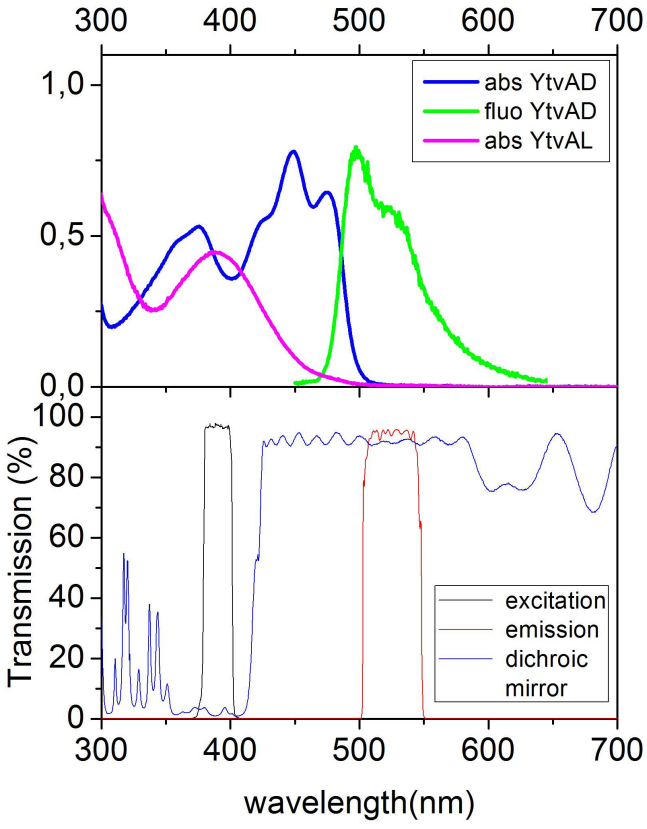

Figure 2.6. Absorption spectra of YtvA dark state (blue) and YtvA light state (pink), emission spectra of YtvA dark state (green) in the upper panel. In the second panel transmission panel of dichroic mirror (blue) and excitation and emission filter (respectively black and red).

E. coli colonies in the growth medium are transferred from the Petri dish to a glass coverslip and measured immediately after. For studies on *E. coli* colonies soaked in a buffered solution, colonies in the growth medium were transferred to an 8-well plate with volume 500 µl (Lab-

Tek) and then covered with 500 µL of a 10 mM phosphate buffer solution, containing 0.9% NaCl (W/V), pH=7.4. We measured fluorescence lifetimes of *E. coli* colonies using a Microtime 200 from Picoquant, based on an inverted confocal microscope (Olympus IX70) as described previously. We did two kind of experiments: i) we illumined *E. coli* colonies in the growth medium directly taken from Petri dish with BL and violet-laser and we fitted experimental data with two exponential; ii) we added to *E. coli* 50 µl of a 10 mM phosphate buffer solution, containing 0.9% NaCl (W/V), pH=7.4 and we observed possible differences from precedent condition.

2.4 Laser Induced Optoacoustic Spectroscopy (LIOAS)

For the LIOAS experiments, samples were excited using the frequency-tripled pulse of a Nd:YAG laser (SL 456G, 6-ns pulse duration, 355 nm, Spectron Laser System, Rugby, Great Britain). The cuvette holder FLASH 100 (Quantum Northwest, Spokane, WA, USA) was temperature controlled to ± 0.02 °C. The signal was detected by a V103-RM ultrasonic transducer and fed into a 5662 preamplifier (Panametrics Inc., Waltham, MA, USA). The pulse fluence was varied with a neutral density filter and measured with a pyroelectric energy meter (RJP735 head connected to a meter RJ7620 from Laser Precision Corp.). The beam was shaped by a 1 × 12 mm slit, allowing a time resolution of ~60 ns by using deconvolution techniques [5]. The experiments were performed in the linear regime of amplitude versus laser fluence, normally ~20 µJ/pulse (corresponding to 30×10^{-11} Einstein for 355 nm excitation, photon energy 337 kJ/mol). The sample concentration was about 15 µM, giving 1.8×10^{-9} mol in the excitation volume $V_0 = 0.12$ mL. These conditions correspond to a ratio of ca. 0.17 photons per protein molecule. New coccine (FLUKA, Neu-Ulm, Germany) was used as calorimetric reference [6]. The time evolution of the pressure wave was assumed to be a sum of monoexponential functions . The deconvolution analysis yielded the fractional amplitudes (φ_i) and the lifetimes (τ_i) of the transients (Sound Analysis 3000, Quantum Northwest Inc., Spokane, WA). The time window was between 20 ns and 5 µs.

LED465 was placed on top of the cuvette in order to keep the sample in the YtvAL state, averaging then 100 shots. For detecting photoacoustic signals originating from YtvAD, we averaged 10 shots, stirring the sample to avoid appreciable accumulation of YtvAL. At the end of the experiments less than 5% of YtvAD was photoconverted, as proven by recording absorption spectra.

2.5 Fluorescence PhotoActivation Localization Microscopy (FPALM)

FPALM measurements were carried out in the lab of Alberto Diaspro, at the Istituto Italiano di Tecnologia (IIT, Genova). FPALM imaging was performed on an inverted fluorescence microscope (NIKON TiE/B). An activation laser (Coherent CUBE 405-100mW) and a readout laser (Coherent Sapphire OPSL 488nm or Coherent Sapphire OPSL 561nm-200mW) lasers are coupled into a collinear path by a dichroic filter (Chroma Tech. Z488RDC). Imaging is performed using a 100x 1.4 NA Nikon objective lens on a back-illuminated electron-multiplying charge-coupled device (CCD) camera (Andor Ixon DU–897E–CS0BV) running at approximately 25 Hz (45 ms exposure time). Dichroic mirrors (Chroma, T505LP) and band-pass dichroic filters allowed selection of the emitted signal (Semrock BLP01-488R-25). Analysis of localized molecules position and rendering of PALM images are performed using MATLAB (The Mathworks). The molecules position is found by means of a gaussian fitting procedure and the localization precision is calculated according to Mortensen et al. 2010. Such a model provides an estimation of the localization precision taking into account also for the excess noise introduced by electron multiplying process of the EMCCD. Before the identification of single molecule events, a roll-ball background subtraction is performed to minimize the effects due to unspecific signal and autofluorescence. The rendering of the super-resolution image is obtained plotting the position of each single event as a gaussian spot with standard deviation corresponding to the calculated localization precision. Before the rendering of the final image, a filter on brightness and molecule dimension is applied and unsuitable events are rejected. E. coli cells were placed on a sterilized and Poly-L-Lysine-coated glass slide. The bacteria were immobilized using 1% agarose gel as mounting medium.

2.6 *In silico* analysis

In a first approach [7], prokaryotic LOV and BLUF proteins were searched by using the BLAST [8] network service at the Swiss Institute of Bioinformatics (SIB) over all annotated prokaryotic genome sequences (completed or in progress), within the UniProt Knowledgebase (Swiss-Prot + TrEMBL) [9] databank using 1 as threshold. As seed sequences we used, respectively: **1)** the LOV core of *B. subtilis* YtvA (accession number O34627) [10] the recovered sequences were further visually inspected for the presence of the substrate Cys62 and of 10 super conserved residues found in LOV domains of demonstrated photochemistry; **2)** the BLUF domain of tll0078 (*Te*PixJ) from *Thermosynechococcus elongatus* strain BP-1 (accession number Q8DMN3); the recovered sequences were further visually inspected for the presence of residues corresponding to Tyr8 and Gln50, responsible for the photocycle [11].

An improved search algorithm has implied the building of a sequence logo (see Figure 3.33 in 3.7.3 paragraph of Results section) and the development of a sequence pattern. To build the sequence logos, prokaryotic and eukaryotic candidates for LOV and BLUF domains were searched by using the BLAST network service at the National Center for Biotechnology Information (NCBI), using the same seed sequences described above. From the recovered sequences a sequence logo was built for the two domains, employing 2000 sequences in each cases and removing those without aligned functional aminoacids, by using WebLogo [12] and Shannon's entropy to quantify the uncertainty of positions [13]. From Logo we defined two patterns in Prosite language [14], in order to obtain a signature that may facilitate the BLAST search. The two patterns, that were then used to search for prokaryotic LOV and BLUF domains are:

[NS]-x(2)-[FPGHSA]-x(4)-[GEQR]-x(9,11)-C for LOV domains;
Y-x(21,27)-[NG]-x(8,9)-[LMVIFTK]-x(6,14)-[FALIYCV]-x(1)-Q for BLUF domains,

where x is any amino acid. With these pattern we performed a search for LOV and BLUF domains over all annotated prokaryotic genome sequences (completed or in progress), within the non-redundant protein sequence database and the SwissProt/UniProt Knowledgebase, at the time point of October 31 of 2013 and using 10 as threshold for the PHI-BLAST algorithm.

Alignment of the recovered sequences was performed with ClustalX using BLOSUM62 as a protein weight matrix without negative values and 10 as gap opening penalty 0.1 as gap extension penality both for pairwise alignment and multiple one [15].

Distance-trees were built based on the obtained alignments, employing MEGA5 [16] according to the neighbour-joining model. The resulting tree is unrooted, and does not provide information on a common ancestor for all sequences. Further the paths between internal and external nodes are not related to the evolutionary time, not yielding a temporal resolution, but only revealing information on changes of protein sequences and on their putative functions.

The precise function of YtvA in *B. subtilis* wasn't known so we performed a search in STRING database [17] to look for additional proteins with functional relationship with it. In particular this database found interactions that include direct (physical) and indirect (functional) associations. They are derived from four different sources:

i) analysis of complete genomes in order to find sequence similarity with proteins of known functions;
ii) description of experiments involving query- protein;
iii) co-expression in same or different organisms of genes codifying proteins related functionally;
iv) published articles.

Chapter bibliography

[1] Raffelberg S., Mansurova M., Gärtner W., and Losi A., "Modulation of the photocycle of a LOV domain photoreceptor by the hydrogen-bonding network.," *J. Am. Chem. Soc.*, vol. 133, no. 14, pp. 5346–56, Apr. 2011.

[2] Raffelberg, S., Gutt, A., Gärtner, W., Mandalari, C., Abbruzzetti, S., Viappiani C., Losi, A., "The amino acids surrounding the flavin 7a-methyl group determine the UVA spectral features of a LOV protein," *Biol. Chem.*, vol. 394, pp. 1517–1528, 2013.

[3] van den Berg P., A., W., Widengren, J., Hink, M., A., Rigler, R., Visser, A., G., "Fluorescence correlation spectroscopy of flavins and flavoenzymes: photochemical and photophysical aspects.," *Spectrochim.Acta A*, vol. 57, pp. 2135–2144, 2001.

[4] Haustein E., Schwille P.,"Single-molecule spectroscopic methods.," *Curr. Opin. Struct. Biol.*, vol. 14, pp. 531–540, 2004.

[5] Rudzki, J., E., Goodman, J., L., Peters, K., S., "Simultaneous determination of photoreaction dynamics and energetics using pulsed, time resolved photoacoustic calorimetry.," *J.Am.Chem.Soc.*, vol. 107, pp. 7849–7854, 1985.

[6] Abbruzzetti, S., Viappiani, C., Murgida, D., H., Erra-Balsells, R., Bilmes, G., M., "Non-toxic, water-soluble photocalorimetric reference compounds for UV and visible excitation.," *Chem Phys.Lett.*, vol. 304, pp. 167–172, 1999.

[7] Mandalari C., Losi A., Gärtner W., "Distance-tree analysis, distribution and co-presence of bilin- and flavin-binding prokaryotic photoreceptors for visible light," *Photochem. Photobiol. Sci.*, vol. 12, pp. 1144–1157, 2013.

[8] Altschul S. F., Madden T. L., Schäffer A. A., Zhang J., Zhang Z., Miller W., and. Lipman D. J, "Gapped BLAST and PSI-BLAST : a new generation of protein database search programs," vol. 25, no. 17, pp. 3389–3402, 1997.

[9] O. Donovan C.,. Martin M. J, Gattiker A., Gasteiger E., Bairoch A., and Apweiler R., "High-quality protein knowledge resource : SWISS-PROT and TrEMBL," vol. 3, no. 3, pp. 275–284, 2002.

[10] Losi A., Polverini E., Quest B., and Gärtner W., "First Evidence for Phototropin-Related Blue-Light Receptors in Prokaryotes," vol. 82, no. May, pp. 2627–2634, 2002.

[11] Fukushima Y., Okajima K., Shibata Y., Ikeuchi M., and Itoh S., "Primary Intermediate in the Photocycle of a Blue-Light Sensory BLUF," pp. 5149–5158, 2005.

[12] Crooks, G.E.; Hon, G.; Chandonia, J.M.; Brenner, S.E., "WebLogo: A Sequence Logo Generator.," *Genome Res.*, vol. 14, pp. 1188–1190, 2004.

[13] Schneider, T.D. and Stephens, R.M., "Sequence Logos: A New Way to Display Consensus Sequences.," *Nucleic Acids Res.*, vol. 18, pp. 6097–6100, 1990.

[14] Sigrist C. J. A., Cerutti L., Hulo N., Gattiker A., Falquet L., Pagni M., Bairoch A., and Bucher P., "PROSITE : A documented database using patterns and pro fi les as motif descriptors," vol. 3, no. 3, pp. 265–274, 2002.

[15] Thompson, J.D.; Higgins, D.G.; Gibson T. J., "CLUSTAL W: improving the sensitivity of progressive multiple sequence alignment through sequence weighting, position-specific gap penalties and weight matrix choice.," *Nucleic Acids Res.*, vol. 22, pp. 4673–4680, 1994.

[16] Tamura, K.; Peterson, D.; Peterson, N.; Stecher, G.; Nei, M.; Kumar S., "MEGA5: Molecular Evolutionary Genetics Analysis Using Maximum Likelihood, Evolutionary Distance, and Maximum Parsimony Methods.," *Mol. Biol. Evol.*, vol. 28, pp. 2731–2739, 2011.

[17] Franceschini A., Szklarczyk D., Frankild S., Kuhn M., Simonovic M., Roth A., Lin J., Minguez P., Bork P., von Mering C., and Jensen L. J., "STRING v9.1: protein-protein interaction networks, with increased coverage and integration.," *Nucleic Acids Res.*, vol. 41, no. Database issue, pp. D808–15, Jan. 2013.

3. Results

3.1 Fluorescence Correlation Spectroscopy (FCS) and the fluorescence decay parameters

In a first approach we performed Fluorescence Correlation Spectroscopy (FCS) measurements in order to understand if YtvA in solution is a monomer or a dimer and to determine fluorescence lifetimes. One purpose was to determine diffusion coefficients. Initially we analyzed the C62S variant, that does not undergo BL-induced photochemistry. Fluorescence decay curves were best fitted with a two-exponential function (eq. 3.1), giving fluorescence lifetimes τ_1=4.8±0.4 ns and τ_2=2.9±0.4 ns, and the associated amplitudes A_1 and A_2 that appear to vary as a function of protein concentration (Figure 3.1).

$$F = A_1 e^{-\frac{t}{\tau_1}} + A_2 e^{-\frac{t}{\tau_2}} \quad \text{(eq. 3.1)}$$

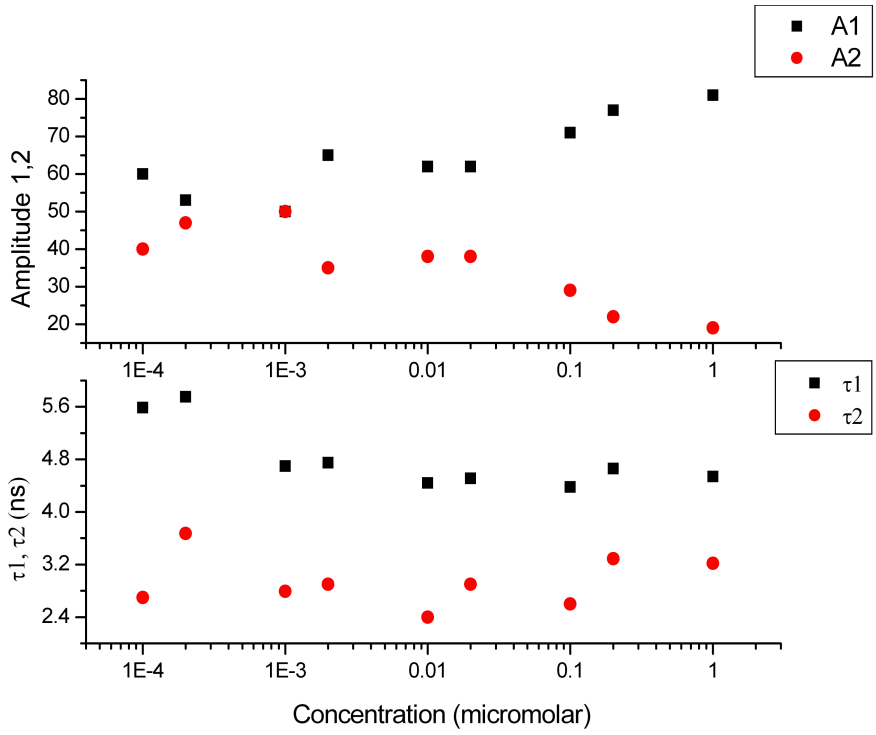

Figure 3. 1. Top, comparison between the amplitudes corresponding to τ_1 and τ_2 (A_1 and A_2), as a function of C62S concentration; bottom, lifetimes as a function of [C62S].

We could see that the longer living component, A_1, increases in percentage with protein concentration, while the shorter living component diminishes. The curves resemble a sigmoid, therefore they could reflect an equilibrium between molecular species or/and an artefact due to secondary photoexcitation for low concentrations and high laser power

From FCS measurements we also noticed that A_1 and A_2 depended on the laser power: in fact we could see that at the lowest BL laser (472 nm) intensity, the longer-living component is larger than A_2, whereas at higher power they are similar (Figure 3.2).

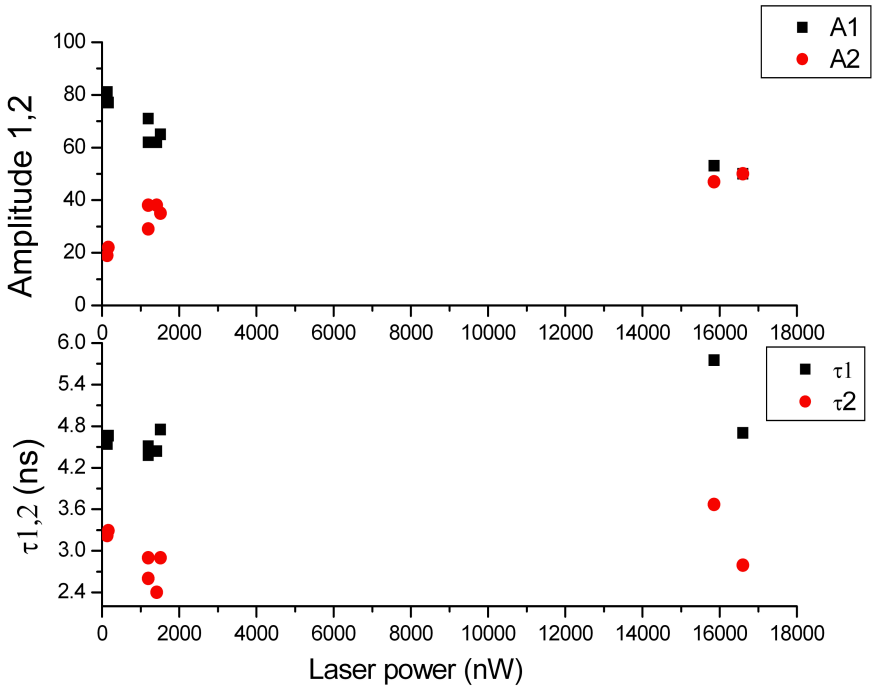

Figure 3.2. Comparison between amplitude of the two transient varying laser power (above) and between time constants (below).

Lifetimes remained constant, τ_1=4.8±0.5 ns and τ_2=2.9±0.4 ns consistent with values recorded at different protein concentrations.

A similar behaviour has been reported for FMN in solution [1] at nanomolar concentration, so we performed the same set of measurements for FMN diluted in buffer and we found a similar laser power dependence at fixed concentrations of 10 nM and 100 nM exciting both with 472 nm ("blue" laser) 405 nm ("violet" laser) (Figure 3.3).

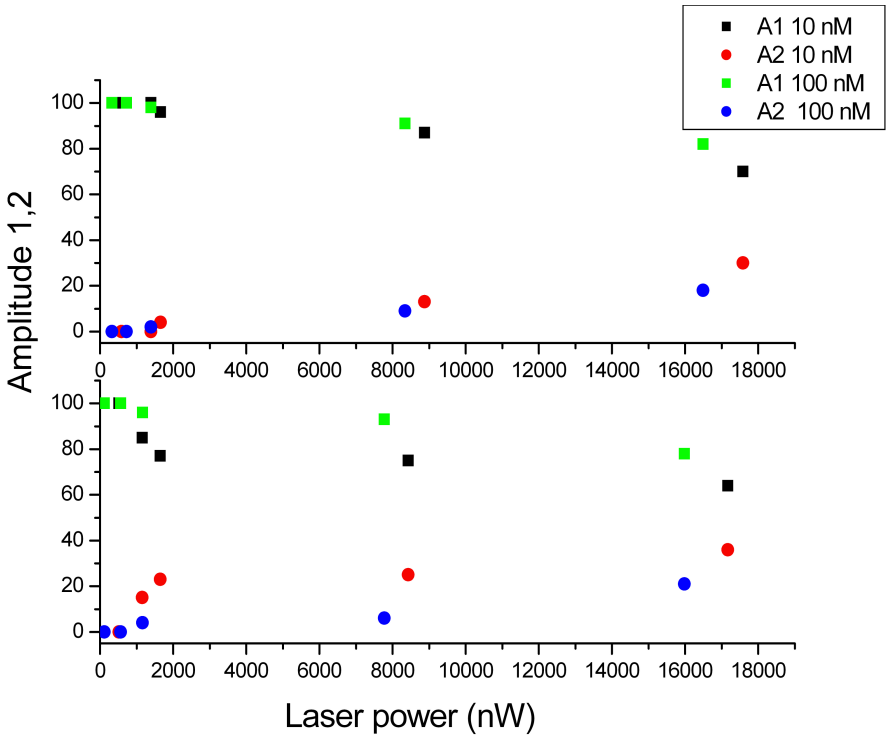

Figure 3.3. Comparison between amplitude of the two transient for blue laser (above) and violet one (below).

At very low laser intensity FMN displayed a fluorescence lifetime equivalent to those found with conventional single photon counting techniques, i.e. a single exponential with τ = 4.27-4.67 ns [2], [3]. Therefore we concluded that the emergence of two fluorescence lifetimes is an intrinsic property of the FMN chromophore at high laser powers/too low concentrations, possibly due to photochemical degradation of the chromophore or secondary photophysics (i.e. excitation of the triplet state), although within the protein the situation can be complicated by the presence of subconformations and by the possible dissociation of FMN in the sub-nanomolar range. Indeed we obtained a single exponential in the case of YtvA-C62S only for low light intensities (0-1000 nW) and high concentration (above 0,1 µM) so we can't obtain single-molecule state, we can't measure autocorrelation function and we can't find diffusion coefficient.

After these preliminary experiments, we analyzed with FCS the fluorescence decay of YtvA-WT, modifiyng the concentrations and the violet laser (405 nm) power in order to identify a suitable working region to avoid multiple excitation artefacts (Figure 3.4).

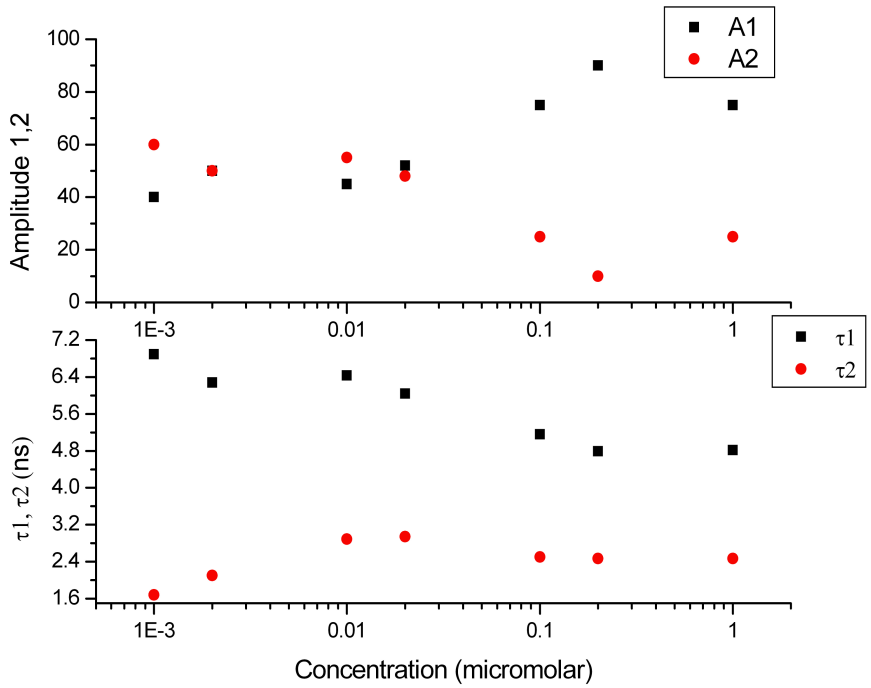

Figure 3.4. Fluorescence decay parameters for YtvA-WT as a function of protein concentration.

In order to determine the fluorescence decay parameters we must work with concentrations around 50-100 nM and a low laser-power (190-1500 nW).

Under these experimental conditions, it was feasible to determine fluorescence lifetimes and associated amplitudes for bound FMN, but it wasn't possible to observe the autocorrelation function and to measure diffusion coefficients because there were present many contributions to fluorescence, it was difficult to discriminate them and we cannot reach single- molecule condition.

Excitation with 472 nm led to a single exponential decay (τ=4.7 ns), possibly revealing a non photoconvertible fraction or free FMN. Violet light excitation (405 nm) induces a photoequilibrium with partial recovery of $YtvA_D$ fluorescence (*vide infra*): under these conditions the fluorescence decay is best fitted with a two-exponential function, giving τ_1=4.6 ns and τ_2=2.1 ns, with A_1 = 33% and A_2 = 67%. τ_2 should thus be the fluorescence lifetime of FMN bound to YtvA-WT in the dark-adapted state. It is not clear whether τ_1 corresponds to free FMN, liberated at the low concentrations used or to a protein fraction that does not form the adduct.

Measurements of fluorescence lifetimes with the confocal microscope-based methodology with violet-light induced photoequilibrium, appears to be more reliable than conventional single photon counting for slow-cycling LOV proteins, in that the conventional method

requires long measuring times and a larger amount of absorbed photons, thus forming considerable amounts of photoadduct and inducing loss of fluorescence intensity.

3.2 From single molecule to steady state spectroscopy: photochromism of YtvA

After BL illumination and accumulation of the photoproduct (light-adapted state YtvAL), it is possible to monitor the thermal recovery to the dark-adapted state (YtvAD) by recording absorption spectra at increasing time intervals (Figure 3.5).

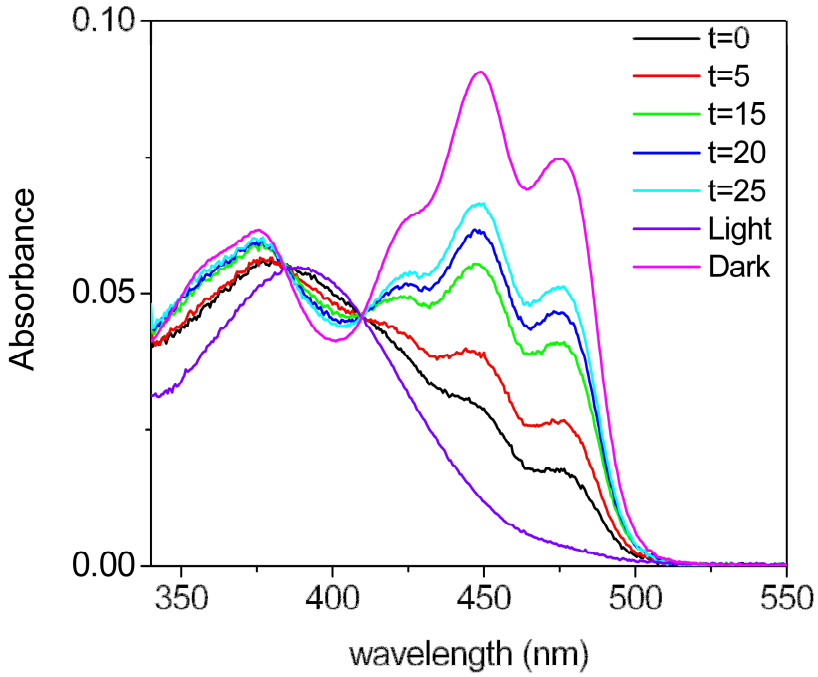

Figure 3. 5. Different absorption spectra for YtvA thermal recovery to the dark-adapted state, at different time interval (expressed in minutes).

In order to check if YtvA is a photochromic system, we tried to induce and monitor YtvAL recovery to YtvAD by illuminating with leds emiting at 356 nm and 405 nm (in the following denominated LED356 and LED405). After few minutes, the system arrived at YtvAL-YtvAD photoequilibrium, where only a small fraction of YtvAD has been recovered (Figure 3.6) as evidenced by the difference spectrum (Figure 3.7).

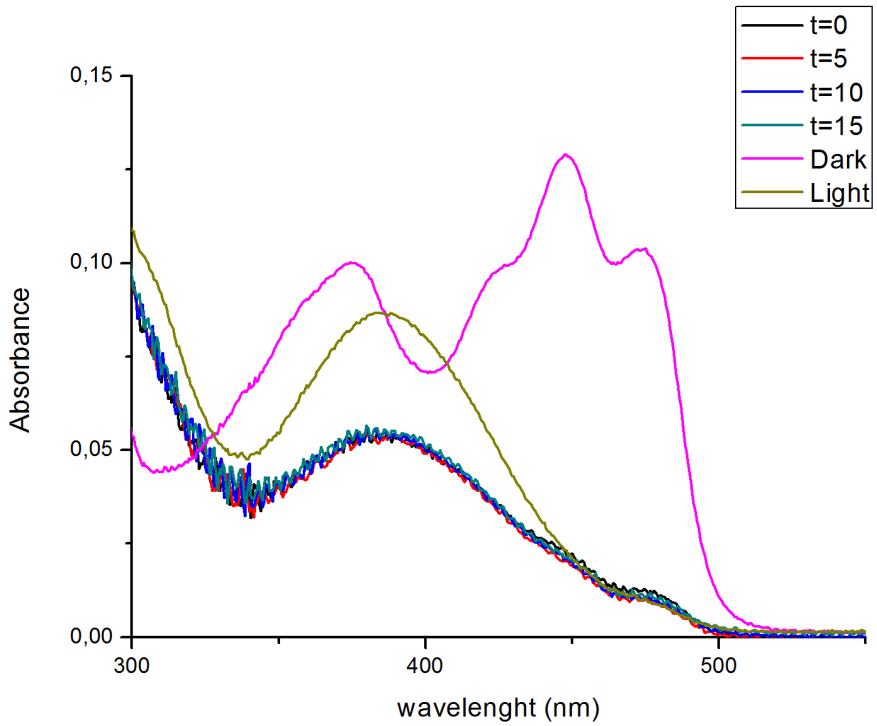

Figure 3. 6. Absorption spectra taken with violet LED405 after t=5 minutes of illumination.

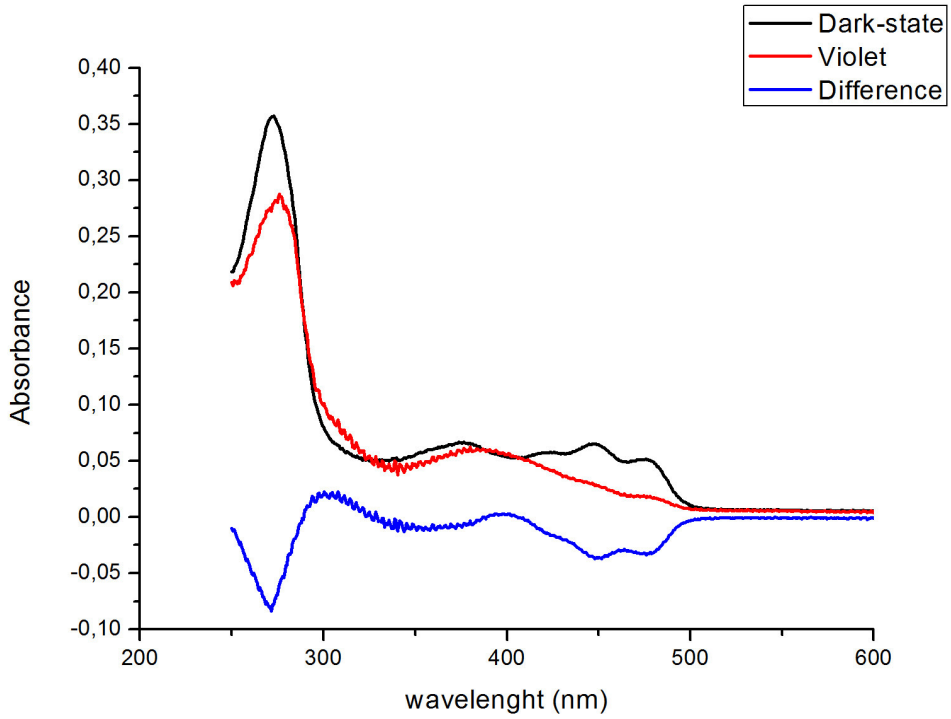

Figure 3.7. Absorption spectra of YtvAD and of the photoequilibrium state reached after LED405 illumination.

The yield of YtvAL-YtvAD photoconversion can be calculated under saturating conditions. The concentrations of both species are readily determined from a simple balance between

rates for forward and reverse photoreactions induced by photons of energy $h\nu$ (h = Planck's constant, ν = photon frequency):

$$YtvAD \underset{h\nu,\ \Phi_{LD},k^{d}_{LD}}{\overset{h\nu,\ \Phi_{DL}}{\rightleftharpoons}} YtvAL \quad \text{(eq. 3.2)}$$

To a first approximation, the back reaction rate of the thermal (dark) relaxation of YtvAL to YtvAD can be neglected in view of its very small value (k^{d}_{LD} ~ 3 × 10−4 s−1 at 20 °C9), compared to light induced reactions at high photon density. Φ_{DL} and Φ_{LD} represent the forward and reverse reaction yields, respectively. Under this approximation, the reverse yield Φ_{LD} can be estimated as:

$$\Phi_{LD} = \frac{SO(YtvAD)}{SO(YtvAL)} \frac{[YtvAD]_{eq}}{[YtvAL]_{eq}} \Phi_{DL} \quad \text{(eq. 3.3)}$$

where *SO(YtvAD)* and *SO(YtvAL)* are defined as the spectral overlaps between the LED emission and the absorption spectra of YtvAL and YtvAD, respectively and are represented as the shaded areas in Figure 3.8. These quantities represent the efficiencies of the molecular species in absorbing incoming photons. $[YtvAL]_{eq}$ and $[YtvAD]_{eq}$ are the concentrations of the two molecular species under photostationary conditions. These concentrations are readily determined from the absorption spectrum of the mixture, which can be described as a linear combination of the pure YtvAL (90%) and YtvAD (10%) spectra under LED356 excitation. Similarly, 9.7% YtvAD and 90.3% YtvAL are obtained under LED405 excitation. Taking into account the forward yields at 465 nm (Φ_{DL} = 0.49) and at 356 nm (Φ_{DL} = 0.3 ± 0.1, from photoacoustic data, see next paragraph), one obtains Φ_{LD} = 0.049 from the photoequilibrium with LED405. A similar value results for the photoequilibrium with LED356, Φ_{LD} = 0.046.

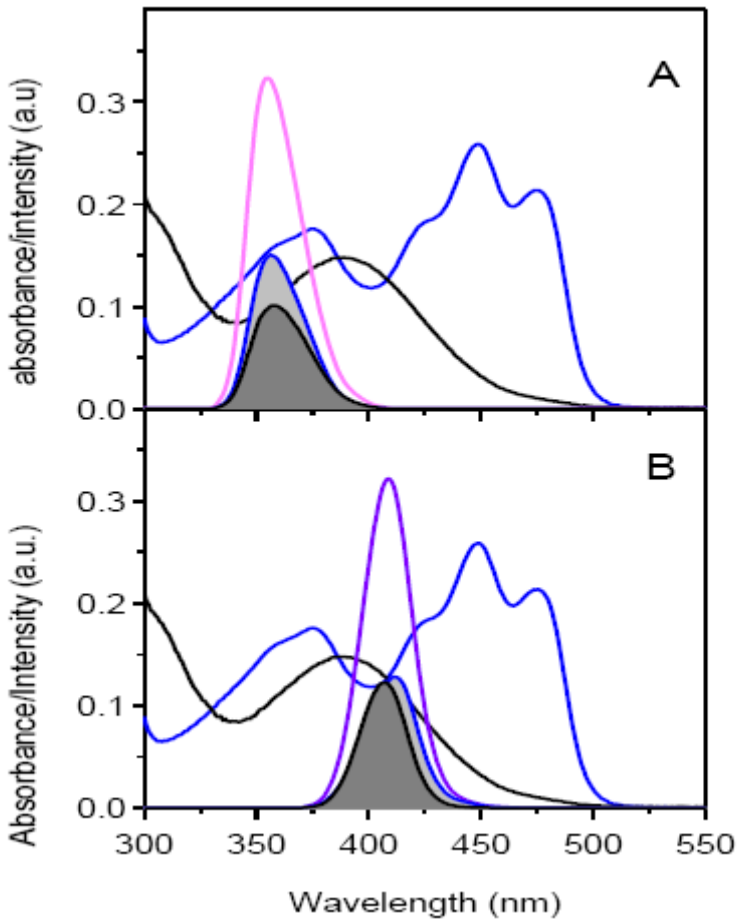

Figure 3.8. Spectral overlap between the absorption spectra of YtvAD (blue), and YtvAL (black) and the 356 nm (A, light pink) and the 405 nm (B, purple) LEDs. The spectral overlaps are represented as shaded areas with the contour coloured as the corresponding absorption spectrum.

The spectra overlaps *SO(YtvAD)* and *SO(YtvAL)*, highlighted as the shaded areas in the plots, can be calculated as the integrals of the products between LED emissions and the corresponding absorption spectra.

The retrieved value for Φ_{LD} is about tenfold lower than the yield for the forward reaction, and is also substantially lower than the figure reported for the LOV2 domain of phototropin [4]. The latter likely arising from an overestimate of the fraction of the dark state which is accumulated at photoequilibrium under near UV excitation. Reverse reaction yields can be estimated also by following the kinetics of establishment of the photoequilibrium, under steady state illumination [5], [6]. After collecting the kinetics at a given LED power, LED465 was applied for 5 minutes to ensure complete recovery of the YtvAL state before submitting the sample to the following illumination cycle with a different power of either LED356 or LED405. When the near UV or violet light is switched on, fluorescence emission is

progressively recovered and, after some time, it saturates. The saturating level of fluorescence emission decreases as the LED power is increased, due to competition with the thermal relaxation of YtvAL to YtvAD. At high LED power the saturating level is independent of the LED power. The rate at which the saturating level is attained increases with the LED power. The above facts are consistent with bidirectional photoswitching between YtvAL and YtvAD induced by LED405 (LED356).

The kinetic model adopted to describe the establishment of the photoequilibrium is detailed below [5], [6].

The concentrations of YtvAD and YtvAL are indicated as D = [*YtvAD*], L = [*YtvAL*], *YtvAtot* is a constant equal to [*YtvAD*]+[*YtvAL*].

The rate of change in D and L can be expressed as:

$$\begin{cases} \dfrac{dD}{dt} = \dfrac{S\Phi}{V}\left(-\dfrac{A_D}{A_D + A_L}\Phi_{DL} + \dfrac{A_L}{A_D + A_L}\Phi_{LD} \right) + k_{LD}^{d} L \\ \dfrac{dL}{dt} = \dfrac{S\Phi}{V}\left(\dfrac{A_D}{A_D + A_L}\Phi_{DL} - \dfrac{A_L}{A_D + A_L}\Phi_{LD} \right) - k_{LD}^{d} L \end{cases} \quad \text{(eq. 3.4)}$$

where Φ is the flux of incoming photons, V is the illuminated volume, A_D and A_L are the absorbances at the excitation wavelength (405 nm or 360 nm) of YtvAD and YtvAL, respectively, $k^{LD}{}_{d}$ is the rate constant for the reverse dark reaction.

Since the following relations hold:

$$\frac{dL}{dt} = -\frac{dD}{dt} \quad \text{(eq. 3.5a)}$$

$$L + D = Ytva_{tot} \Rightarrow L = Ytva_{tot} - D \quad \text{(eq. 3.5b)}$$

we can solve only the rate equation for YtvAD.

Since the fluorescence quantum yields for YtvAD and YtvAL are: $\Phi_{F,D} = 0.22$ $\Phi_{F,L} = 0$. Then the fluorescence emission from a solution containing a mixture of YtvAD and YtvAL only arises from molecules in the YtvAD state.

$$F = F_D = \Phi_{F,D}\left(1 - 10^{-A_D}\right) I_0 \approx \Phi_{F,D}\left(A_D \ln 10\right) I_0 = \Phi_{F,D}\left(\varepsilon_D D l \ln 10\right) I_0 \quad \text{(eq. 3.6)}$$

Fluorescence intensity is fitted using the above expression, where D is obtained by integration of:

$$\frac{dD}{dt} = \frac{S\Phi}{V}\left(-\frac{A_D}{A_D + A_L}\Phi_{DL} + \frac{A_L}{A_D + A_L}\Phi_{LD} \right) + k_{LD}^{d} L \quad \text{(eq. 3.7a)}$$

Which is further simplified by using: *L=Ytvatot-D* and considering that

$$\Phi = \frac{P}{S}\left(1 - 10^{-A}\right) \approx \frac{P}{S} A \ln 10 = \frac{P}{S}\left(A_D + A_L\right)\ln 10 \quad \text{(eq. 3.7b)}$$

where *P* is the light power, *V* is the illuminated volume, thus the differential equation which accounts for the time course of the concentration of YtvAD becomes:

$$\frac{d[YtvAD]}{dt} = \frac{P}{V}\ln 10\left(-A_D\Phi_{DL} + A_L\Phi_{LD}\right) + k_{LD}\left([YtvA_{tot}] - [YtvAD]\right) \quad \text{(eq. 3.8)}$$

A similar relation holds for the concentration of YtvAL.

Saturation curves measured at different LED powers were globally analyzed and fitted to the solution of the above rate equation by optimizing parameter Φ_{DL}, the other parameters being known quantities. The global fitting of the kinetics recorded at several illumination powers (Figure 3.9, Figure 3.10) afforded Φ_{LD} = 0.06 ± 0.01 (LED356) and Φ_{LD} = 0.05 ± 0.01 (LED405), perfectly consistent with the determination from the photoequilibrium data.

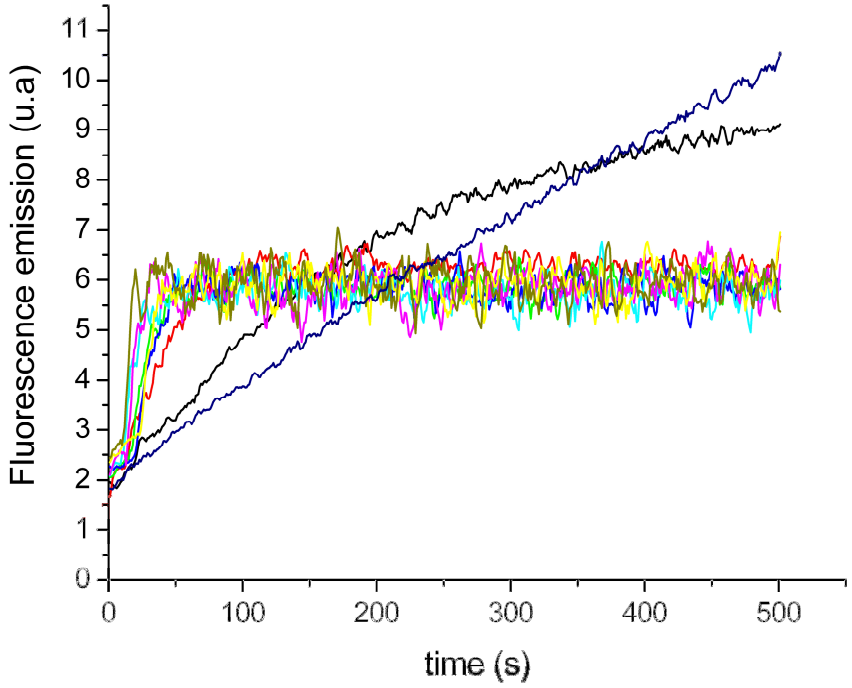

Figure 3. 9. Fluorescence recovery at different powers of **LED405** violet led for YtvA- wild type (blue = thermal recovery, 0 mW; black = 0.15 mW, red = 1.70 mW; green= 3.24 mW; blue= 4.79 mW; cyan= 6.34 mW; magenta= 7.88 mW; yellow= 9.43 mW; olive green= 11 mW). Light-adapted protein solutions were prepared by 5-min irradiation with LED465 (*T* = 20°C, λex = 330 nm, λem = 500 nm).

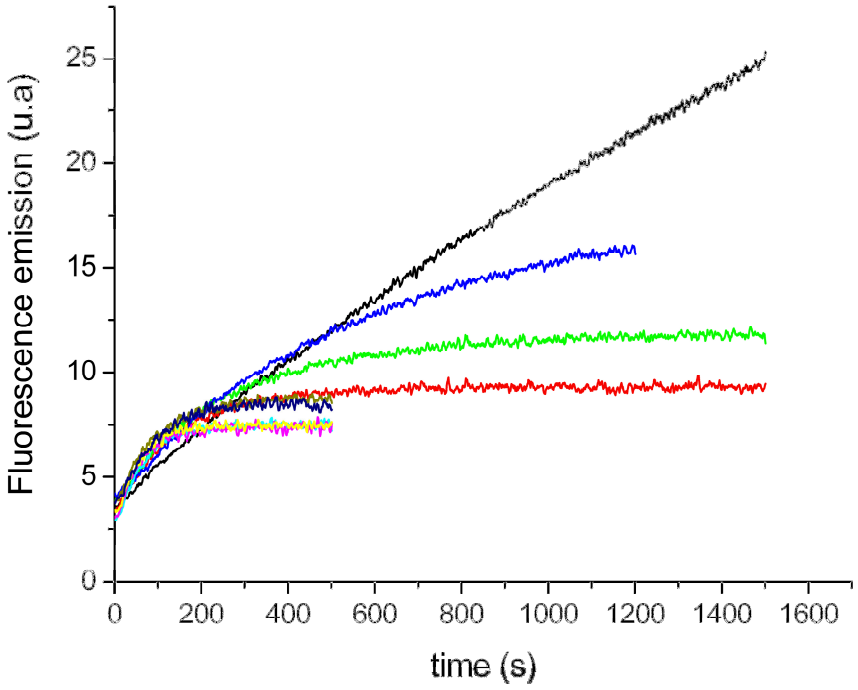

Figure 3.10. Fluorescence recovery at different powers of **LED356** UVA led for YtvA- wild type (black = thermal recovery, 0 mW; blue = 0.08 mW, green= 0.18 mW; red = 0.35 mW; olive green= 0.53 mW; blue= 0.7 mW; cyan= 1.15 mW; yellow= 1.22 mW; magenta= 1.32 mW;). Light-adapted protein solutions were prepared by 5-min irradiation with LED465 (T = 20°C, λex = 330 nm, λem = 500 nm).

The stability in spectral properties of the photoreceptor under steady state illumination is noticeably high, as confirmed by the data reported in Figure 3.11 where YtvA was repeatedly subjected to photoconversion cycles between YtvaD and YtvAL using LED465 and LED405, for about 3000 s. The change in the fluorescence emission (or absorption at 450 nm) after reactivation was very small indicating that irreversible bleaching was below 5 %.

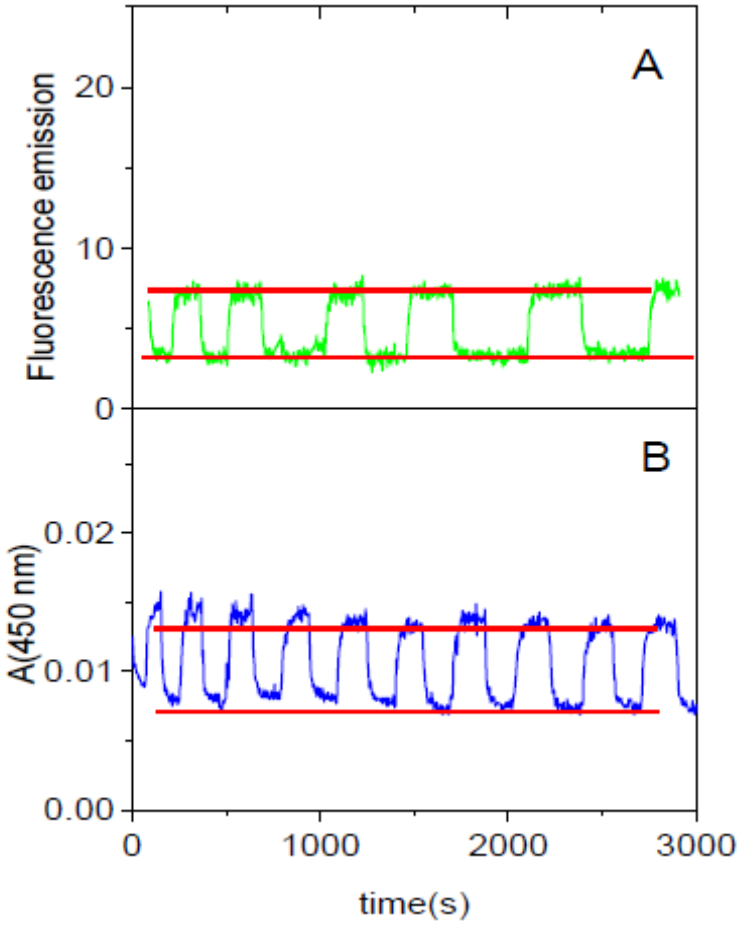

Figure 3.11. Fluorescence emission (A, excitation at 330 nm, detection at 500 nm) and absorbance at 450 nm (B) of an YtvA solution subjected to repeated photo-bleaching/photo-reactivation cycles between YtvAL and YtvAD. YtvAL was generated with LED465 (2.7 mW) while YtvAD was partially regenerated with LED405 (5.4 mW). Red solid lines are drawn to indicate the levels of the signals for the photoequilibrium mixture YtvAD/YtvAL (high fluorescence, high absorbance) and YtvAL (low fluorescence, low absorbance). The fluorescence emission at t =0 represents the signal for YtvAD. The drift in the absorption values is due to instrumental instability and not to bleaching of the chromophore, as indicated by the stability in the changes in absorbance between the D and L states.

3.3 From steady state to time-resolved spectroscopy

UVA/Violet light-induced YtvAL-YtvAD conversion is further confirmed by nanosecond laser flash photolysis. Photoexcitation of YtvAL with 355 nm laser pulses leads to absorbance changes consistent with formation of the YtvAD state, with a kinetics falling below the resolution of the experimental setup, suggesting that this reaction proceeds from the singlet state, as proposed for the LOV2 domain of phototropin [4]. This photochemistry contrasts that of YtvAD which upon BL excitation forms a reactive triplet state within the time resolution of the experimental setup, with 0.6 quantum yield, that decays into the photoadduct on the microsecond time scale (Figure 3.12a) [7]. Additional evidence that 355 nm illumination leads to back conversion to YtvAD is provided by time resolved photoacoustic data. It was shown previously that 475 nm excitation of YtvAD is accompanied by a fast (lifetime below ~20 ns) contraction corresponding to triplet formation, followed by a slower (~1.6 μs) and larger ongoing contraction [8]. The latter was interpreted as the formation of the adduct in YtvAL. A similar pattern of structural volume changes is observed, starting from YtvAD, with 355 nm excitation (blue curve in Figure 3.12b). The L-to-D photoconversion instead leads to a photoacoustic signal (magenta curve in Figure 3.12b) characterized by a fast (lifetime below ~20 ns) and small expansion, $\Delta V_{LD} = 0.55$ ml einstein^{-1}. Taking into account that the molar volume contraction for adduct formation (i.e. for the D-to-L conversion) is $\Delta V_{R,DL} = -6.2$ ml einstein^{-1} Φ_{LD} is readily calculated as the ratio $\Phi_{LD} = \Delta V_{LD}/\Delta V_{DL} = 0.04$, in good agreement with the above estimates.

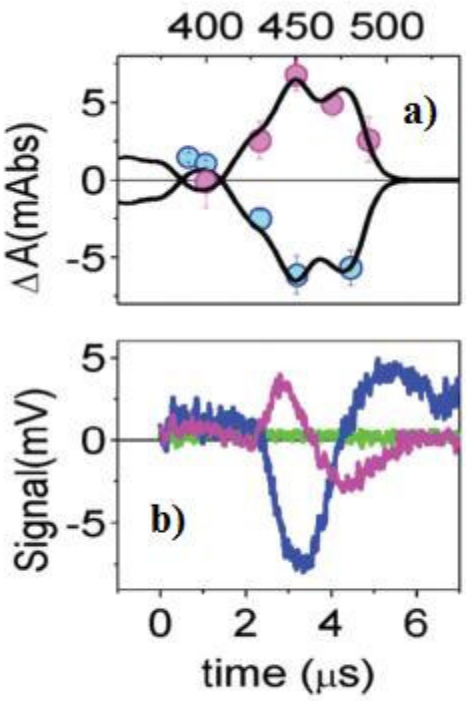

Figure 3.12. (a) Comparison between the absorbance changes measured at t = 7 μs after 475 nm excitation of a YtvAD solution (blue circles) (elaborated from [7]), the absorbance change measured at t =7 μs after excitation at 355 nm of a YtvAL solution (magenta circles), and the steady state absorbance changes between YtvAL and YtvAD (black solid curves). **(b)** Photoacoustic signal measured at T_β=0 = 3.4 °C for the photocalorimetric reference compound (green, new coccine), and after photoexcitation at 355 nm of YtvAD (blue trace) and of YtvAL (magenta).

These measurements in solutions indicate that YtvA is a photochromic protein that can be swiched between a fluorescent (YtvAD) and a non-fluorescent (YtvAL) state, by alternating blue and violet light illumination.

3.4 From the cuvette to a coverslip: super-resolution microscopy

The photoswitching between YtvAD and YtvAL is observed also for molecules deposited on a coverslip, or expressed within *Escherichia coli*. We have exploited this property to perform sub-diffraction localization of individual molecules deposited on a coverslip (Figure 3.13) or in *E. coli* over-expressing wild-type YtvA. Collection and localization of individual fluorescent YtvA molecules is performed by imaging a layer of proteins. The layer was obtained by placing a drop (20 µl) of protein solution (100 nM) on a glass coverslip. Switching between the fluorescent and the dark state is obtained using a low-level 405 nm activation laser and a 488 nm readout laser continuously running. Localization of YtvA molecules could be performed with an average precision of 18 nm.

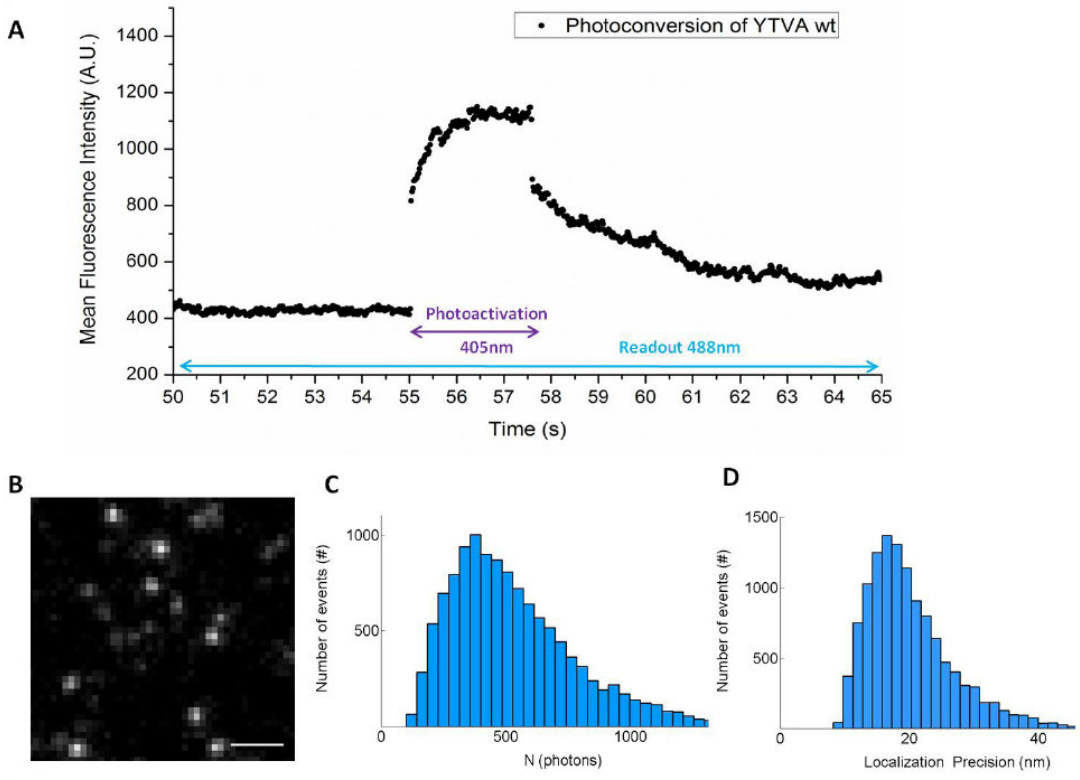

Figure 3.13. Single molecule collection and localization of YtvA. An immobile sample is obtained drying a thin layer of protein on a sterile glass slide and photoactivation experiments are performed using a PALM microscope. Panel A shows the behavior of the mean fluorescence intensity vs time when readout and activation laser are switched on. Single molecule regime has been obtained with a low-level 405 nm activation laser and a 488 nm readout laser continuously running. The activation and excitation laser powers were at 0.35 kW/cm^{-2} and1.7 kW/cm^{-2}, respectively. Fluorescence emission recovery after 405 nm photoactivation can be described by the kinetic model for photoequilibrium and fitting afforded the same photoconversion yield retrieved for bulk samples (data not shown).Panel B shows a representative image of single molecules of YtvA. The number of photons collected for each molecule and the localization precision are reported in panels C and D, respectively. The analysis is performed after the collection and localization of approximately 12,000 events. Images were acquired with a frame rate of 20 frames s^{-1}. Scale bar, 1 µm (B).

Super-resolution experiments are carried out by collecting and analyzing individual fluorescent molecules of YtvA, following the procedure previously reported for Fluorescence PhotoActivation Localization Microscopy (FPALM) [9].

FPALM images of living *E. coli* (Figure 3.14) show the intracellular distribution of YtvA molecules, with an average localization precision (35 nm) (Figure 3.15), similar to the one observed for the molecules deposited on a coverslip. A comparison between the conventional wide-field fluorescence image (Figure 3.14b) and the FPALM image (Figure 3.14c) shows the remarkable resolution improvement and clearly demonstrates the suitability of YtvA for super-resolution applications in cells, thanks to its photochromic properties.

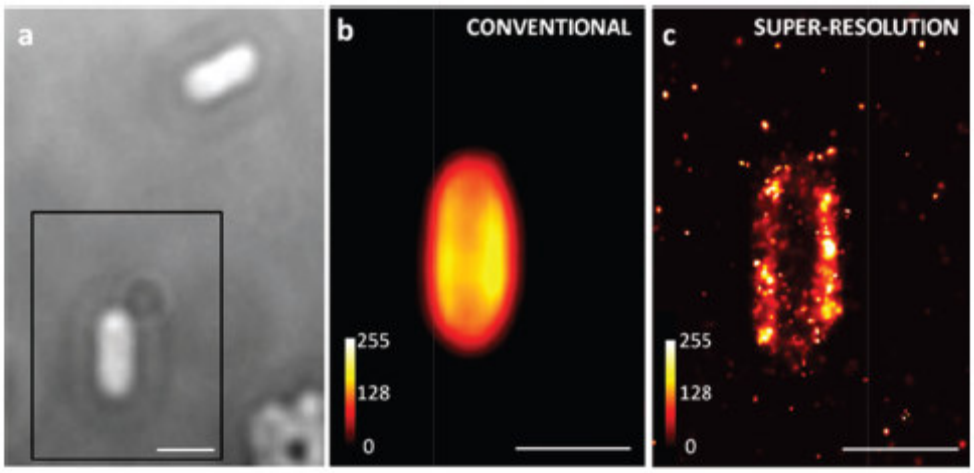

Figure 3.14. Super-resolution imaging of *Escherichia coli* over-expressing wild-type YtvA. Transmitted image **(a),** conventional fluorescence image obtained by adding the total signal from all the frames **(b)** and super-resolution (FPALM) image (c) of a single *E. coli* cell.

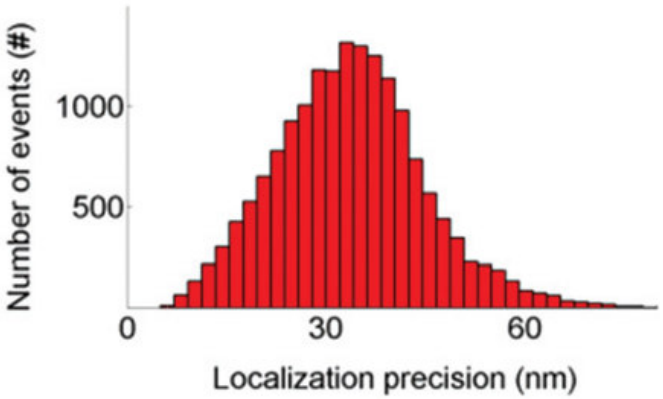

Figure 3.15. Localization precision of photons collected during the FPALM experiments described above.

From these experiments it appears that YtvA preferentially accumulates at the periphery of *E. coli* cells, nearby the membranes or the cells wall. It remains to be established if this is an artefact of the heterologous system of overexpression, that may lead to artifactual accumulation within inclusion bodies.

Also Fluorescence Lifetime Imaging Microscopy (FLIM) images under two-photon excitation (TPE) of living *E. coli* were acquired, showing fluorescent molecules with a lifetime around 2.2 ns (the lifetime observed for bulk YtvAD solutions, see. paragraph 3.1 on FCS) clustering around a few spots (Figure 3.16).

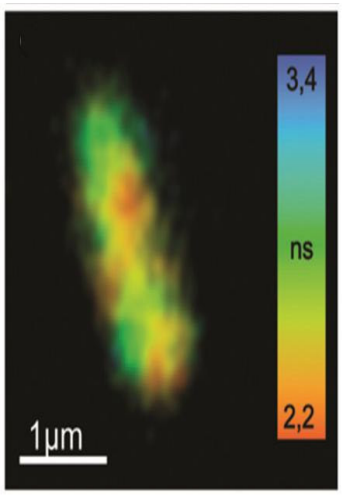

Figure 3.16. FLIM image of an *E. coli* cell.

The spatial distribution is similar to the one observed in some of the FPALM images (Figure 3.14).

3.5 Optimizing parameters for applications: mutagenesis studies

3.5.1 Spectral parameters and fluorescence lifetimes

Following the identification of two amino acids that are potentially UVA-absorbance regulators by sequence alignment of LOV domains (see Figure 3.34 in paragraph 3.7.1), positions 30 (threonine) and 37 (asparagine, YtvA numbering) were mutated. Whereas none of the mutations performed had a significant effect on the lowest energy transition I (λ_{max} = 448/475 nm), remarkable shifts in spectral properties are observed in the UVA range. Interestingly, the most significant changes are caused by T30 substitution with an apolar residue (A, V), whereas negligible effects are observed for mutations of N37 (Figure 3.17, Table 3.1).

Table 3.1: Spectral parameters and fluorescence anisotropy (A).

	[a]Dark state Abs. maxima/nm		[b]F_{max} /nm	[c]τ_F λ_{ex} / nm		[d]$\tau_{F1/2}$ /ns (fraction 1/2)	[e]*A* λ_{ex} /nm	
	UVA	**Blue**		**355**	**450**	**405 nm**	**355**	**450**
FMN_{aq}	372	445/472	526	0.25	0.25	4.7/-- (1/--)	< 0.01	0.01
YtvA-WT	359_s/375	448/475	497	0.16	0.22	4.6 /2.1 (0.33/0.67)	0.25	0.33
N37C	359_s/ 375	448/475	498	0.20	0.22	4.8/2.1 (0.89/0.11)	0.23	0.30
N37F	358_s/ 374	448/475	496	0.20	0.26	4.8/2.7 (0.47/0.53)	0.22	0.30
N37V	359_s/ 375	448/475	496	0.20	0.26	5.1/2.1 (0.73/0.27)	0.23	0.31
T30A	354/ 370	448/475	496	0.22	0.25	4.8/2.1 (0.85/0.15)	0.20	0.30
T30S	358_s/373	448/475	497	0.28	0.27	4.4/2.2 (0.74/0.26)	0.24	0.31
T30V	354/371	448/475	497	0.18	0.18	4.9/2.6 (0.72/0.28)	0.21	0.31
T30V/N37C	354/372	448/475	497	0.17	0.16	5.0/2.2 (0.66/0.34)	0.26	0.32
Q66H	358_s/ 374	448/475	496	0.08	0.11	4.6/1.3 (0.60/0.40)	0.28	0.34
Q66K	358_s/ 374	450/476	499	0.21	0.27	4.6/2.7 (0.75/0.25)	0.22	0.32
R63K	359_s/375	448/475	497	0.20	0.22	4.9/2.5 (0.55/0.45)	0.23	0.31

[a]: shoulders (suffix "s") /vibrational bands in the same transition are separated by a slash; **[b]:** fluorescence maximum**; [c]:** fluorescence quantum yield**; [d]:** fluorescence lifetime with violet light-induced photoequilibrium (FCS)**;** in parenthesis, the fractions associated to each component; **[e]:** *A* = fluorescence anisotropy**.**

This is also confirmed by the observation that the double mutation T30V/N37C produces spectral features virtually identical to T30V (Table 3.1). YtvA-WT exhibits a UVA maximum at 375 nm with a shoulder at ca. 359 nm, whereas in T30A/V the band is blue-shifted and resolved in two distinct peaks (λ_{max} = 354/370 nm,
Table ***3.1***, Figure 3.17).

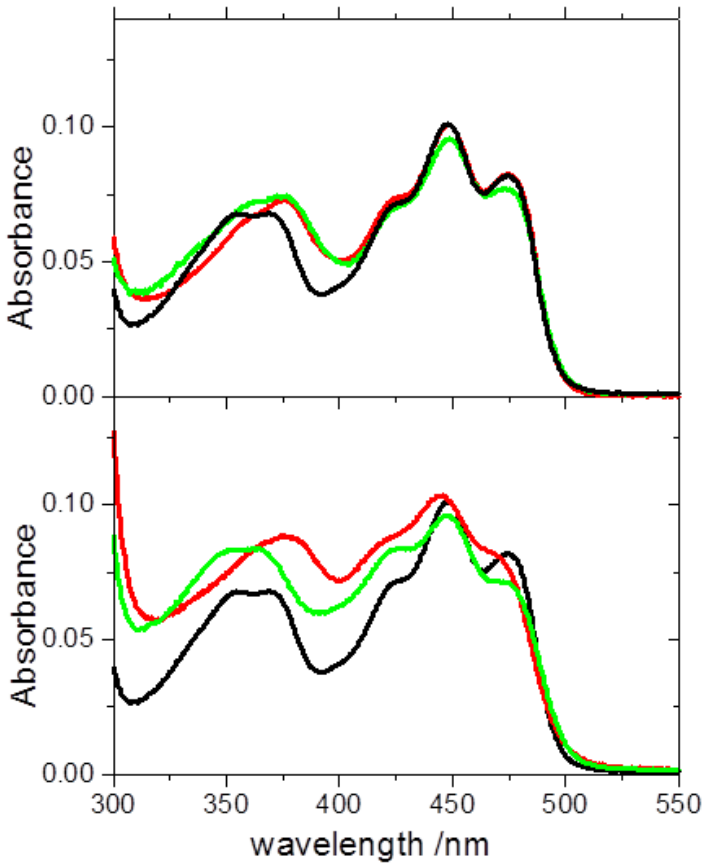

Figure 3.17. Absorption spectra of YtvA proteins in the dark-adapted state: a) T30A (black line), WT (red) and N37C (green); b) T30A (black line), N104A (red) and N94A (green).

A similar blue-shift of the UVA transition was formerly reported for N94A (Figure 3.17) [10]. Interestingly, N94 is interacting with position 3 of the isoalloxazine ring, and is, as T30, directly in line with the calculated transition dipole moment for the UVA band [11]. Including two other positions into this investigation, Q66 and R63, we find that the transition I (blue-light region) and the fluorescence maxima are solely and minimally affected by Q66K. Fluorescence anisotropy, that depends on the extent and rate of chromophore rotational

diffusion during the lifetime of the excited state, appears virtually unaffected by all mutations. Interestingly, Q66H has a much lower value of Φ_F and a faster fluorescence lifetime, indicating a mechanism of dynamic quenching: this is possibly due to electron transfer from histidine to the flavin excited state [12]. Q66L and Q66P showed a very low chromophore loading and where not further investigated.

Measurements of fluorescence lifetimes with the confocal microscope-based methodology gave a single value, τ_F=4.7±4.9 ns, under BL illumination and two values under photoequilibrium conditions with violet illumination: τ_{F1}=4.6±5.1 ns and τ_{F2}=1.3±2.7 ns (Table 3.1). The longer lifetime τ_{F1} corresponds to a non-photoconvertible fraction, possibly a small amount of free FMN, given the identical fluorescence lifetime, whereas τ_{F2} originates from the small percentage of protein molecules driven back to the fluorescent state by violet light [13] The shorter lifetime, τ_{F2}, should therefore correspond to the fluorescence lifetime of bound FMN, although we cannot exclude it is bound to the protein in a non specific manner/alternative conformation (Figure 3.18).

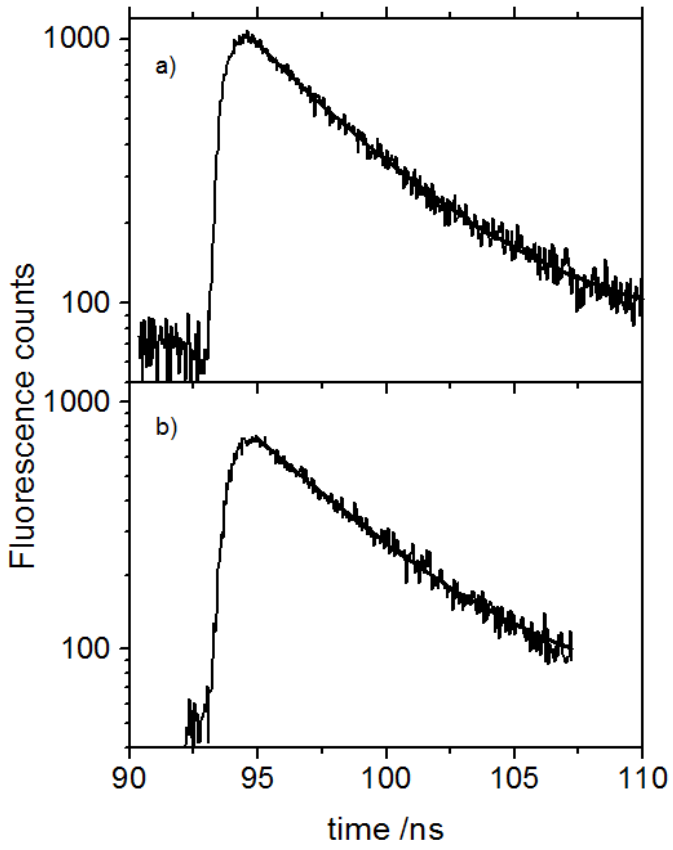

Figure 3.18. Fluorescence decay of T30A under: a) violet illumination (405 nm), photoequilibrium condition; the best fitting is with a double exponential function (superimposed to the experimental curve), giving τ_{F1}= 4.8 ns and τ_{F2} = 2.1 ns; b) BL illumination (475 nm), giving a single τ_{F1}=4.6 (Table 3.1).

This method appears thus to be, for slow-cycling LOV proteins, more reliable than conventional single photon counting, in that the conventional method requires long measuring times and a larger amount of absorbed photons, thus forming considerable amounts of photoadduct and inducing loss of fluorescence intensity and two-exponential fittings of fluorescence decays as possibly being artifacts [7], [8].

3.5.2 Photocycle dynamics and efficiency

All investigated mutated proteins formed a triplet state and a photoadduct with yields comparable to, or even higher than YtvA-WT (Table 3.2). The only exception again is Q66H, with a lower quantum yield (Φ_{DL}) possibly due to quenching of the flavin triplet state by the introduced, nearby histidine via electron transfer [14].

Table 3. 2: Triplet state properties and adduct formation efficiency.

	[a]Φ_T	[b]τ_T /µs	[c]Φ_{DL} ill. range =		[d]Φ_{LD} LED405	
			UVA	**Blue**	**Photoeq.**	**Kin. mod.**
YtvA-WT	0.46	1.8	0.32	0.49	0.049 [13]	0.050 [13]
N37C	0.62	2.0	0.30	0.52	--	--
N37F	0.60	3.1	0.34	0.28	0.060	0.047
N37V	0.54	2.3	0.36	0.58	0.100	0.044
T30A	0.63	1.5	0.33	0.28	0.038	0.040
T30S	0.45	0.8	0.28	0.40	0.046	0.040
T30V	0.69	1.3	0.25	0.61	0.057	0.030
T30V/N37C	0.63	1.3	0.26	0.51	--	--
Q66H	0.59	4.2	0.12	0.20	0.050	0.030
Q66K	0.77	6.3	0.28	0.40	0.027	0.025
R63K	0.51	2.2	0.23	0.40	0.080	0.100

[a]: triplet quantum yield as determined by LIOAS based on the energy level of the triplet state as 200 kJ/mol; λ_{ex} = 355 nm; [b]:triplet lifetime, flash photolysis, λ_{ex} = 355 nm; [c]:as determined from the time-course of fluorescence bleaching induced by LED356 and LED465; YtvA-WT was used as reference, with Φ_{DL} = 0.32 [13] and 0.49 [7] for UVA and BL illumination, from independent LIOAS and flash photolysis measurements. [d]: as determined from the from the photoequilibrium absorption spectra and from the kinetic model applied to rates fluorescence recovery as a function of LED405 power. In the latter case the average fitting error is 25%.

Interestingly, mutations at T30 tend to shorten the triplet lifetime, τ_T, probably reflecting the fact that at the triplet state level the protein microenvironment has started to respond to the modified electronic structure of the chromophore.
Both mutations of Q66 considerably increase τ_T, in line with previous data that have suggested a role of the extended HB network in modulating the dynamics of the photocycle [10].

LIOAS and fluorescence measurements indicate that UVA and violet light are able to induce a photoequilibrium in all cases investigated, as was previously demonstrated with YtvA-WT [13]. All mutated proteins exhibit photochromism, as underscored by the possibility to determine fluorescence lifetimes of bound FMN under photoequilibrium conditions (Figure 3.18, Table 3.1).
By means of absorption and fluorescence spectroscopy it is possible to directly visualize the UVA/Violet-inducible photoequilibrium and to estimate the value of Φ_{LD} as previously demonstrated with YtvA-WT. This is done either by establishing a photoequilibrium and applying eq.3.3, or by following the kinetics of fluorescence recovery under violet light with different LED power and applying the kinetic model (eqs. 3.4-3.8). In some cases (N37C and T30V/N37C), the signal-to-noise ratio was not sufficient to allow the determination of Φ_{LD}, but in general the protein variants investigated did not show a large deviation from YtvA-WT (Table 3.2). An example of fluorescence recovery curves and kinetic fitting is given in Figure 3.19.

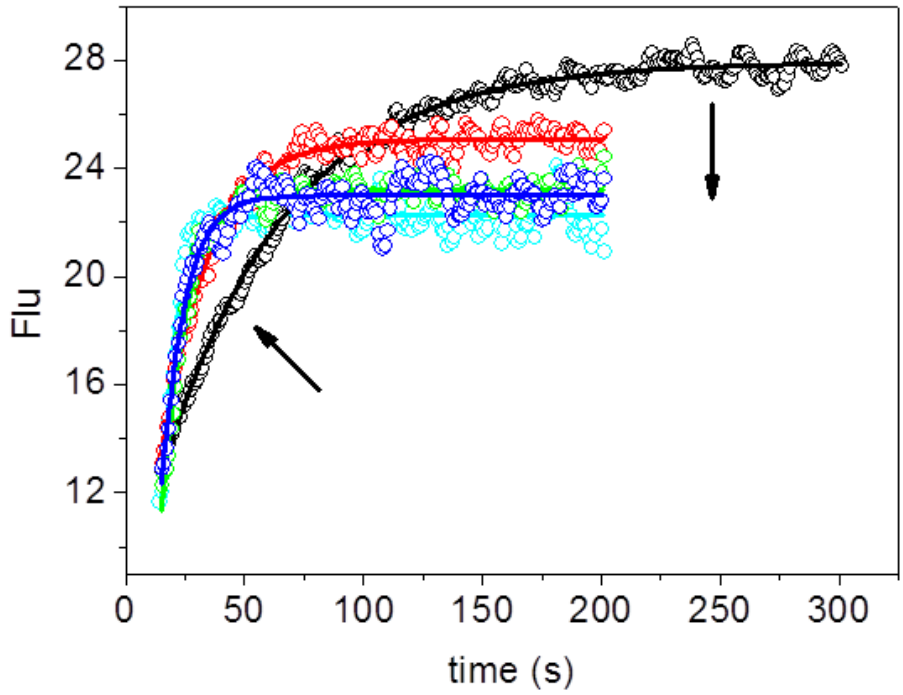

Figure 3.19. Fluorescence emission recovery of YtvA-T30S under violet illumination with LED405 (the arrows indicate increasing LED power, between 0.05 mW and 0.8 mW). Light adapted protein solutions were prepared by 5 min irradiation with LED465. T = 20 °C; λ_{ex} = 330 nm, λ_{em} = 500 nm.

3.5.3 Kinetics of the thermal dark-recovery reaction

The lifetime τ_{rec} for the completion of the photocycle (thermal recovery to the dark-adapted state with breakage of the covalent FMN-Cys bond) is in some cases considerably faster than in YtvA-WT, at 20°C (Table), e.g., for N37F/V, T30A/S, Q66H. Also other mutations have previously shown such a feature, e.g. R63K, N94A/S or Q123N (Table 3.3) [10],[15].

Table 3.3: Recovery kinetics, (20°C), and Arrhenius and Eyring parameters.

	$\tau_{rec,20°}$/s	A/ s^{-1}	E_a/kJ mol^{-1}	$\Delta H^{\#}$ /kJ mol^{-1}	$\Delta S^{\#}$/kJ $mol^{-1}K^{-1}$
YtvA-WT	**6240**	**6.9 x10^{14}**	**104**	**101**	**+0.031**
N37C	3300	5.7 x10^{7}	63	60	-0.10
N37F	1470	6.5 x10^{12}	90	87	-0.008
N37V	930	1.15 x10^{11}	49	76	-0.033
T30A	1690	2.6 x10^{11}	82	80	-0.034
T30S	1625	8.4 x10^{8}	68	65	-0.082
T30V	4280	4.9 x10^{9}	75	72	-0.067
T30V/N37C	5260	2.2 x10^{7}	62	60	-0.110
Q66H	1650	1.2 x10^{12}	86	83	-0.022
Q66K	2510	3.6 x10^{14}	95	92	+0.006
R63K	485	6.9 x 10^{9}	70	68	-0.065
N94D	1250	3.4 x10^{23}	151	148	+0.20
YtvA-N94A	140	4.9 x10^{18}	117	115	+0.10
YtvA-N94S	300	7.2 x10^{15}	103	100	+0.05
YtvA-N104D	6890	4.9 x10^{16}	115	112	+0.066
YtvA-N104A	2250	4.0 x10^{8}	67	65	-0.09
YtvA-N104S	1120	9.2 x10^{10}	78	76	-0.043
YtvA-Q123N	72	5.0 x10^{9}	65	62	-0.067

The temperature dependence of the recovery reaction demonstrates that a faster photocycle may be related to a more favorable (larger) activation entropy or to a more favorable (smaller) activation enthalpy (Table 3.3, Figure 3.20). Although the phenomenon is complex, the relation between the activation entropy and enthalpy is linear, revealing a compensation, most probably related to the network of weak interactions within the cavity [10].

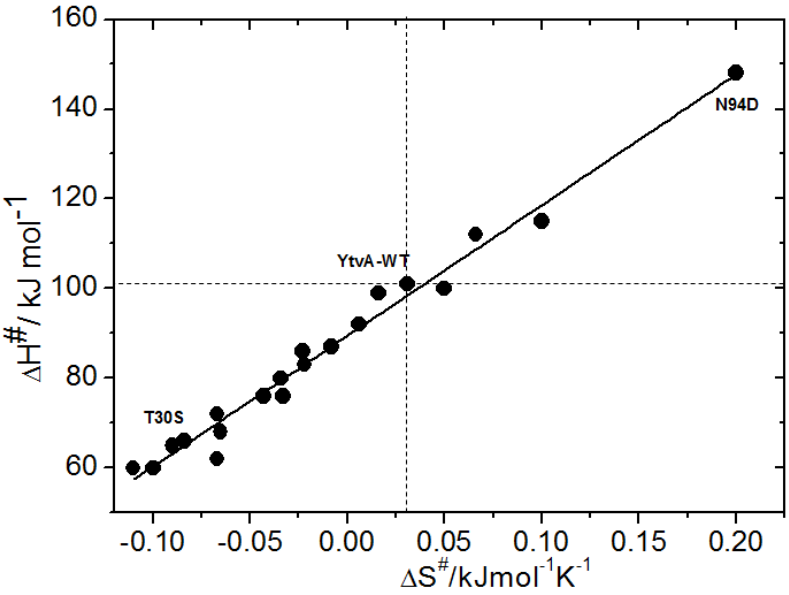

Figure 3.20. Activation enthalpy-entropy correlation in the recovery reaction of YtvA-WT and mutated YtvA proteins. The mutations T30S and N94D give comparably short τ_{rec} with respect to YtvA-WT (see Table 3.3) but for T30S this appears to be linked to a more favorable (lower) $\Delta H^{\#}$, whereas for N94D the faster kinetics is related to a larger $\Delta S^{\#}$.

3.6 From *vitro* to *vivo* applications

When a dark adapted *E. coli* culture (taken directly form agar plates and smeared on a coverslip) over-expressing YtvA (which is fully in its YtvAD state) is exposed to LED465, the fluorescence emission by YtvAD is reduced due to the photoreaction leading to the formation of the non-fluorescent adduct YtvAL. When blue light is turned off and cells are kept in the dark, fluorescence emission intensity increases with time, as a consequence of the dark relaxation to YtvAD. Figure 3.21 shows several subsequent dark relaxation kinetics following illumination of the cell culture for 5 minutes. In these experiments it is not possible to monitor the photoconversion of YtvAD to YtvAL upon LED465 illumination since the detection system was saturated by the fluorescence emission excited by the intense actinic beam. The kinetics of the dark relaxation is quite reproducible from cycle to cycle, with some loss (~10%) in the fluorescence emission level attained upon recovery of YtvAD.

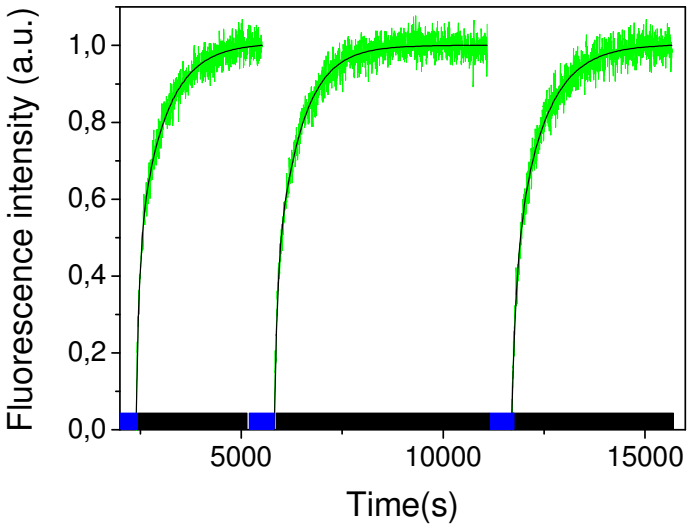

Figure 3.21. Cyclic dark recovery of YtvAL to YtvAD in *E. coli* colonies overexpressing YtvA from agar plates and smeared on a coverslip, after illumination with LED465, monitored through fluorescence emission of YtvAD. The blue bars indicate illumination periods with LED465, black bars indicate that the colonies were kept in the dark. T=25°C.

Control experiments on *E. coli* colonies overexpressing YtvA-C62S , for which the photocycle is inhibited, showed no modulation of the fluorescence intensity upon illumination (Figure 3.22), thus demonstrating that the observed cyclic effect is indeed related to the photochemistry of the photoreceptor.

As a further control, the fluorescence emission intensity by *E. coli* colonies not transformed to overexpress YtvA, was at least two orders of magnitude smaller than the level observed for transformed bacteria (Figure 3.22).

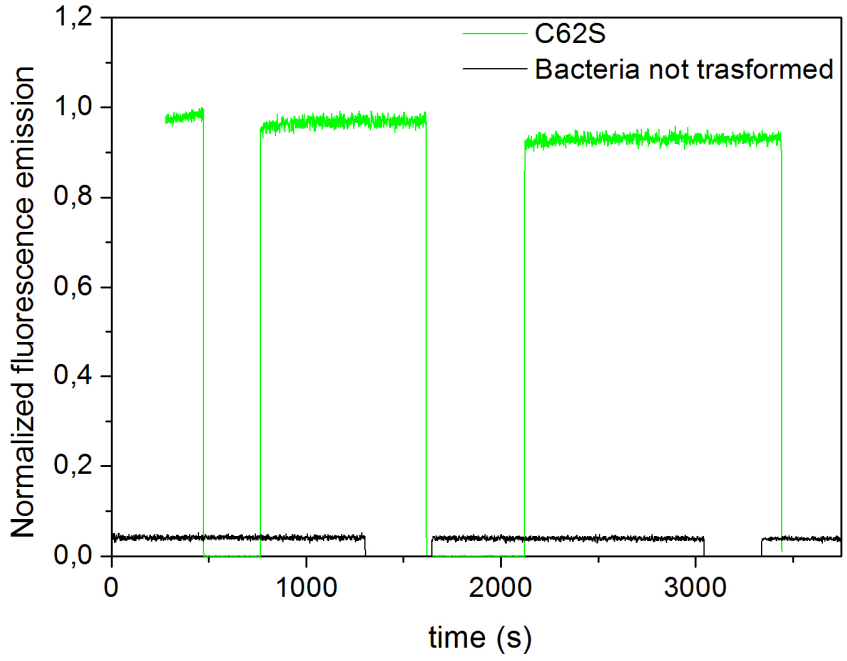

Figure 3.22 The observed photoconversion is indeed related with the photochemistry of YtvA. When fluorescence from not transformed *E. coli* colonies are measured, the emission is very much weaker than for the transformed ones (black trace) and does not shown any photoconversion. When colonies transformed to express the YtvA-C62S, for which the photochemistry is fully inhibited, are measured , a strong fluorescence emission is observed which is not modulated by blue light.

The first striking feature of the kinetics in Figure 3.21 is that under these conditions the relaxation becomes much faster than expected on the basis of previous experiments on purified proteins, which showed that in a homogeneous solution YtvAL relaxes to YtvAD with an exponential decay characterized by a lifetime of about 3000 s at 25°C. This difference can be appreciated in Figure 3.23 which compares the relaxation kinetics observed for the colonies smeared on coverslips (green curve) and for the purified protein in solution (blue curve). Furthermore, for YtvA molecules inside *E. coli* the dark relaxation is best described by a stretched exponential decay ($y = e^{[-(t/\tau)^{\beta}]}$), whose time constant and stretching exponent, reported in Table 3.4, suggest that YtvAL is much less stabilized, and that kinetics is characterized by a rather distributed nature.

Table 3.4. Apparent time constants for the YtvAL to YtvAD relaxation at 25 °C.

		τ_d (s)	β_d	τ_w (s)	β_w	$\gamma=\tau_w/\tau_d$	
		Dried protein					**Solution τ (s)**
Purified protein		250±20	0.70±0.05	-	-	13	3200±50
		Cells smeared on coverslip		**Cells soaked in buffer**			
B. subtilis	*wt*	360±10	0.70±0.05	4080±40	1	11	3200
E. coli	*wt*	263±3	0.51±0.01	2100±10	1	8.0	3200
	R63K	275±38	0.56±0.05	312±12	0.94±0.05	1.13	246
	N37C	286±5	0.6±0.1	912±2	0.811±0.002	3.2	1930
	T30S	485±46	0.59±0.01	1209±2	0.991±0.003	2.5	1150
	T30A	351 ± 28	0.62±0.06	592 ± 59	1	1.7	1027
	N94A	80±30	0.5±0.1	120±30	1	1.5	85
	N94D						599
	N104D	290±20	0.66±0.04	1100±200	1.05±0.03	3.8	2780
	N104A	140±40	0.5±0.1	620±10	0.98±0.02	4.4	1505
	Q123N	64±2	0.56±0.05	74±7	1	1.1	32 (66%) 71 (34%)
	Q66H	242±32	0.64±0.03	753±56	0.98±0.02	3.1	1024

β: coefficient of stretched exponential; $\gamma=\tau_w/\tau_d$ ratio between apparent time constant of "wet" and "dry" conditions.

When *E. coli* colonies are soaked in a physiological buffer (Na-phosphate buffer pH = 7.4, 0.9% NaCl), the kinetics becomes much slower and comparable to the one observed for purified proteins in solution (red curve in Figure 3.23). In addition, the kinetics is much less distributed and approaches a pure exponential decay, with lifetime a bit shorter (~2000 s) than the one observed for YtvA purified in solution.

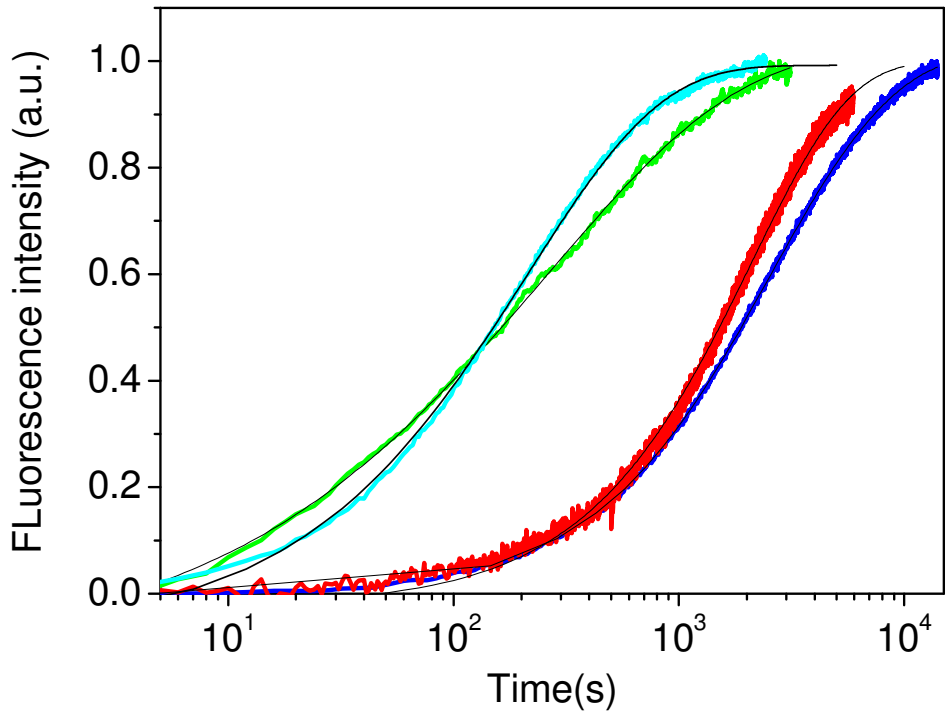

Figure 3.23. Dark relaxation of YtvAL to YtvAD, as monitored by the recovery of fluorescence emission after switching off LED465. Blue, buffered YtvA solution; red *E. coli* colonies overexpressing YtvA taken form agar plates and soaked in 10 mM phosphate buffer solution, containing 0.9% NaCl (W/V), pH=7.4; green, *E. coli* colonies overexpressing YtvA from agar plates, but smeared on a coverslip; cyan, YtvA solution dried on a glass coverslip. T=25°C. Black solid lines are the fit with stretched exponential relaxations except for YtvA solution, for which fitting was obtained with an exponential decay.

The above experiments suggest a major effect of the cellular environment on the stabilization of YtvAD, which appears to be strongly modulated by the water content of the system. We thus decided to investigate the behavior of dried purified proteins.

Figure 3.23 shows the kinetics of the changes in fluorescence emission by YtvA molecules dried on a coverslip, subject to illumination with LED465 or LED405, and subsequently left in the dark. Fluorescence emission is decreased by LED465 (LED405) illumination due to formation of YtvAL. Unlike the case of the experiments on *E. coli* cells, for dried proteins it proved feasible to follow also the kinetics of the forward YtvAD to YtvAL photoconversion, thanks to the much higher fluorescence signal of the sample, which required lower amplification at the photomultiplier on top of the photometer. Photoconversion to YtvAL is not complete under these experimental conditions, since the actinic blue light by LED465 must be kept anyway at a low level to avoid saturation of the detection system. Hence, a mixture of YtvAD and YtvAL is always present in the state generated by shining blue light.

When left in the dark, fluorescence increases with time due to thermal recovery of YtvAL to YtvAD. It can be easily appreciated from Figure 3.24, that YtvAD recovery in the dark is attained through a rather fast decay, which is best described by a stretched exponential relaxation. The time constant and the stretching exponent are quite stable from cycle to cycle, and an average value is reported in Table 3.4.

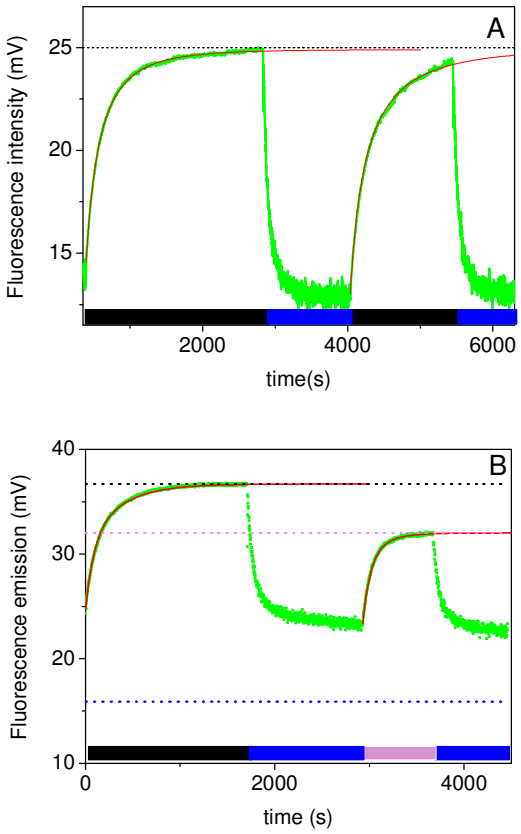

Figure 3.24. Fluorescence emission by YtvA dried on a glass coverslip and subject to successive photoconversion (blue light illumination with LED465) and dark recovery cycles. Illumination and dark recovery cycles are indicated at the bottom of the figure by blue and black bars, respectively. The power of LED465 on the focal plane of the microscope was 19 μW. Red solid lines are the result of a best fit with a stretched exponential relaxation with τ= 250±20 s and β = 0.70±0.05. The black dotted line is the level of initial fluorescence emission by YtvAD. B. Fluorescence emission by YtvA dried on a glass coverslip and subject to successive dark recovery, YtvAD-to-YtvAL photoconversion (blue light illumination with LED465), YtvAL-to-YtvAD (violet light illumination with LED 405). Illumination and dark cycles are indicated at the bottom of the figure by blue, violet and black bars. The power of LED465 and LED405 on the focal plane of the microscope were 19 μW and 7 μW, respectively. Red solid lines are the result of a best fit with a stretched exponential relaxation (τ = 170±10 s and β = 0.70±0.05 for the dark relaxation, τ = 100±5 s and β = 0.90±0.05 for the relaxation under LED405 illumination). The black dotted line is the fluorescence emission by YtvAD, the violet dotted line is the fluorescence emission by the mixture obtained with LED405. The emission by pure YtvAL is shown as a blue dotted line. The level was estimated by illuminating with high LED465 power (84 μW) and then measuring the resulting emission immediately after switching off the actinic beam.

The level of fluorescence emission reached after dark relaxation is not affected by illumination, indicating that photobleaching occurs to a minor extent. To allow for an easier visual comparison with the other experimental conditions, the dark recovery signal is also plotted in Figure 3.23 (cyan curve), along with the fitting with a stretched exponential decay. While the time scale for the relaxation is similar to the one observed for *E. coli* overexpressing YtvA, the kinetics appears less distributed, indicating a lower degree of stretching (Table 3.4). Experiments conducted by monitoring the absorbance changes at 436 nm after photoconversion with LED465 demonstrate that the recovery of the YtvAD absorbance occurs with a stretched exponential relaxation which is very similar to the one retrieved by monitoring the fluorescence emission, with τ = 380±5 s and β = 0.62±0.05. Different data sets show some variability, most likely due to changes in water content of the sample, in response to changes in the ambient humidity. This is appreciable in the data reported in Figure 3. 24B, where data from similar experiments are reported. In this case, the dark relaxation was observed to occur with a slightly shorter time constant (Table 3.4). Figure 3.24B also shows the effect of exposing YtvAL to LED405. Since the violet radiation is inducing both the YtvAL-YtvAD and YtvAD-YtvAL reactions, the observed relaxation time becomes shorter, and the process becomes more exponential, with a larger stretching exponent (Table 3.4). The equilibrium fluorescence level in this case is intermediate between those of YtvAD and YtvAL.

Fluorescence decay curves were fitted with two exponential using blue light and violet light because landscape of cellular environment is very different from that one of protein solution and there is certainly free FMN so it must be consider (see Table 3.5).

The obvious concern when working with hydrated cells is that when soaked in a buffer, even if isotonic and thus preventing cells rupture by trivial osmotic effects, cells may anyway release the photoactive proteins to the surrounding medium and thus expose them to an environment identical to the one experienced by purified proteins in solution. To rule out this possibility we have collected FPALM images of *E. coli* cells over-expressing YtvA, both direclty taken from agar plates and soaked in the isotonic buffer employed in the above experiments (Figure 3.25).The cellular distribution of the fluorescent proteins is similar in both cases, with accumulation of molecules near the cell wall. Although the background fluorescence emission outside the cells is substantial, the amount of photoswitchable proteins is a negligible fraction, demonstrating that leakage of the expressed YtvA is small. Thus, the amount of water of the environment outside the cells appears to influence the photocycle

dynamics for YtvA proteins located inside the cells, but not the cellular shape and YtvA localization.

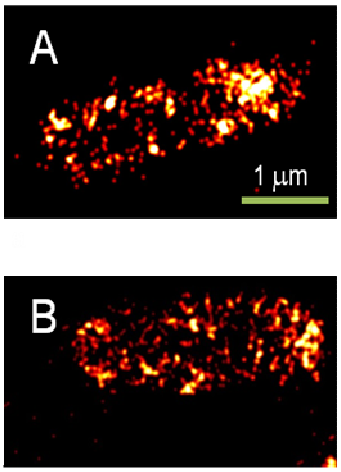

Figure 3.25. FPALM images of *E. coli* cells overexpressing YtvA taken directly from agar plates (A) and soaked in isotonic buffer (B).

3.6.1 Photoconversion studies on YtvA mutants

The above empirical correlation between the dark relaxation time constant and level of hydration implies some major degree of coupling between the flavin fluorophore and the surrounding environment. FMN is effectively protected from interactions with solutes as demonstrated by the lack of quenching by molecular oxygen on singlet and triplet excited states (Aba Losi, unpublished). It is therefore important to identify specific amino acids surrounding the chromophore, which are capable of transducing the interaction with the solvent. We have previously developed several YtvA mutants at specific amino acids nearby the chromophore, which allowed to identify residues with large effects on the photocycle rate constants [16].

We have taken the ratio γ between the time constants measured for bacteria soaked in isotonic buffer (τ_w) and smeared directly in coverslip (τ_d) as an indication of the sensitivity of the dark relaxation to hydration. For wt YtvA, γ has a value of about 10 when the dark relaxation is measured either in *B. subtilis* (γ=11) or *E. coli* (γ=8). A similar value is measured for the purified recombinant protein (γ=13). While all mutations appear to decrease the value of γ, some residue afford values close to unity, almost completely removing the effect of the excess solvent in the surrounding medium. Figure 3.26 shows the topological arrangement of the amino acids surrounding the FMN chromophore considered. Mutations which resulted in values of γ close to one are highlighted in red. A special place is held by Arg63, a residue which is located near the phosphate of the chromophore. When Arg63 is mutated to Lys, γ becomes 1, indicating that this is a very critical point for coupling the dark relaxation process to the solvent. Mutation R63K most likely leads to formation of a salt bridge between the phosphate and the Lys, thus inhibiting, or at least limiting, interactions with the bulk solvent.

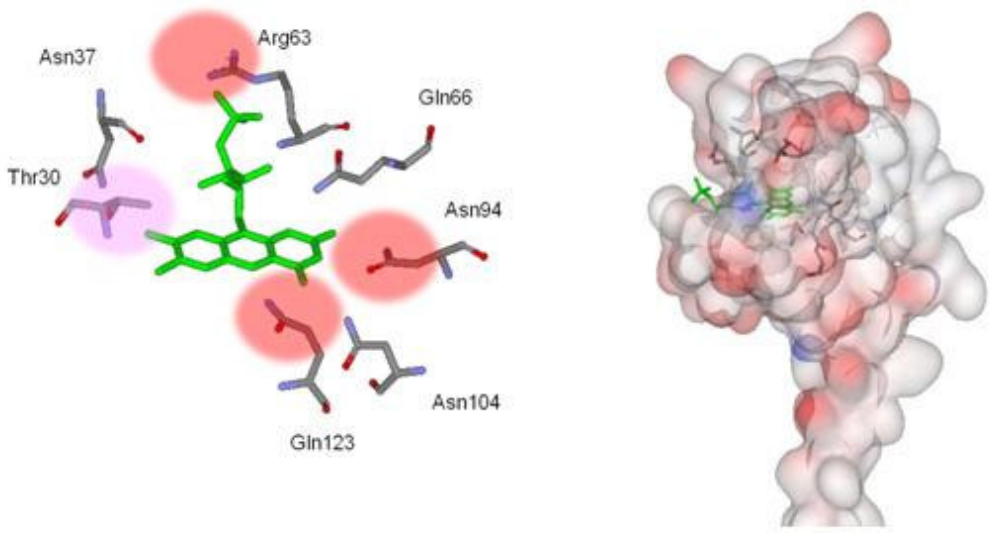

Figure 3.26. Left. Closeup of the amino acids surrounding the chromophore investigated in this study. Right. Solvent accessible surface visualization of the protein with the chromophore in green and the amino acids considered in this study represented in capped sticks.

We also measured fluorescence decay lifetimes for *E. coli* cells overexpressing YtvA and mutated YtvA-proteins (Table 3.5). It is evident that, different from the situation with purified proteins, *in vivo* fluorescence decay are best fitted with a two-exponential function also in the case of BL illumination, probably due to a heteregoneus protein photoactivation pattern.

Table 3.5: time constants (in ns) of fluorescence decays for different mutants.

	472 nm		405 nm	
	$^{a}\tau_{F1/2}$ /ns (fraction 1/2) **dry**	$^{a}\tau_{F1/2}$ /ns (fraction 1/2) **wet**	$^{a}\tau_{F1/2}$ /ns (fraction 1/2) **dry**	$^{a}\tau_{F1/2}$ /ns (fraction 1/2) **wet**
YtvA-WT	4.56 /1.98 (0.35/0.65)	4.71/1.67 (0.41/0.59)	4.35/1.77 (0.35/0.65)	4.62/1.66 (0.41/0.59)
C62S	4.48/2.34 (0.42/0.58)	4.85/2.76 (0.49/0.51)	4.86/2.15(0.4/0.6)	4.99/2.26 (0.51/0.49)
N37C	4.74/2.06 (0.36/0.64)	4.96/1.72 (0.38/0.62)	4.86/1.78 (0.44/0.56)	4.56/1.77 (0.37/0.63)
Q123N	4.69/1.7 (0.35/0.65)	4.87/1.62 (0.48/0.52)	4.79/1.49 (0.43/0.57)	5.07/1.43 (0.44/0.56)
T30A	4.68/1.76 (0.44/0.56)	4.54/1.68 (0.48/0.52)	4.75/1.76 (0.48/0.52)	4.76/1.27 (0.49/0.51)
T30S	4.55/1.93 (0.46/0.54)	4.71/1.53 (0.43/0.57)	4.71/1.86 (0.41/0.59)	4.63/1.66 (0.48/0.52)
N104D	4.91/1.71 (0.39/0.61)	5.14/1.63 (0.42/0.58)	4.87/1.49 (0.45/0.55)	5.08/1.46 (0.46/0.54)
Q66H	4.52/1.65 (0.39/0.61)	4.87/1.55 (0.44/0.56)	4.91/1.59 (0.46/0.54)	4.99/1.37 (0.44/0.56)
N94A	5.11/1.85 (0.44/0.56)	4.9/1.73 (0.45/0.55)	5.02/1.7 (0.45/0.55)	5.03/1.63 (0.43/0.57)
R63K	4.45/1.57 (0.43/0.57)	4.53/1.37 (0.45/0.55)	4.68/1.55 (0.45/0.55)	4.79/1.41 (0.46/0.54)

[a]: fluorescence lifetime with violet light-induced photoequilibrium (FCS)**;** in parenthesis, the fractions associated to each component.

3.7 *In silico* research and analysis of novel FL-Blues

In this part of the work we tried to improve genome mining for uncovering LOV proteins within public databanks. Besides, we also performed search and analysis of BLUF photoreceptors and built distance trees for these two kind of prokaryotic photoreceptors.

3.7.1 Protein search and distribution: patterns of super conserved residues

A new search for FL-Blues obeyed more stringent criteria than the previous ones, [17] by employing a lower threshold during databanks blasting and by visually inspecting the recovered proteins not only for the presence of residues directly involved in photochemistry, but also for a series of conserved amino acids present in proteins for which photochemistry has been experimentally demonstrated. This criterion defined ten super conserved residues in LOV domains (Figure 3.27) and twelve in BLUF domains (Figure 3.28), six and seven of which, respectively, in close vicinity to the flavin chromophore (marked with triangles on top of the alignment).

As a whole at June 2012 we recovered and analyzed 496 LOV proteins in 377 bacterial species/strains, 751 BLUF proteins in 558 bacterial species/strains; additionally, 24 LOV proteins are described in 17 Archaea (Appendix 1 signed in gray). The represented phyla include, to date: Acidobacteria (Acido), Actinobacteria (Ac), Bacteroidetes/Chlorobi group (Bact/Ch), Chlamydiae/Verrucomicrobia group (Verr), Chloroflexi (Chl), Cyanobacteria (Cya), Deinococcus-Thermus (DeTh), Firmicutes (F), Lentisphaerae (Lent), Nitrospirae (Nit), Planctomycetes (Pl), Spirochaetes (Spi), unclassified bacteria (U) and Euryarchaeota (EuA). In some, but not all of these groups, phototrophy (obliged or facultative) is present as anoxygenic photosynthesis (Acido, Bact/Ch, Chl, F, P), oxygenic photosynthesis (Cya), or microbial rhodopsin-based (Acido, Ac, Bact/Ch, Chl, DeTh, F, Cya, P, EuA) [19], [20]. However it should be noted that phototrophy does not necessarily imply the presence of photosensory receptors discussed here: as an example photosynthetic Firmicutes (*Heliobacteria*) and many cyanobacteria (eg. *Prochlorococcus*), do not possess kind of photoreceptors.

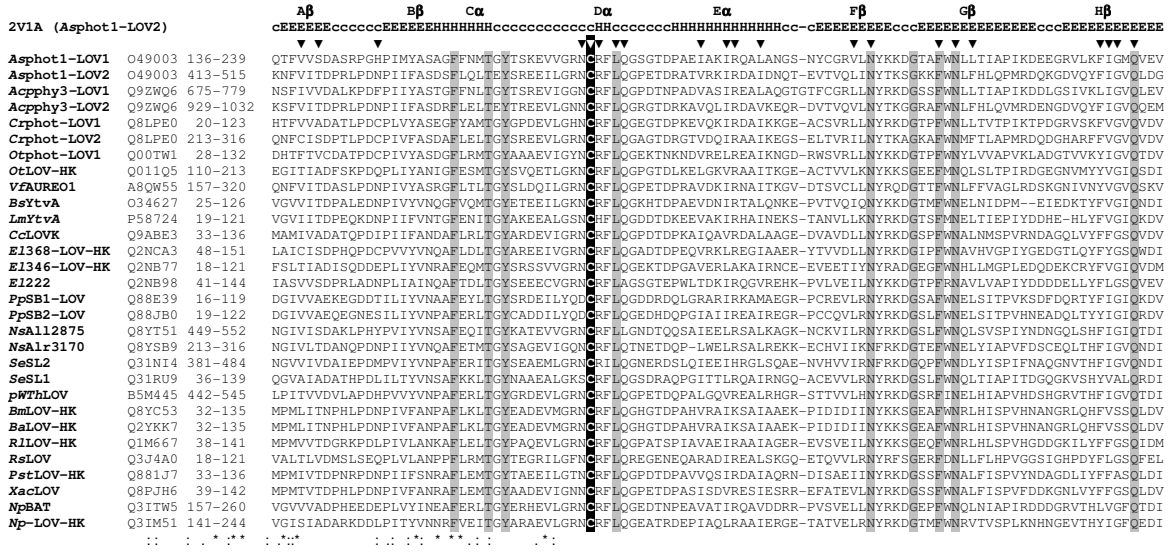

Figure 3.27. Criteria for selecting photochemically competent LOV domains. Alignment of selected LOV domains with described photochemistry (with the exception of the two bottom lines, showing archaeal LOV domains, not yet characterized) and secondary structures elements detected for the indicated structure (PDB code 2V1A9): E = strands, H = helices, c = unordered, loops, turns. Above, the most common nomenclature used. Triangles indicate residues interacting with the chromophore (within 4 Å distance); the white triangle denotesthe substrate cysteine involved in LOV-type photochemistry. The 10 super conserved amino acids are evidenced and marked with a * sign. : and . = high and low conservative substitutions respectively. From left: protein literature name, Uniprot code, aa interval encompassing the LOV core. *As = Avena sativa;Ac = Adiantum capillus veneris*; *Cr =Chlamydomonas reinhardtii*; *Ot =Ostreococcus tauri; Vc = Vaucheria frigida*;*Bs = Bacillus subtilis*; *Lm = Listeria monocytogenes*; *Cc = Caulobacter crescentus*; *El = Erythrobacter litoralis*;*Pp = Pseudomonas putida*; *Ns = Nostoc sp. PCC 7120*; *Se = Synechococcus elongatus PCC 7942*; *pWTh*LOV= *bacterium enrichment culture clone pWTh*LOV*; Bm= Brucella melitensis*; *Ba = Brucella abortus*; *Nostoc sp. PCC 7120*;*Rl = Rhizobium leguminosarum*; *Rs = Rhodobacter sphaeroides*;*Pst=Pseudomonas syringae pv. tomato*; *Xac = Xanthomonas axonopodis pv. citri*; *Np = Natromonas pharaonis*. LOV proteins of the ZTL/FKF1/LKP2 family, bearing an insertion in the Eα-Fα loop and binding FAD (flavin adenin dinucleotide) as chromophore, also have the ten super conserved residues, with the exception of LKP2 [18].

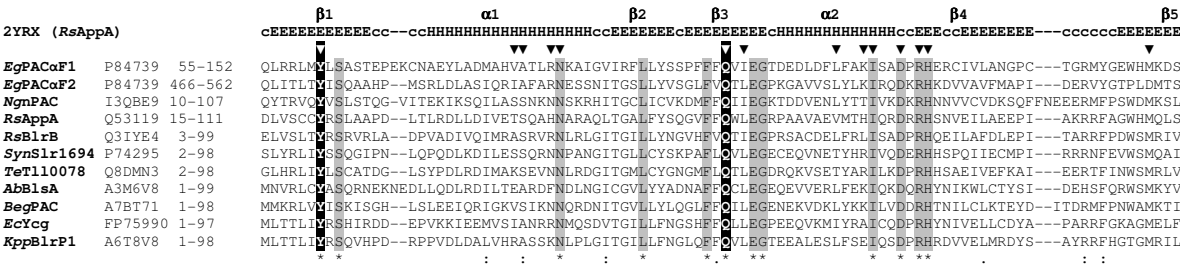

Figure 3.28. Criteria for selecting photochemically competent BLUF domains. Alignment of selected BLUF domains with described photochemistry, with the 12 super conserved amino acids in evidence.Underlined triangles denote the Tyr-Gln couple involved in BLUF-type photochemistry. See figure 3.27 for the remaining legenda.*Eg = Euglena gracilis;Ng = Naegleria gruberi*;*Rs = Rhodobacter sphaeroides*; *Syn = Synechocystis sp.* PCC 6803;*Te = Thermosynechococcus elongatus*; *Ab = Acinetobacter baumannii*;*Beg = Beggiatoa sp. PS*; *Escherichia coli*; *Ec = Escherichia coli*; *Kpp = Klebsiella pneumoniae subsp. pneumoniae*.

Many soluble photoreceptor are modular, in that they bear quite often one or more associated effector and/or regulatory domain [17]. Functionally we can distinguish major groups of proteins including: histidine-kinases; phosphatases; GGDEF/EAL domains, involved in the

turnover of cyclic diguanylate, c-di-GMP (as diguanylate cyclase/phosphodiesterase respectively), and/or in protein-protein interactions; transcription factor of the helix-turn-helix family and chemotaxis proteins bearing MCP (Methyl-accepting chemotaxis proteins) modules. Heme-binding domains are restricted to a few BLUF-protein, such as the SCHIC (Sensor containing heme instead of cobalamin) domain of *Rhodobacter sphaeroides* AppA [21] and some putative globin domains, e.g. in a LOV protein from *Leptospirillum ferrodiazotrophum*. Adenylate/guanylate cyclases are extremely rare, although they appear to be functional and light-regulated [22].

Standalone photochemically competent domains, without fused partners, also are quite common.

LOV proteins show a large percentage of histidine kinases (HK) of the two-component system, a prototypical signal transduction device in Bacteria and Aarchaea, found with many variations in nature [23], [24]. Interestingly, there are no BLUF-based kinases. In this case the preferred associated domains are related to the metabolism of c-di-GMP (GGDEF and EAL) [25] (Table 3.6).

3.7.2 Phylogenetic analysis and distance-trees

Preliminary, we observe that there are some differences in bootstrap values in the three trees calculated from different distances, but most clusters are conserved. In general, from the calculated trees, we can see that most photoactive domains coming from organisms of the same phylum/ class, fall in the same cluster or are neighbours. There are also some clusters encompassing proteins from organisms of the same taxon, but belonging to different groups. We also observed some exceptions to this: for example gammaproteobacteria fall together with Bacteroides and Actinobacteria (Figure 3.29). Most of the proteins with the same effector domains falls in the same cluster, underscoring that clustering of photoactive domains may be related either to group affinities or to functional similarities.

As initial step, for LOV domains we separately built the Archaea and Bacteria distance-trees to detect clusters. Then we joined the sequences of both groups and analyzed the total trees obtained from all prokaryotic LOV domains, including those from Archaea, whose presence do not appreciably affect bacterial clusters in that they remain segregated. Figure 3.29 represents the tree obtained using *p*-distance; highly conserved clusters are shown compressed.

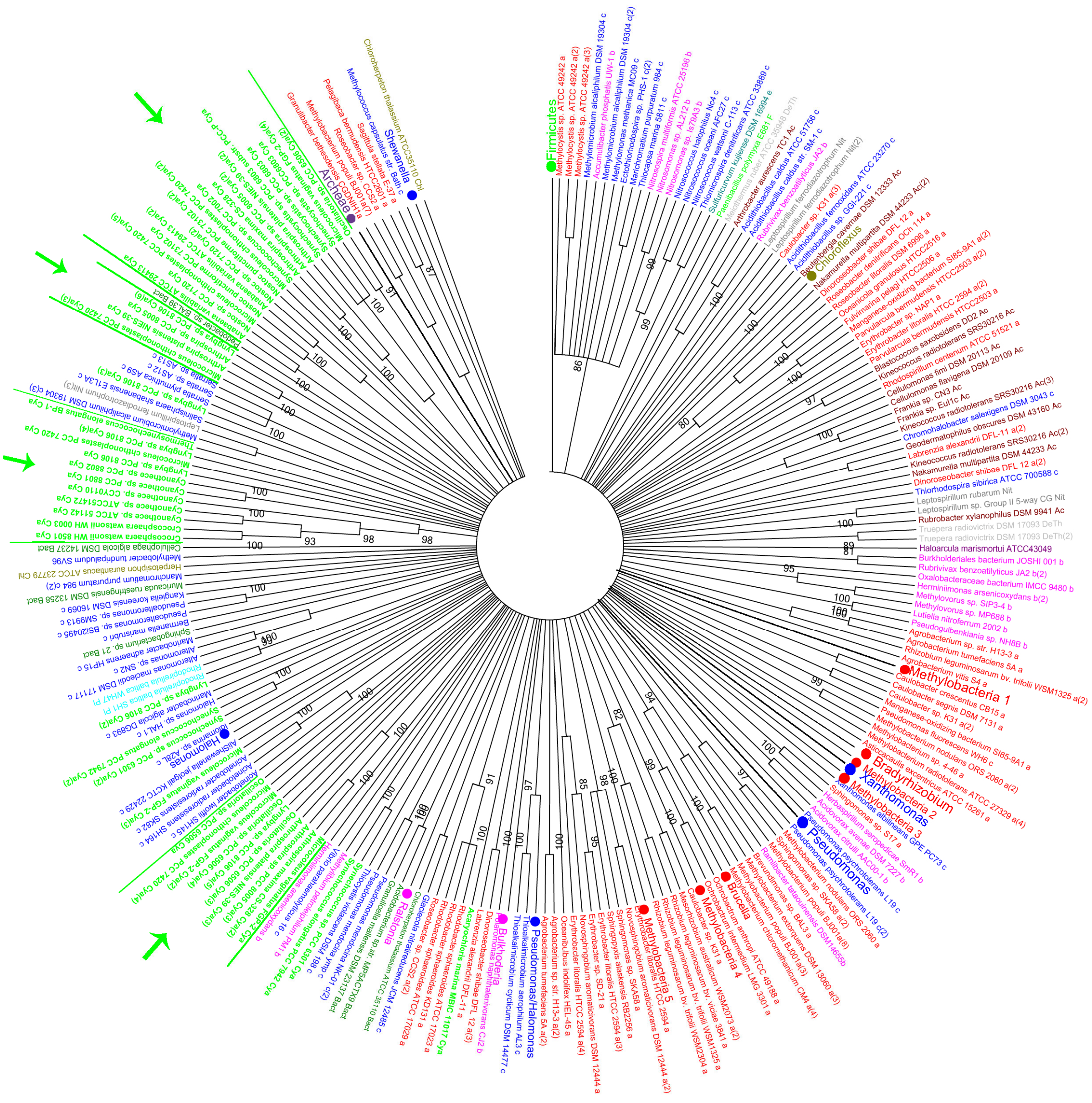

Figure 3.29. p-distance LOV domains tree. Only bootstraps values > 80 are shown. Color code: light green, Firmicutes and Cyanobacteria; red, alphaproteobacteria and Acidobacteria; magenta, betaproteobacteria; blue, gammaproteobacteria; Steel blue, epsilonproteobacteria and Spirochaetes; light gray, Deinococcus-Thermus; brown, Actinobacteria; gray, Nitrospirae; gold, Chloroflexi; purple, Euryarchaeota; green, Bacteroidetes/Chlorobi; cyan, Planctomycetes; navy, Lentisphaerae; yellow, Verrucomicrobia; purple, uncultured.

The same analysis was applied to BLUF sequences to uncover similarity or differences with clusters identified in the overall LOV domains trees. We submit the trees obtained to 1,000 bootstrapping cycles to test the accuracy of the branching patterns. The results is shown in Figure 3.30.

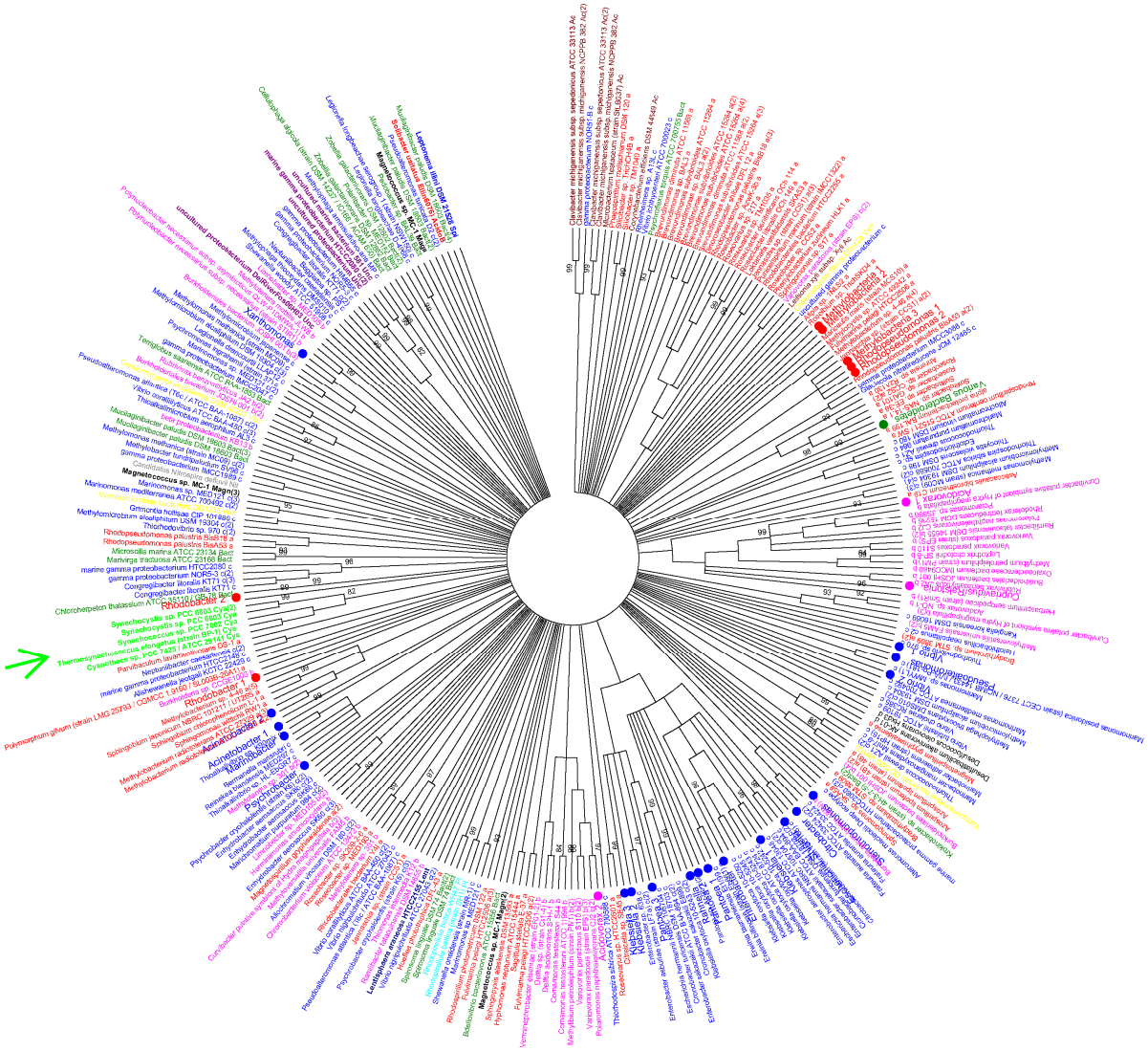

Figure 3.30. p-distance BLUF domains tree. Only bootstraps values > 80 are shown. Color code: light green, Firmicutes and Cyanobacteria; red, alphaproteobacteria and Acidobacteria; magenta, betaproteobacteria; blue, gammaproteobacteria; Steel blue, epsilonproteobacteria and Spirochaetes; light gray, Deinococcus-Thermus; brown, Actinobacteria; gray, Nitrospirae; gold, Chloroflexi; purple, Euryarchaeota; green, Bacteroidetes/Chlorobi; cyan, Planctomycetes; navy, Lentisphaerae; yellow, Verrucomicrobia; purple, uncultured.

In the trees shown we took into account branches with a bootstrapping value > 40 instead of the usual 70 or 90%, because a considerable amount of information would be lost with a higher threshold. Proteins are indicated via the name of the organisms. In case of multiple domains presence in the same organism MEGA5 puts a default number succession referred to that of the comprehensive tables (see Appendix 1).

It can be seen that bacteria having co-presence of LOV and BLUF domains, fall in the same clusters in both trees, showing that the evolution of these photoreceptors is to some extent parallel to phylogeny.

Notable clusters in LOV distance-tree

All LOV domains from Firmicutes are clustered together except for *P. polymyxa.* The latter separation appears to be functionally driven: proteins from Firmicutes shows mostly two domains, LOV+STAS (Sulphate Transporter and AntiSigma factor antagonist) (Appendix 1) resembling YtvA from *B. subtilis*, whereas the LOV protein from *P. polymyxa* is a phosphatase of the SPOIIE type. Within the large YtvA-like cluster we can see two major sub-groups, corresponding to the majority of Bacillaceae and to Listeriaceae. LOV domains from *B. megaterium*, *P. donghaensis* and *B. seleniti reducens* complete this isolated cluster.

Archaeal LOV domains also remain segregated, despite having different associated functions nevertheless limited to kinases and transcriptional regulators.

Other phyla are not so markedly separated as the Firmicutes and the domain of Archaea, but the sequences examined appear in most cases to cluster according to the functional modules associated to the LOV domain. We give some examples in the following.

Cyanobacterial LOV domains fall in four major clusters, indicated with green arrows in Figure 3.29. From the top, we found a first cluster mainly grouping complex and large GGDEF-EAL proteins, that constitute 60% of cyanobacterial LOV proteins, and a LOV-cyclase from *Microcoleus chthonoplastes*. A second group is a functionally mixed small cluster (GGDEF/EAL and kinases). The third cluster includes simpler proteins built as RR+LOV+GGDEF (RR = response regulator). The fourth cluster groups the majority of cyanobacterial LOV-kinases.

LOV proteins from *Pseudomonadales* have different functional domains and they fall accordingly in different clusters, *P. syringae* and *P. savastanoi* LOV-kinases are all together, whereas *P. putida* and *P. mendocina* have short-LOV and fall together with other gamma-proteobacteria and are all short-LOV.

As for Methylobacteriaceae, a class of alphaproteobacteria amongst the richest in photoreceptors, LOV domains (all linked to His-Kinase domains) appear to be separated according to protein architectures. The different clusters are shown as large red points in Figure 3.29. Methylobacteria 1 and 5 enconpass proteins a LOV+Kinase structure; Methylobacteria 2 and 3 include LOV+Kinase+RR; in Methylobacteria 4 most proteins are build as LOV+PAS+Kinase.

Notable clusters in BLUF distance-tree

The few Cyanobacterial BLUF domains, all belonging to the short-BLUF type, remain segregated. This is different to LOV domains, probably related to the many different functional and regulative domains associated within the full-length proteins in that case.

BLUF domains from Methylobacteriaceae again form separated clusters: Methylobacteria 1 and 2 contain short-BLUF proteins. Interestingly, the species pattern of BLUF-Methylobacteria 1 coincides with LOV- Methylobacteria 3 (*M. chloromethanicum*, different strains of *M. extorquens*, *M. populi*, *M. radiotolerans*) There is also a large cluster encompassing Methylobacteria 3 and proteins from different proteobacteria classes.

An interesting cluster is composed by various Bulkhoderiales (betaproteobacteria) with *A. biprosthecum* C19 which is a *Caulobacterales* alphaproteobacterium. Most species of this group have only BLUF proteins among the three classes analyzed here, with the exception of *R. tataouinensis* DSM 14655, *O. bacterium* IMCC9480 and *M. petroleiphilum* PM1 (Appendix 1). Within this cluster we can identify two set of species equal to LOV-tree: *B. bacterium* JOSHI 001 is with *R. benzoatilyticus* JA2 and *Acidovorax avenae* ATCC 19860 is together with *A. avenae sub. Citrulli* AAC00-1.

Another important protein architecture is built of BLUF+EAL domains. *Klebsiella* 1, *Enterobacter, Pantoea* 1,2, *Klebsiella* 2,3 and *Escherichia/ Shigella* contain protein of this kind and are together in a cluster with Citrobacter, Cronobacter, Rahnella and Erwinia. According to this structure there is also a little cluster formed by *B. avium* and *F. aurantia*.

AppA proteins built of BLUF+SCHIC domains are restricted to the various sequenced strains of *Rhodobacter sphaeroides*. Their BLUF domains segregate in a cluster denominated *Rhodobacter* 1 (Figure 3.30).

Comparison between distance and maximum parsimony trees

To test the validity of distance-trees we use another method to obtain topology, namely the maximum-parsimony method [26] given the high degree of similarity among the sequences analyzed. Clusters that are conserved in both trees and that have high bootstrap values are considered reliable. In general clusters are quite conserved between the two types of trees (see Figure 3.31 and Figure 3.32) but there are differences in the precise location of branches with lower bootstrap values (40-70%). This is expected because there we haven't enough phylogenetic information so we can't distinguish exactly among taxa. For LOV domains smaller cluster are conserved, having high bootstrap values in both types of tree, instead there are major differences in larger clusters. As for BLUF trees we can observe that most of small and large clusters are conserved. In general we can be sure of most of the branching patterns obtained, even if we haven't enough information to discriminate particular dichotomies.

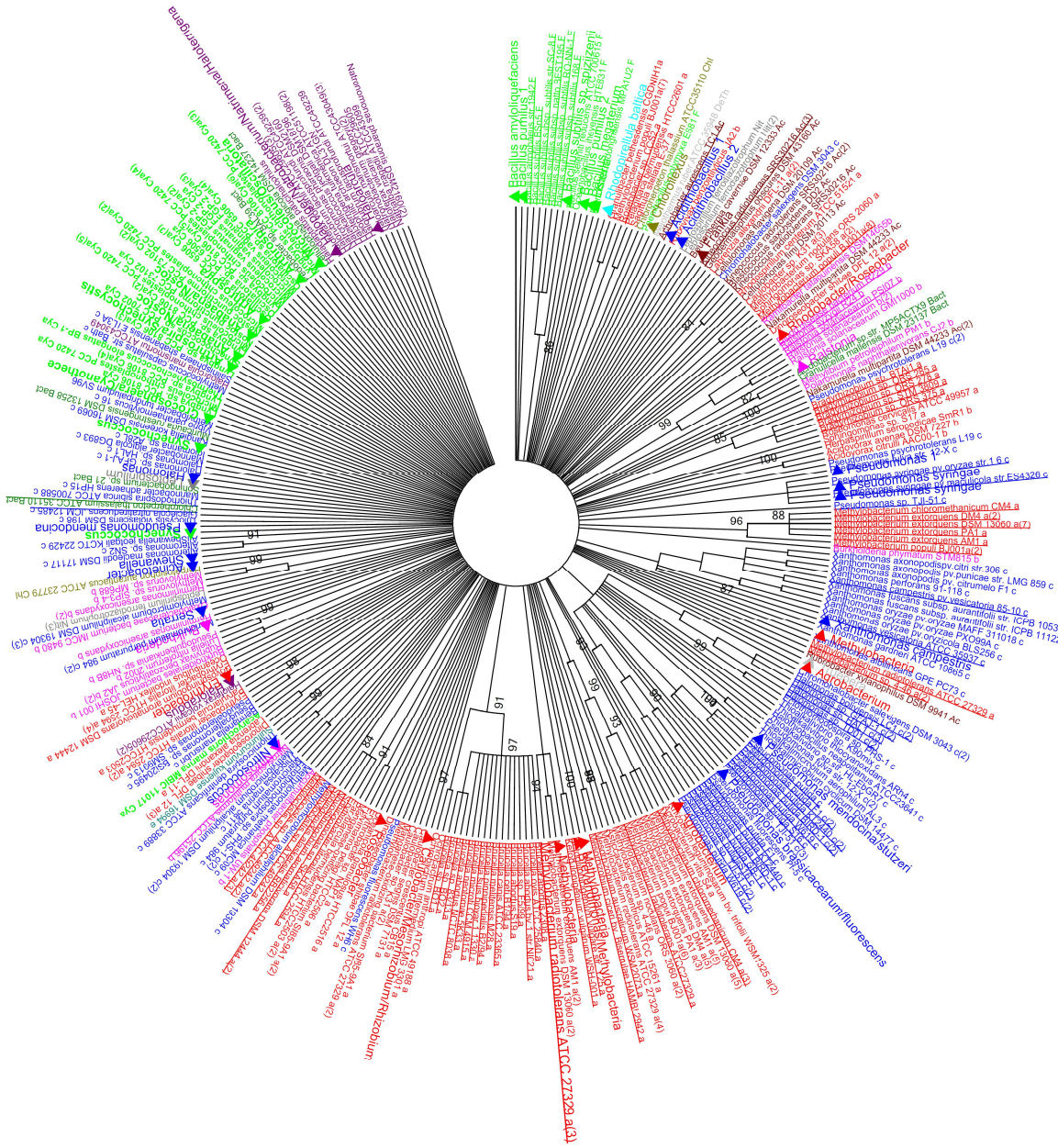

Figure 3.31. Maximum- parsimony LOV domains tree. Only bootstraps values > 80 are shown. Color code: light green, Firmicutes and Cyanobacteria; red, alphaproteobacteria and Acidobacteria; magenta, betaproteobacteria; blue, gammaproteobacteria; Steel blue, epsilonproteobacteria and Spirochaetes; light gray, Deinococcus-Thermus; brown, Actinobacteria; gray, Nitrospirae; gold, Chloroflexi; purple, Euryarchaeota; green, Bacteroidetes/Chlorobi; cyan, Planctomycetes; navy, Lentisphaerae; yellow, Verrucomicrobia; purple, uncultured.

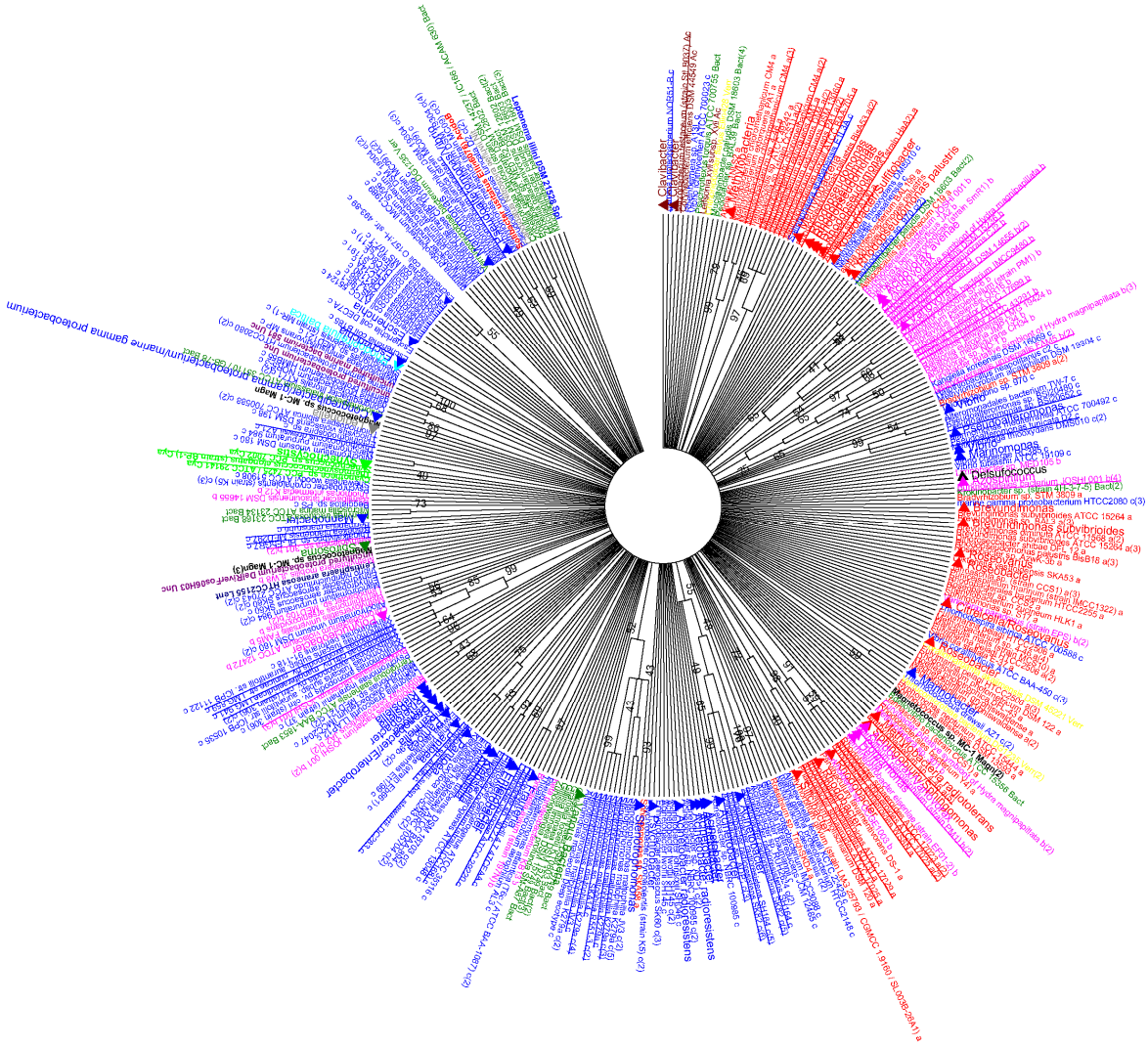

Figure 3.32. Maximum- parsimony BLUF domains tree. Only bootstraps values > 80 are shown. Color code: light green, Firmicutes and Cyanobacteria; red, alphaproteobacteria and Acidobacteria; magenta, betaproteobacteria; blue, gammaproteobacteria; Steel blue, epsilonproteobacteria and Spirochaetes; light gray, Deinococcus-Thermus; brown, Actinobacteria; gray, Nitrospirae; gold, Chloroflexi; purple, Euryarchaeota; green, Bacteroidetes/Chlorobi; cyan, Planctomycetes; navy, Lentisphaerae; yellow, Verrucomicrobia; purple, uncultured.

3.7.3 Optimization of sequence search: sequence LOGOs for LOV and BLUF domains

Crucial step in phylogenetic analysis of photoreceptors is to obtain aligned sequences with corresponding aminoacids for fotochemistry. We tried to perform this first search using another algorithm which allows us to include criterion more stringent. We did database mining for prokaryotic Fl-Blues by using sequence logos and search patterns that significantly facilitate the search.

Surveys in databases yield so-called sequence logos, obtained from an alignment of ca. 2000 proteins (eukaryotic and prokaryotic), for each of the two photosensing domains (Figure 3.33). It is evident that, beyond the essential presence of amino acids functional to the photocycle, other residues are highly conserved. From these residues we built sequence patterns that highly facilitated the subsequent search for prokaryotic LOV and BLUF domains.

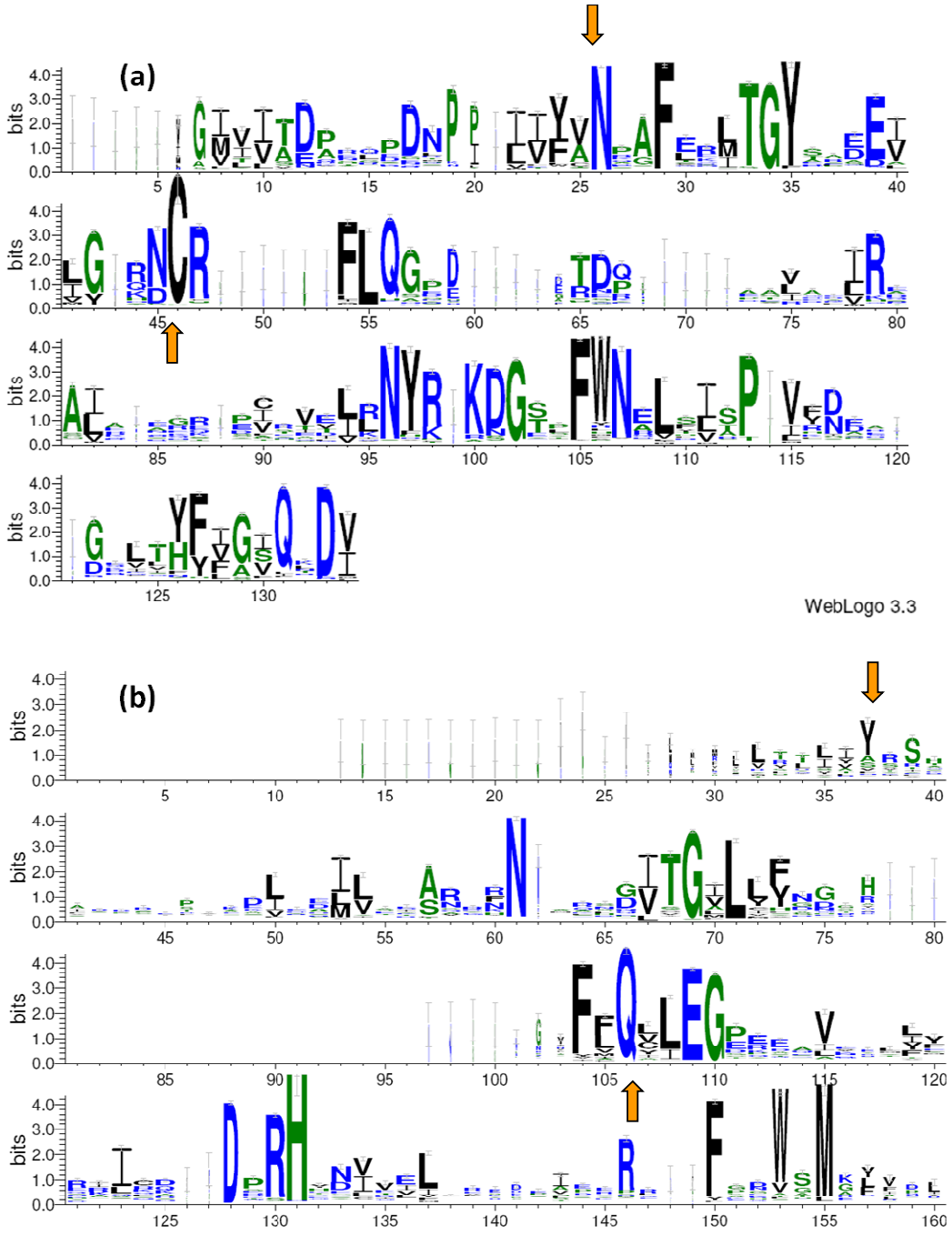

Figure 3.33. Amino acids sequence logos [27], [28] for (a) LOV and (b) BLUF domains. The vertical axis gives the value of Shannon entropy expressed in bits, the horizontal axis lists the aa number of the primary structure. Colors of the one-letter codes are related to the hydrophobicity: blue, hydrophilic aa (R, K, D, E, N, Q) green, neutral (S, G, H, T, A,P), black, hydrophobic (Y, V, M, C, L, F, I, W). Orange arrows mark the beginning and end of the interval used to define the subsequent search patterns.

Using PHI-BLAST and a threshold of 10 at point of 31 October 2013 we found 1390 LOV-proteins in 658 bacterial species/strains and 167 proteins in 82 archeal species instead 1705 BLUF sequences in 453 bacterial species/strains. We reassumed our results in histogram in Figure 3.34.

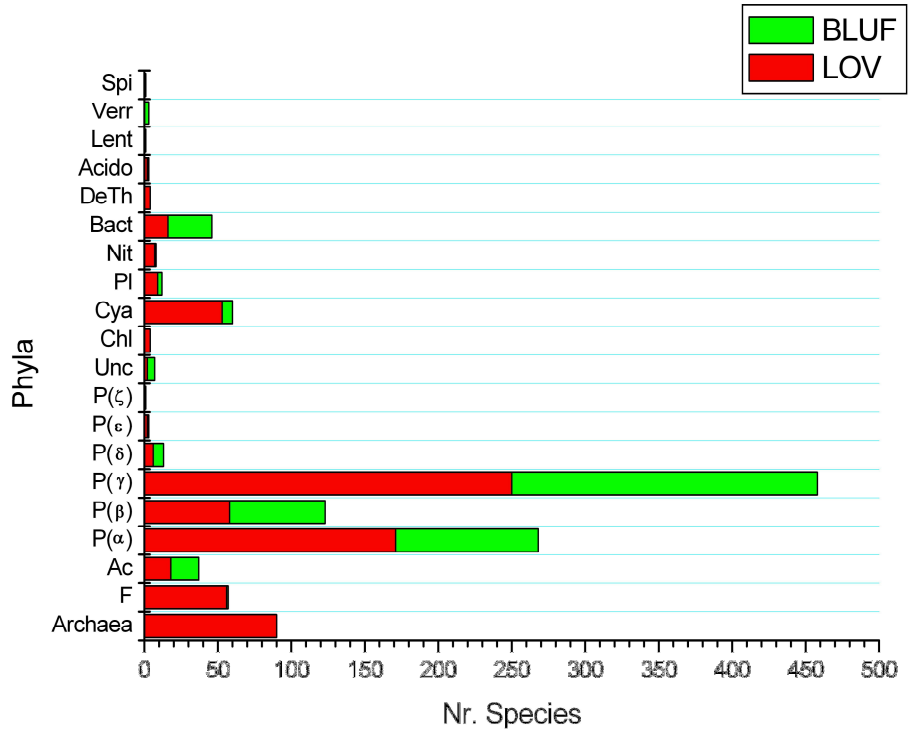

Figure 3.34. Histogram of distribution for species bearing at least one LOV (red) or/and one BLUF (green) protein in the diverse phyla (for proteobacteria also classes are given). Spi = Spirochaetes; Verr = Verrucomicrobia; Lent = Lentisphaerae; Acido = Acidobacteria; DeTh = Deinococcus-Thermus; Bact = Bacteroidetes/Chlorobi; Nit = Nitrospirae; Pl = Planctomycetes; Cya = Cyanobacteria; Chl = Chloroflexi; Unc = Uncultured; P = Proteobacteria; Ac =Actinobacteria; F = Firmicutes; see Appendix1 for a detailed list.

As for domains the LOV and BLUF scenario for the superkingdom of bacteria was very different but it is very similar to the first search presented above. Of the 1390 LOV proteins detected, ca. 50% are HK of the two-component systems [29], in some cases built with additional sensing and regulatory domains (Table 3.6). PAS domains, the superfamily to which LOV domains belong [30] are often present, possibly with a regulative function or further sensing function. About 18% bacterial LOV proteins bear GGDEF or GGDEF+EAL domains that act as cyclases and phosphodiesterases for c-di-GMP formation or hydrolysis [25]. Short-LOV proteins are present in about the same percentage, whereas 8,5% of the proteins are YtvA-like, solely found in the Firmicutes. Only 8 proteins carry a HTH motif for DNA-binding, in HTH+LOV or LOV+HTH arrangements, configuring one-component systems [31]. Also, 20 proteins are one-component systems where a LOV domain is directly linked to a response regulator (RR).

Instead BLUF proteins are dominated by short-proteins (64%) and by the large occurrence of EAL domains (34%), putatively involved in c-di-GMP metabolism, sometimes these domains are degenerated and enzymatically inactive EAL domains, as illustrated above for YcgF in *E.*

coli [32] (Appendix 1). A notable new entry is a BLUF protein found in *Enterococcus gallinarum*, the first of this type in a member of the phylum Firmicutes.

Table 3.6: major associated functions to prokaryotic LOV and BLUF domains.

Bacteria	Tot.	His-Kinase	GGDEF /EAL	Phosphatase	HtH	RR	"Short"
LOV	1390	704 (51%)	250 (18%) (54)	18 (1%)	10 (1%)	31 (2%)	258 (18%)
BLUF	1705	-	580 (34%) (5GGDEF) (12 +)	-	5(<1%)	-	1098 (64%)
Archaea						-	
LOV	167	107 (64%)	-	-	51 (31%)	9(<1%)	-

In 162 species/strains both LOV and BLUF proteins are present. Some major examples of bacteria literally “packed” with LOV and BLUF proteins are given in Table 3.7. There are presently no hints about the molecular functioning of a possible BL-sensing network in these organisms. We recall that the largest co-presence of soluble photoreceptors in Bacteria is given by the LOV and bilin-GAF superfamilies [33].

Table 3.7: Examples of bacteria having multiple LOV and BLUF proteins in co-presence.

	Class (phylum) /order	LOV proteins	BLUF proteins
Aureimonas ureilytica	P(α)/Rhizobiales	2X LOV-HK	2 X short-BLUF
Methylobacterium populi[a]	P(α)/Rhizobiales	7XLOV-HK 1 X short LOV	2 X short-BLUF
Sphingobium xenophagum	P(α)/ Sphingomonadales	2 X LOV-RR 1 X LOV-HK	2 X short-BLUF
Herminiimonas arsenicoxydans	P(β)/ Burkholderiales	3XLOV-GGDEF/EAL	1 X short-BLUF
Methylomicrobium alcaliphilum	P(γ)/ Methylococcales	2 Xshort LOV 1X LOV-HK	3 X short-BLUF 1 X BLUF-GGDEF/EAL

[a]: all bacteria of the genus *Methylobacterium* are rich in LOV, BLUF and bilin-binding domains (see Appendix 1).

Application of above outlined search criteria yielded 167 archaeal LOV proteins in 85 species of Euryarchaeota, belonging to the two classes of *Halobacteria* and, screened for the first time, *Methanomicrobia*. The most striking difference between archaeal and bacterial LOV proteins is that a large percentage (30%) of the halobacterial protagonists carry fused HTH effector domains (all from *Halobacteria*), whereas this motif is found in only 0.6% of all bacteria. The general architecture of these putative photo-regulated DNA-binding proteins is depicted in Figure 3.35 and can be generalized as (RR/GAF/ or PAS)+LOV+*n*PAS+*k*GAF+HTH, with n = 0-8, *and* k = 0-2, where: RR = response regulator, receiver domain; PAS (the same fold as LOV domains); GAF = domain found in cGMP-specific phosphodiesterases, cyanobacterial adenylate cyclases, and formate hydrogen lyase transcription activator FhlA [34] (see Appendix1 for a detailed legenda). One of the detected arrangements closely resembles the *Bat* protein of *Halobacterium salinarum*, a redox- and putatively light-sensing transcription regulator that mediates production of bacteriorhodopsin in the purple membrane [35]. *H. salinarum* Bat bears a PAS domain lacking the reactive cysteine of canonical LOV proteins. The remaining archaeal proteins are LOV-kinases of the two-component systems [29], with solely RR, GAF and PAS domains as additional building units. We note that none of the archaeal LOV proteins have been investigated so far.

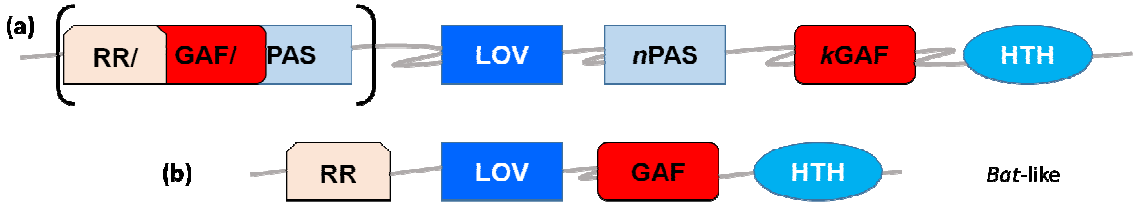

Figure 3.35. (a) General architecture for archaeal LOV-HTH proteins: in most cases a photosensing LOV domain is preceded by a response regulator (RR), a GAF or a PAS domain, and followed by a variable number of PAS (n = 0-8) and GAF (k = 0-2) domains; at the C-terminus of the protein, there is a DNA-binding domain of the helix-turn-helix (HTH) type. **(b)** One of the arrangements detected resembles the Bat protein of *Halobacterium salinarum*, a redox-sensing transcription regulator that has been reported to mediate production of bacteriorhodopsin in the purple membrane [35]. *H. salinarum* Bat has been described as a putative light-sensor, but it does not bear the cysteine involved in the photocycle of LOV domains.

The distance-tree built with archaeal LOV domains (Figure 3.36) again depicts a scenario different from the bacterial ones, for which major deteminants for group clustering were the effector/regulative domains associated to the photosensing units [33]. In the case of Archaea, LOV domains of *Methanomicrobia* cluster separately from *Halobacteria*, emphasizing the difference in metabolism and habitats for these two classes. It is still too early, nevertheless, to draw any stringent conclusion on the evolutionary history of LOV domains in Archaea, given that up to now only two classes are represented.

Figure 3.36. Unrooted distance tree for archaeal LOV domains, obtained with the neighboring-joining algorithm. On the nodes we report the bootstrap values >80; red branches are related to Halobacteria; purple lines mark Methanomicrobia that cluster separately as a class.

3.7.4 From sequence to function: hints from *in silico* analysis

In the following we report a STRING analysis of YtvA from *B. subtilis*, to search for functional relatives and gain further hints for its function within the cell. STRING is a database that includes known and predicted protein-protein interactions, of functional and/or physical origin [36] (see paragraph 2.6 in Materials and Methods). From STRING analysis we found actually that YtvA is strictly related to (Figure 37):

- rsbT (133 aa), a switch protein/serine-threonine kinase that controls the activity of the stressosome providing the crucial link between the upstream module (communication of environmental stress) and the downstream module (integration of the environmental signals with signals of energy stress) that compose the signal transduction pathway controlling the altyernative transcription factor σ^B. RsbT phosphorylates and inactivates its specific antagonist protein rsbS thanks to its serine kinase activity. Upon phosphorylation of rsbS, rsbT is released to stimulate rsbU, a PP2C phosphatase, thereby initiating the signaling cascade;
- rsbS (121 aa), an antagonist of rsbT and a negative regulator of σ^B activity. Non-phosphorylated rsbS binds to rsbT, preventing its association with rsbU. It requires any one of rsbRA, rsbRB, rsbRC or rsbRD to sequester rsbT. When rsbS and the rsbR paralog(s) are phosphorylated, they release rsbT, which can then bind and activate rsbU;
- rsbP (403 aa), a serine phosphatase and a positive regulator of σ^B activity. It dephosphorylates rsbV in response to an energy stress;
- rsbU (335 aa), a serine phosphatise and a positive regulator of σ^B activity. It dephosphorylates rsbV in response to environmental stress conveyed from the rsbXST module;
- rsbV (109 aa), an anti-anti-sigma factor (antagonist of rsbW) and a positive regulator of σ^B activity. Non- phosphorylated rsbV binds to rsbW, preventing its association with σ^B. Once phosphorylated, rsbVreleases rsbW, which is then free to complex with and inactivate σB;
- rsbX (199 aa), a serine phosphatase and a negative regulator of σ^B activity. It dephosphorylates rsbS and plays a role both in maintaining low σ^B activity during growth and in reestablishing prestress σ^B activity after induction. It could have a negative feedback role by indirectly communicating σ^B protein levels;

- rsbQ (269 aa), a regulator of RsbP phosphatise and a positive regulator required for energy stress activation of the σ^B transcription factor. It could be required for rsbP phosphatase activity;
- rsbW (160 aa), a serine-protein kinase RsbW and a negative regulator of σ^B activity. It phosphorylates and inactivates its specific antagonist protein, rsbV. Upon phosphorylation of rsbV, rsbW is released and binds to σ^B, thereby blocking its ability to form an RNA polymerase holoenzyme (E-σ^B).

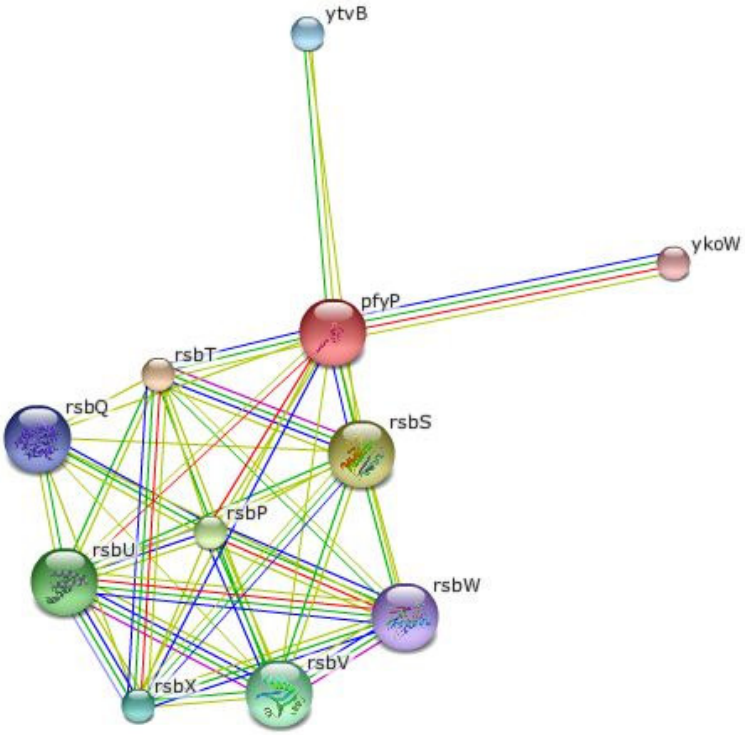

Figure 37. Network between YtvA (or pfyP =photoactive flavin yellow protein) and proteins related to it by genic neighbourhood (green lines), by gene fusion (red lines), co-occurrence (blue lines) and text-miming (olive-green).

The proteins more linked to YtvA are rsbT, rsbS and rsbP, that are involved in the first steps of stressosome-mediated responses. We could observe that genes codifying proteins involved in stessosome's response are co-expressed with high sequence conservation (black squares) in Bacilli but also in other Firmicutes (*O. iheyensis* and Listeriae) (Figure 38). In others organisms belonging to different phyla there isn't co-expression of genes and homology of sequence (pink or white squares).

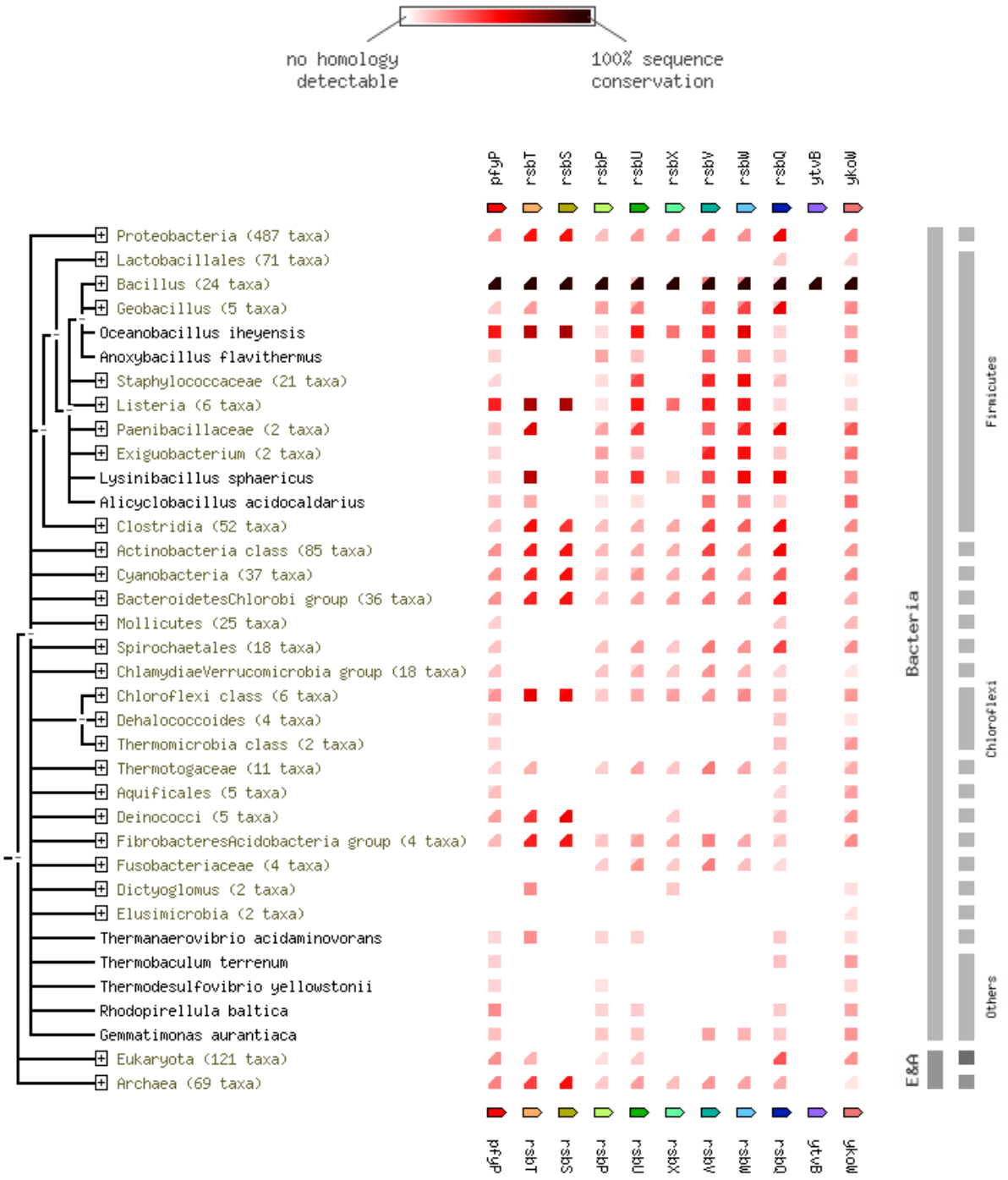

Figure 38. Co-presence of genes in prokariotic genomes.

These genes are also neighbour in Firmicutes DNA so we can say that they are probably functionally related (Figure 39). Furthermore they are the sole organisms with YtvA-like proteins built with a LOV and a STAS domain. We can conclude that combination of these proteins is specific for *Bacilli* and for *Firmicute*s in general.

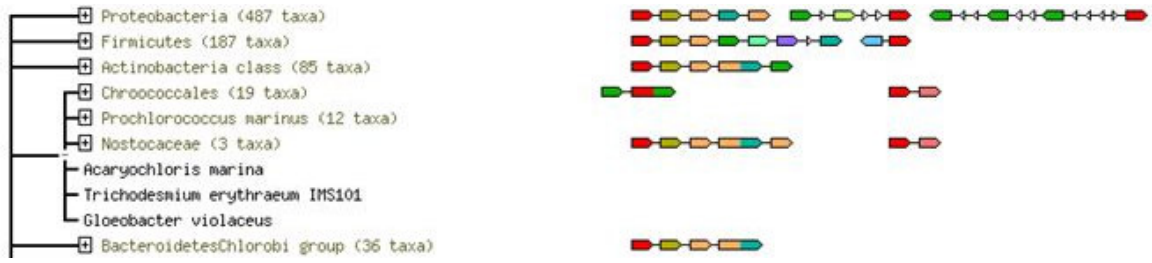

Figure 39. Neighbourhood of genes.

Chapter bibliography

[1] van den Berg P., A., W., Widengren, J., Hink, M., A., Rigler, R., Visser, A., G., "Fluorescence correlation spectroscopy of flavins and flavoenzymes: photochemical and photophysical aspects.," *Spectrochim.Acta A*, vol. 57, pp. 2135–2144, 2001.

[2] Koziol B., Markowicz B., Kruk M., Plytycz J., "Riboflavin as a Source of Autofluorescence in Eisenia fetida Coelomocytes," *Photochem. Photobiol.*, vol. 82, pp. 570–573, 2006.

[3] Berezin M. Y., Achilefu S., "Fluorescence Lifetime Measurements and Biological Imaging.," *Chem. Rev.*, vol. 110, pp. 2641–2684, 2010.

[4] Kennis J. T. M., van Stokkum I. H. M., Crosson S., Gauden M., Moffat K.and van Grondelle R., "The LOV2 domain of phototropin: a reversible photochromic switch," *J. Am. Chem. Soc.*, vol. 126, pp. 4512–4513, 2004.

[5] Voliani V., Bizzarri R., Nifosì R., Abbruzzetti S., Grandi E., Viappiani C., Beltram F., "Cis–Trans Photoisomerization of Fluorescent-Protein Chromophores.," *J. Phys. Chem. B*, vol. 112, no. 34, pp. 10714–10722, 2008.

[6] Bizzarri R., Serresi M., Cardarelli F., Abbruzzetti S., Campanini B., Viappiani C., Beltram F., "Single Amino Acid Replacement Makes Aequorea victoria Fluorescent Proteins Reversibly Photoswitchable.," *JACS*, vol. 132, no. 1, pp. 85–95, 2010.

[7] Losi A., Polverini E., Quest B., and Gärtner W., "First Evidence for Phototropin-Related Blue-Light Receptors in Prokaryotes," *Biophys. J.*, vol. 82, no. May, pp. 2627–2634, 2002.

[8] Losi A., Quest B., Gärtner W., "Listening to the blue: the time-resolved thermodynamics of the bacterial blue-light receptor YtvA and its isolated LOV domain.," *Photochem. Photobiol. Sci.*, vol. 2, pp. 759–766, 2003.

[9] Hess S. T., Girirajan T. P. K., and Mason M. D., "Ultra-high resolution imaging by fluorescence photoactivation localization microscopy.," *Biophys. J.*, vol. 91, no. 11, pp. 4258–72, Dec. 2006.

[10] Raffelberg S., Mansurova M., Gärtner W., and Losi A., "Modulation of the photocycle of a LOV domain photoreceptor by the hydrogen-bonding network.," *J. Am. Chem. Soc.*, vol. 133, no. 14, pp. 5346–56, Apr. 2011.

[11] Climent T., Gonza R., and Mercha M., "Theoretical Insight into the Spectroscopy and Photochemistry of Isoalloxazine , the Flavin Core Ring," *J. Phys. Chem. A*, vol. 110, pp. 13584–13590, 2006.

[12] Penzkofer A., Bansal A. K., Song S. H., and Dick B., "Fluorescence quenching of flavins by reductive agents.," *Chem.Phys.*, vol. 336, pp. 14–21, 2007.

[13] Losi A., Gärtner W., Raffelberg S., Cella Zanacchi F., Bianchini P., Diaspro A., Mandalari C., Abbruzzetti S., and Viappiani C., "A photochromic bacterial photoreceptor with potential for super-resolution microscopy.," *Photochem. Photobiol. Sci.*, vol. 12, no. 2, pp. 231–5, Feb. 2013.

[14] Tsentalovich, Y. P., Lopez, J. J., Hore, P. J., and Sagdeev, R. Z., "Mechanisms of reactions of flavin mononucleotide triplet with aromatic amino acids.," *Spectrochim.Acta A*, vol. 58[9], pp. 2043–2050, 2002.

[15] Tang Y., Cao Z., Livoti E., Krauss U., Jaeger K.-E., Gärtner W., and Losi A., "Interdomain signalling in the blue-light sensing and GTP-binding protein YtvA: a mutagenesis study uncovering the importance of specific protein sites.," *Photochem. Photobiol. Sci.*, vol. 9, pp. 47–56, 2010.

[16] Raffelberg, S., Gutt, A., Gärtner, W., Mandalari, C., Abbruzzetti, S., Viappiani C., Losi, A., "The amino acids surrounding the flavin 7a-methyl group determine the UVA spectral features of a LOV protein," *Biol. Chem.*, vol. 394, pp. 1517–1528, 2013.

[17] Losi A. and Gärtner W., "Bacterial bilin- and flavin-binding photoreceptors.," *Photochem. Photobiol. Sci.*, vol. 7, pp. 1168–1178, 2008.

[18] Ito S.,. Song Y. H, and Imaizumi T., "LOV Domain-Containing F-Box Proteins : Light-Dependent Protein Degradation Modules in Arabidopsis," vol. 2, no. January, pp. 1–10, 2012.

[19] Atamna-Ismaeel N. , Finkel O., Glaser F., von Mering C. and Vorholt J. A., Koblizek M., Belkin S. and Beja O., "Bacterial anoxygenic 45 photosynthesis on plant leaf surfaces.," *Environ. Microbiol. Rep.*, vol. 4, pp. 209–216, 2012.

[20] Yutin N. and Koonin E., "Proteorhodopsin genes in giant viruses.," *Biol. Direct*, vol. 7, p. 34, 2012.

[21] Domains H. S., Moskvin O. V, and Gomelsky M., "The PpaA / AerR Regulators of Photosynthesis Gene Expression from Anoxygenic Phototrophic Proteobacteria Contain Heme-binding SCHICH domains," *J. Bacteriol*, vol. 192, no. 19, pp. 5253–5256, 2010.

[22] Stierl M., Stumpf P., Gueta R., Hagedorn R., Gärtner W., Petereit L., Efetova M., Schwarzel M., Oertner G., Nagel G., and Hegemann P., "Light Modulation of Cellular cAMP by a Small Bacterial Photoactivated Adenylyl Cyclase , bPAC , of the Soil Bacterium," 2011.

[23] West A. H. and Stock A. M., "Histidine kinases and response regulator proteins in two-component signaling systems.," *Trends Biochem. Sci.*, vol. 26, pp. 369–376, 2001.

[24] Szurmant H., White R. A. and Hoch J. A., "Sensor complexes regulating two-component signal transduction.," *Curr. Opin. Struct. Biol.*, vol. 17, pp. 706–715, 2007.

[25] Sondermann H., Shikuma N. J., and Yildiz F. H., "You've come a long way: c-di-GMP signaling," *Curr. Opin. Microbiol.*, vol. 15, no. 2, pp. 140–146, 2012.

[26] Mount D. W., "Maximum Parsimony Method for Phylogenetic Prediction.," *CSH Prot.*, 2008.

[27] Schneider, T.D. and Stephens, R.M., "Sequence Logos: A New Way to Display Consensus Sequences.," *Nucleic Acids Res.*, vol. 18, pp. 6097–6100, 1990.

[28] Crooks, G.E.; Hon, G.; Chandonia, J.M.; Brenner, S.E., "WebLogo: A Sequence Logo Generator.," *Genome Res.*, vol. 14, pp. 1188–1190, 2004.

[29] Hoch J. A., "Two-component and phosphorelay signal transduction.," *Curr. Op. Microbiol*, vol. 3, pp. 165–170, 2000.

[30] Hefti J., Francoijs M.H., de Vries K.J., Dixon S.C., Vervoort R., "The PAS fold: A redefinition of the PAS domain based upon structural prediction.," *FEBS J.*, vol. 271, pp. 1198–1208, 2004.

[31] Ulrich L. E., Koonin E. V, and Zhulin I. B., "One-component systems dominate signal transduction in prokaryotes," vol. 13, no. 2, pp. 52–56, 2005.

[32] Tschowri N., Busse S., and Hengge R., "The BLUF-EAL protein YcgF acts as a direct anti-repressor in a blue-light response of *Escherichia coli*," pp. 522–534, 2009.

[33] Mandalari C., Losi A., Gärtner W., "Distance-tree analysis, distribution and co-presence of bilin- and flavin-binding prokaryotic photoreceptors for visible light," *Photochem. Photobiol. Sci.*, vol. 12, pp. 1144–1157, 2013.

[34] Sigrist P., C.J.; Cerutti, L.; Hulo, N.; Gattiker, A.; Falquet, L.; Pagni, M.; Bairoch, A.; Bucher, "PROSITE: a documented database using patterns and profiles as motif descriptors.," *Br. Bioinf.*, vol. 3, pp. 265–274, 2002.

[35] Baliga N. S., Pan M., Goo Y. A., Yi E. C., Goodlett D. R., Dimitrov K., Shannon P., Aebersold R., Ng W. V., and Hood L., "Coordinate regulation of energy transduction modules in Halobacterium sp . analyzed by a global systems approach," vol. 99, no. 23, pp. 14913–14918, 2002.

[36] Franceschini A., Szklarczyk D., Frankild S., Kuhn M., Simonovic M., Roth A., Lin J., Minguez P., Bork P., von Mering C., and Jensen L. J., "STRING v9.1: protein-protein interaction networks, with increased coverage and integration.," *Nucleic Acids Res.*, vol. 41, no. Database issue, pp. D808–15, Jan. 2013.

4. Conclusions

The multiple approach employed in this work to study Fl-Blues, has brought to several novel results, opening at the same time new questions and future perspectives.

Photochromism of the LOV protein YtvA from *B. subtilis* has been fully characterized here, including the associated quantum efficieny and the first super-resolution measurements in living cells. The broad variety of LOV domains, with respect to their photocycle dynamics and functional roles, make this class of photoreceptors promising tools for the above depicted applications, clearly shown here for YtvA [1]. This is especially advantageous when taking their small size and their high thermal and photochemical stability into account (Figure 3.11 in par. 3.2 Results section). Although super-resolution experiments reported here exploited just the wild type photoreceptor expressed in *Escherichia coli*, it can be seen that the localization precision of ca. 35 nm obtained with YtvA is at least comparable to those reported for photoconvertible GFP-derivatives. The development of chimeric structures with suitable peptides will allow labelling specific cellular structures. Furthermore, given that LOV proteins are hypoxia tolerant, different to the chromophore of GFP that needs oxygen to develop [2], YtvA and other LOV domains could be employed for super-resolution experiments also in anaerobic or microaerobic cells/compartments. A further development could be represented by the detection and localization of these novel bacterial photoreceptors within their natural hosts, that would be of great help in understanding their functions and relevance. In addition, these biological photoreceptors exhibit double application potential: besides being tools for super-resolution microscopies, their photo-switching ability, if connected to an on-/off-regulation of fused enzyme activities (as found naturally occurring in many photoreceptors), opens perspectives for new paradigms in optogenetics (Table 3.6). Photoinduced switching between the YtvAD and YtvAL states allows controlling the activity of the photoreceptor and it is foreseen that tuning of photochemical and fluorescence emission yields by engineered mutations, will improve control of the functional states of coupled enzymatic units.

This tuning attempts have been initiated in this work, with the analysis of several mutated YtvA proteins (par. 3.5). To try to optimize optical parameters and photocycle dynamics, we mutated amino acids interacting with FMN, several of which affect the dynamics of the photocycle and, in some cases, the quantum yields of adduct formation (Tables 3.1 and 3.2).

A net of hydrogen bonds formed around the chromophore by polar amino acids, had been previously shown to largely modulate the photocycle of YtvA [3]. Here we identified an amino acid localized in close vicinity to the C(7a) atom of FMN (T30 in YtvA), i.e. at the apolar part of the isoalloxazine ring, as a major determinant for the spectral features of the LOV protein YtvA in the UVA range [4] (Figure 3.17). Its substitution with an apolar residue, such as alanine, converts a typical *As*phot-LOV2-like spectrum into a LOV1-like spectrum. N37, although important for the duration of the photocycle as previously reported for the equivalent N425 position in *As*phot1-LOV2 [5], does not seem to be involved in spectral tuning.

The quite large blue shift in the UVA range, induced in YtvA by T30A and N94A substitutions, is in line with the solvatochromic analysis of FMN (i.e. blue shift in the UVA range with decreased HB-donor ability of the microenvironment) and with the proposed polarization directions for transition II, ca. 350-375 nm [6], [7]. (Figure 4.1).

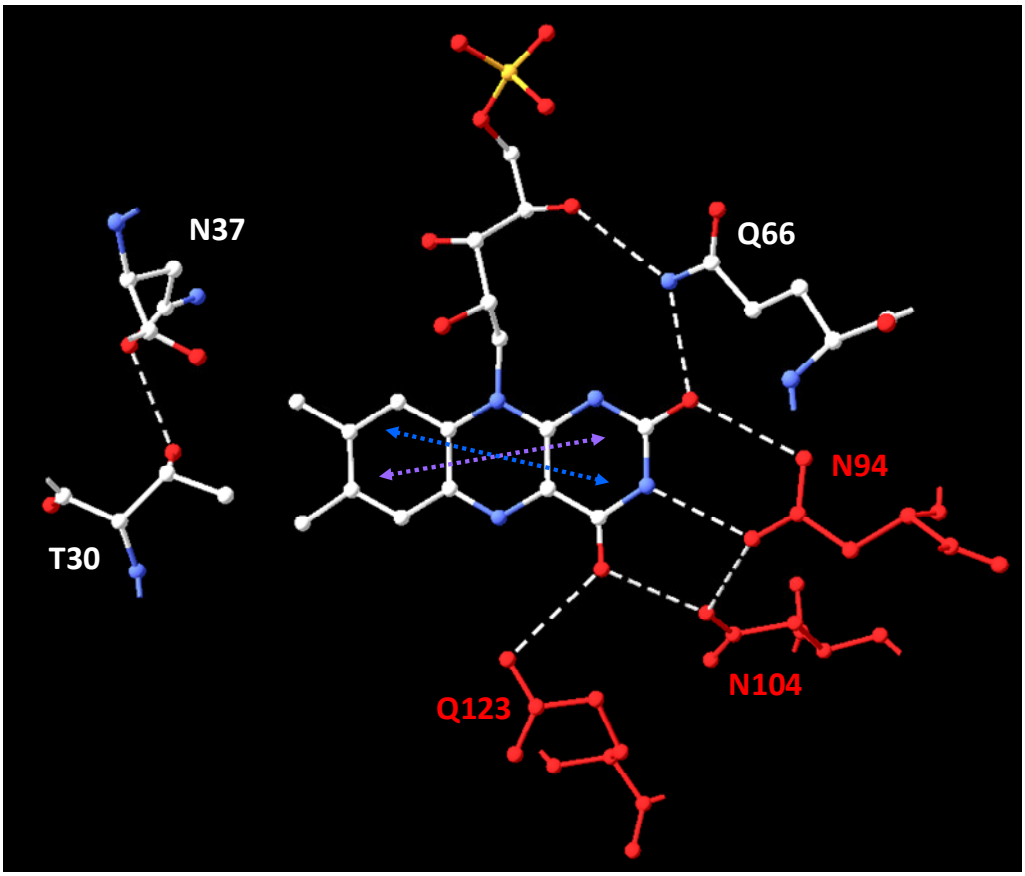

Figure 4. 1. Graphics of the binding cavity in YtvA-LOV (dark adapted state, PDB accession number 2pr5), showing the three residues modified in this work (T30, N37 and Q66) in white; in red, the three polar amino acids form a HB network around the polar part of the isoalloxazine ring in YtvA-LOV that were the subject of a previous investigation [3]. The calculated polarization directions of the low-energy ππ* transitions are also shown, blue, I with λ_{max} at ca. 450 nm; violet, II with λ_{max} at ca. 350-375 nm [6], [7].

The advantage of a mutation at T30 over N94 for tuning the spectral properties of YtvA (or other LOV domains), is the larger stability of the proteins in the former case, comparable to YtvA-WT; N94 is instead important for chromophore stabilization and is, accordingly, part of a pool of 10 super conserved amino acids within the LOV series. A survey of literature data confirms that, in the majority of cases, LOV proteins having a threonine at the position corresponding to T30 in YtvA, exhibit indeed the same UVA pattern, with a maximum at ca. 375 nm [8], [9], [10], [11], [12], [13], [14], [15], whereas a serine, an alanine or a valine in that position results in a phot-LOV1 pattern with a double 350-370 nm peak [8], [13], [16], [17], [18], [19], [20], [21], [22], [23], [24], [25], [26]. There is at least one exception of this observation, namely, the recently published LOV protein from *Listeria monocytogenes* that has a threonine in position 30, but still exhibits a 350-370 nm UVA pattern [27].
The ability to tune spectrally LOV domains might be important for advanced biotechnological applications with such proteins [28], [29], with special emphasis on spectral separation between the dark-adapted state and the adduct, an important aspect to maximize photochromicity [1]. Interestingly, for mutations investigated in this work, the absorption maximum of the adduct is barely affected, also in the case of T30A. Nevertheless, mutations at T30 apparently do not affect the value of Φ_{LD} that is solely increased for R63K, suggesting that localized structural factors might be involved in the process. Surely, for further studies on the photochromism of LOV domains, a wider range should be of proteins should be employed in order to identify criteria for optimization of Φ_{LD}. We note that all examined variants exhibit photochromism and can be brought into a violet/UVA induced photoequilibrium.

Since applications depicted above are supposed to be performed *in vivo*, we started a set of measurements, to follow YtvA photocycle in *E. coli* over-expressing the protein. It could be observed that the dark recovery of dark-state is much faster than for purified proteins and that the process is non-exponential. Soaking cells in a physiological buffer, resulted in a recovery kinetics very similar to that of purified proteins (Figure 3.23 and Table 3.4in par. 3.6). In other words, hydratation seems to affect the photocycle of YtvA expressed in cells.
E. coli cultures over-expressing mutants of YtvA have been also analyzed, pointing in the same direction of a clear drop in the rate constant with decreased hydration levels. Not surprisingly, the mutations affect the HB network and hence are possibly changing the response to the level of hydration. This analysis is still *in fieri* and proposes interesting considerations both from the chemical-physics and applicative points of view. Finally, we note that photoequilibrium-based measurements of fluorescence lifetimes with the confocal

microscope-based methodology, appear to be, for slow-cycling LOV proteins, more reliable and much faster than conventional single photon counting. The latter requires in fact long-lasting measuring times and a larger amount of absorbed photons, thus forming considerable amounts of photoadduct and inducing loss of fluorescence intensity possibly inducing artifacts during fitting of fluorescence deacy curves [12], [30]. Furthermore the methodology reported here has turned to be applicable also to cell cultures.

From the *in silico* analysis we recovered a scenario that underscores the large presence of soluble photoreceptors in the prokaryotic world, even if our knowledge of the physiological role of LOV and BLUF proteins in prokaryotes remain sparse [28]. Novel genome projects have recently brought in some hints as for the functional role of Fl-Blues, that still remain to be largely demonstrated [31]. From this phylogenetic analysis we can try to draw some conclusions about the evolution of the LOV and BLUF photosensing paradigms. Clustering in the distance-trees built according to sequence comparison among the photoperceptive domains, seems to be dictated by two intermixed factors: group proximity and full-protein architecture, i.e. associated effector/regulative domains (Figures 29, 32). The first factor is actually quite loose, and works well only in segregating YtvA-like proteins of the phylum Firmicutes (Figure 3.29) and of the superkingdom Archaea in the LOV-domains tree (Figure 3.35). In particular archeal distance-tree indicates that for LOV domains clustering occurs mainly according to groups, and not in relation to putative molecular functions, that is instead a prominent feature for bacteria [31]. LOV domains of *Methanomicrobia* cluster separately from *Halobacteria*, emphasizing the difference in metabolism and habitats for these two classes. It is still too early, nevertheless, to draw any stringent conclusion on the evolutionary history of LOV domains in Archaea, given that up to now only two classes are represented. Instead, within the superkingdom bacteria, the second factor seems to play a major role, less evident for BLUF proteins that are mostly constituted of standalone photosensing domains. This observation may explain the reported incongruencies observed between the LOV and SSU rRNA phylogenetic trees, and the scattered distribution of LOV domains [32]. It can be seen that bacteria having co-presence of LOV and BLUF domains, fall in the same clusters in both trees, showing that the evolution of these photoreceptors is to some extent parallel to phylogeny.

Up to now we can say that proteins containing LOV and BLUF domains are extremely modular, could have diverse functions in different organisms and could be part of disparate pathways of evolution. Roughly speaking, BL seems to operate both as a stress factor and as a

source of environmental information able to elicit adaptative responses in metabolism, growth patterns, and interactions with other organisms. The functional domain linked to LOV and BLUF are very different from each other, so we can formulate the hypothesis that they tend to be specialized in different metabolic pathways. This observation is important not only to understand evolutionary and specialization pathways, but also for optogenetic applications because it has turned to be very useful to have natural systems able to perform and activate different actions in cells [33].

We have also tried to accelerate the homology search of these domains since the ever growing information of genomic information calls for more elaborate tools to screen new genomes (and metagenomes) for the presence of BL-photoreceptor genes and the identification of their genomic neighborhood. Here we have proposed search patterns based on a sequence logo (Figure 3.33), that is built by identifying conservation of aminoacids in a definite position of a linear chain. Though still in its infancy, search criteria are now being developed that allow a more sophisticated search for potential photoreceptors, and also allow suggesting scenarios by which BL-photoreceptors have an impact on the gene regulation. The usefulness of such search criteria has been demonstrated here for the first time for Archaea in which a manifold of BL-sensing photoreceptors could be identified. None of these archaeal species have been probed so far for their response to and lifestyle changes caused by blue light. It has now to be accepted that the generic stress response mechanisms, well studied in several bacterial species, have now to be extended to blue-light environmental inputs for diverse prokaryotic organisms [34].

Chapter bibliography

[1] Losi A., Gärtner W., Raffelberg S., Cella Zanacchi F. Bianchini P., Diaspro A., Mandalari C., Abbruzzetti S., and Viappiani C., "A photochromic bacterial photoreceptor with potential for super-resolution microscopy.," *Photochem. Photobiol. Sci.*, vol. 12, no. 2, pp. 231–5, Feb. 2013.

[2] Drepper, T.; Gensch, T.; Pohl M., "Advanced in vivo applications of blue light photoreceptors as alternative fluorescent proteins.," *Photochem. Photobiol. Sci.*, vol. 12, pp. 1125–1134, 2013.

[3] Raffelberg S., Mansurova M., Gärtner W., and Losi A., "Modulation of the photocycle of a LOV domain photoreceptor by the hydrogen-bonding network.," *J. Am. Chem. Soc.*, vol. 133, no. 14, pp. 5346–56, Apr. 2011.

[4] Raffelberg, S., Gutt, A., Gärtner, W., Mandalari, C., Abbruzzetti, S., Viappiani C., Losi, A., "The amino acids surrounding the flavin 7a-methyl group determine the UVA spectral features of a LOV protein," *Biol. Chem.*, vol. 394, pp. 1517–1528, 2013.

[5] Brosi R., Illarionov B., Mathes T., Fischer M., Joshi M., Bacher A., Hegemann P., Bittl R., Weber S., and Schleicher E. Brosi R., Illarionov B., Mathes T., Fischer M., Joshi M., Bacher A., Hegemann P., Bittl R., Weber S., "Hindered Rotation of a Cofactor Methyl Group as a Probe for Protein - Cofactor Interaction," *J.Am.Chem.Soc.*, no. 132, pp. 8935–8944, 2010.

[6] Johansson L. B., Davidsson A., Lindblom G., and Naqvi K. R., "Electronic transitions in the isoalloxazine ring and orientation of flavins in model membranes studied by polarized light spectroscopy.," *Biochemistry*, vol. 18, pp. 4249–4253, 1979.

[7] Climent T., Gonzalez-Luque R., and Mercha M., Serrano- Andres L., "Theoretical Insight into the Spectroscopy and Photochemistry of Isoalloxazine , the Flavin Core Ring," *J. Phys. Chem. A*, vol. 110, pp. 13584–13590, 2006.

[8] Salomon M., Christie J. M., Knieb E., Lempert U., and Briggs W. R., "Photochemical and mutational analysis of the FMN-binding domains of the plant blue light receptor phototropin.," *Biochemistry*, vol. 39, pp. 9401–9410, 2000.

[9] Swartz T. E., Corchnoy S. B., Christie J. M., Lewis J. W., Szundi I., Briggs W. R., and Bogomolni R. A., "The photocycle of a flavin-binding domain of the blue light photoreceptor phototropin.," *J.Biol.Chem.*, vol. 276, pp. 36493–36500, 2001.

[10] Onodera A., Christie J. M., Kasahara M., Mochizuki N., Asamizu E., Tabata S., Fukuzawa H., Briggs W. R., and Nagatani A., "Analysis of phototropin-like gene of Chlamydomonas reinhardtii.," *Plant Cell Physiol.*, vol. 43, p. S230, 2002.

[11] Christie J. M., Salomon M., Nozue K., Wada M., and Briggs W. R., "LOV (light, oxygen, or voltage) domains of the blue-light photoreceptor phototropin (nph1):

binding sites for the chromophore flavin mononucleotide.," *PNAS*, vol. 96, pp. 8779–8783, 1999.

[12] Losi A., Polverini E., Quest B., and Gärtner W., "First Evidence for Phototropin-Related Blue-Light Receptors in Prokaryotes," *Biophys. J.*, vol. 82, no. May, pp. 2627–2634, 2002.

[13] Swartz, T.E.; Tseng, T.S.; Frederickson, M.A.; Paris, G.; Comerci, D.J.; Rajashekara, G.; Kim, J.G.; Mudgett, M.B.; Splitter, G.A.; Ugalde, R.A. et al., "Blue-Light-Activated Histidine Kinases: Two-Component Sensors in Bacteria.," *Science (80-.).*, vol. 317, pp. 1090–1093, 2007.

[14] Hendrischk A. K., Moldt J., Fruhwirth S. W., and Klug G., "Characterization of an Unusual LOV Domain Protein in the alpha-Proteobacterium Rhodobacter sphaeroides.," *Photochem. Photobiol.*, vol. 85, pp. 1254–1259, 2009.

[15] Djouani-Tahri E. B., Christie J. M., Sanchez-Ferandin S., Sanchez F., Bouget F. Y., and Corellou F., "A eukaryotic LOV-histidine kinase with circadian clock function in the picoalga Ostreococcus.," *Plant J.*, vol. 65, pp. 578–588, 2011.

[16] Kottke T., Heberle J., Hehn D., Dick B., and Hegemann P., "Phot-LOV1 : Photocycle of a Blue-Light Receptor Domain from the Green Alga Chlamydomonas reinhardtii," *Biophys. J.*, vol. 84, no. 2, pp. 1192–1201, 2003.

[17] Islam S. D. M., Penzkofer A., and Hegemann P., "Quantum yield of triplet formation of riboflavin in aqueous solution and of flavin mononucleotide bound to the LOV1 domain of Phot1 from Chlamydomonas reinhardtii," *Chem. Phys.*, vol. 291, pp. 97–114, 2003.

[18] Holzer W. and Penzkofer A., "Absorption and emission spectroscopic characterisation of the LOV2-domain of phot from Chlamydomonas reinhardtii fused to a maltose binding protein," *Chem. Phys.*, vol. 302, pp. 105–118, 2004.

[19] Kasahara M., Swartz T. E., Olney M. A., Onodera A., Mochizuki N., Fukuzawa H., Asamizu E., Tabata S., Kanegae H., Takano M., Christie J. M., Nagatani A., and Briggs W. R., "Photochemical Properties of the Flavin Mononucleotide- Binding Domains of the Phototropins from Arabidopsis , Rice , and Chlamydomonas reinhardtii 1," *Plant Physiol.*, vol. 129, no. June, pp. 762–773, 2002.

[20] Iwata T., Nozaki D., Tokutomi S., and Kandori H., "Comparative Investigation of the LOV1 and LOV2 Domains in Adiantum Phytochrome3.," *Biochemistry*, vol. 44, pp. 7427–7434, 2005.

[21] Purcell E. B., Mcdonald C. A.,. Palfey B. A, and. Crosson S, "An Analysis of the Solution Structure and Signaling Mechanism of LovK , a Sensor Histidine Kinase Integrating Light and Redox Signals †," pp. 6761–6770, 2010.

[22] Nash A. I., Mcnulty R., Elizabeth M., Swartz T. E., Bogomolni R. A., Luecke H., and Gardner K. H., "Structural basis of photosensitivity in a bacterial DNA-binding protein," 2011.

[23] Jentzsch K., Wirtz A., Circolone F., Drepper T., Losi A., Gärtner W., Jaeger K.-E., "Mutual Exchange of Kinetic Properties by Extended Mutagenesis in Two Short LOV Domain Proteins from Pseudomonas putida.," *Biochemistry*, vol. 48, pp. 10321–10333, 2009.

[24] Krauss U., Losi A., Gärtner W., Jaeger K.-E., and Eggert T., "Initial characterization of a blue-light sensing, phototropin-related protein from Pseudomonas putida: a paradigm for an extended LOV construct.," *Phys.Chem.Chem.Phys.*, vol. 7, pp. 2229–2236, 2005.

[25] Narikawa R., Zikihara K., Okajima K., Ochiai Y., Katayama M., Shichida Y., Tokutomi S., and Ikeuchi M., "Three Putative Photosensory Light, Oxygen or Voltage (LOV) Domains with Distinct Biochemical Properties from the Filamentous Cyanobacterium Anabaena sp. PCC 7120.," *Photochem.Photobiol.*, vol. 82, pp. 1627–1633, 2006.

[26] Cao Z., Livoti E., Losi A., and Gärtner W., "A Blue Light-inducible Phosphodiesterase Activity in the Cyanobacterium Synechococcus elongatus.," *Photochem.Photobiol.*, vol. 86, pp. 606–611, 2010.

[27] Chan R. H., Lewis J. W, and Bogomolni R. A., "Photocycle of the LOV-STAS Protein from the Pathogen Listeria monocytogenes," pp. 361–369, 2013.

[28] Losi A. and Gärtner W., "The evolution of flavin-binding photoreceptors: an ancient chromophore serving trendy blue-light sensors.," *Annu. Rev. Plant Biol.*, vol. 63, pp. 49–72, Jan. 2012.

[29] Walter J., Hausmann S., Drepper T., Puls M., Eggert T., and Dihné M., "Flavin Mononucleotide-Based Fluorescent Proteins Function in Mammalian Cells without Oxygen Requirement.," *PLoS One*, vol. 7, p. e43921, 2012.

[30] Losi A., Quest B., Gärtner W., "Listening to the blue: the time-resolved thermodynamics of the bacterial blue-light receptor YtvA and its isolated LOV domain.," *Photochem. Photobiol. Sci.*, vol. 2, pp. 759–766, 2003.

[31] Mandalari C., Losi A., Gärtner W., "Distance-tree analysis, distribution and co-presence of bilin- and flavin-binding prokaryotic photoreceptors for visible light," *Photochem. Photobiol. Sci.*, vol. 12, pp. 1144–1157, 2013.

[32] Krauss U., Minh B. Q., Losi A., Gärtner W., Eggert T., von Haeseler A., and Jaeger K.-E., "Distribution and phylogeny of light-oxygen-voltage-blue-light-signaling proteins in the three kingdoms of life.," *J. Bacteriol.*, vol. 191, no. 23, pp. 7234–42, Dec. 2009.

[33] Pathak, G.P.; Vrana, J.D.; Tucker, C.L., "Optogenetic control of cell function using engineered photoreceptors.," *Biol. Cell*, vol. 105, pp. 59–72, 2013.

[34] Losi A., Mandalari C., Gärtner W., "From plant infectivity to growth patterns: the role of blue-light sensing in the prokaryotic world", Plants, accepted for publication, 2014..

Acknowledgments

Foremost, I want to thank dr. Losi, dr. Abbruzzetti and all the molecular biophysics group in Parma, for giving me the opportunity to work with them in such a fascinating research on novel photoreceptors. I want to thank them for their patience, support and attention during all three years. They are an example for me for their competence and generosity.

I want to thank also dr. Polverini for giving me precious help to learn bioinformatics techniques and dr. Bedotti for lab assistance (and not only).

I am particularly grateful to prof. Gärtner of the Max Planck Institute for Chemical Energy Conversion, and his group for biomolecolar assistance and for careful work in the preparation of samples. I thank also prof. Diaspro and his group at the Italian Institute for Technology of Genova, dr. Cella Zanacchi and dr. Bianchini for super-resolution microscopy.

I thank also dr. Allegri, my Ph. D mate, for the illuminating conversations.

Last but not least to my family for their love.